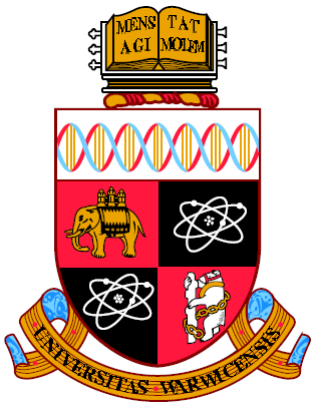

Study of Supercritical Coal-Fired Power Plant Dynamic Responses and Control for Grid Code Compliance

by

Mihai Draganescu

A thesis submitted to the University of Warwick for the degree of Doctor of Philosophy in Engineering

University of Warwick, School of Engineering

August 2015

Contents

List of Figures

List of Tables

Acknowledgements

I would like to thank God for empowering me to do this research and to write this thesis.

I would like to express my gratitude towards Professor Jihong Wang for giving me the opportunity to undertake this research. She offered me guidance and total support, which proved to be invaluable to me throughout the research period. I learned a lot from her professional and life experience, which I treasure and will use along my entire life. I am grateful for having her as my supervisor and I thank her for all the teachings I received.

I would like to thank Dr. Yongmann Chung and Professor Kang Li for the work they carried out by reading and reviewing my thesis.

I would like to thank my parents for giving me the right upbringing. Special thanks go towards my wife Adina for her love, care and understanding, which she offered me throughout this period. I am addressing my thanks as well to my aunt Mioara who always encouraged me to continue my education and never stopped believing in me.

Declaration

I declare that this thesis represents entirely my own work, conducted under the supervision of Prof. Jihong Wang, except where otherwise stated.

The thesis has not been submitted for a degree at another university.

Abstract

The thesis is concerned with the study of the dynamic responses of a supercritical coal-fired power plant via mathematical modelling and simulation. Supercritical technology leads to much more efficient energy conversion compared with subcritical power generation technology so it is considered to be a viable option from the economic and environmental aspects for replacement of aged thermal power plants in the United Kingdom. However there are concerns for the adoption of this technology as it is unclear whether the dynamic responses of supercritical power plants can meet the Great Britain Grid Code requirement in frequency responses and frequency control.

To provide answers to the above concerns, the PhD research project is conducted with the following objectives: to study the dynamic responses of the power plant under different control modes in order to assess its compliance in providing the frequency control services specified by the Great Britain Grid Code; to evaluate and improve the performance of the existing control loops of the power plant simulator and in this regard a controller based on the Dynamic Matrix Control algorithm was designed to regulate the coal flow rate and another controller based on the Generalized Predictive Control algorithm was implemented to regulate the temperature of the superheated steam; to conduct an investigation regarding frequency control at the power plant level followed by an analysis of the frequency control requirements extracted from the Grid Codes of several European and non-European countries.

The structure and operation of the supercritical power plant was intensively studied and presented. All the simulation tests presented in this thesis were carried out by the mean of a complex 600 megawatts power plant simulator developed in collaboration with Tsinghua University from Beijing, China.

The study of the conducted simulation tests indicate that it is difficult for this type of power plant to comply with the frequency control requirements of the Great Britain Grid Code in its current control method. Therefore, it is essential to investigate more effective control strategies aiming at improving its dynamic responses. In the thesis, new Model Predictive Control power plant control strategies are developed and the performance of the control loops and consequently of the power plant are greatly improved through implementation of Model Predictive Control based controllers.

List of Abbreviations

B	Boiling Point
B & W	Babcock & Wilcox
CARMA	Controller Auto-Regressive Moving-Average
CCS	Coordinated Control System
CP	Critical Point
DMC	Dynamic Matrix Control
FGPI	Fuzzy Gain Scheduling Proportional and Integral
FL	Fuzzy Logic
FOPTD	First Order Plus Time Delay
GB	Great Britain
GPC	Generalized Predictive Control
HP	High Pressure
MAC	Model Algorithmic Control
MIMO	Multi Input Multi Output
MPC	Model Predictive Control
MPHC	Model Predictive Heuristic Control
MW	Megawatt
PI	Proportional-Integral
PID	Proportional-Integral-Derivative
QP	Quadratic Programming

RC	Registered Capacity
SCR	Selective Catalytic Reduction System
SH	Superheater
SISO	Single Input Single Output
SMOC	Shell Multivariable Optimizing Controller
TSO	Transmission System Operator
UCTE	Union for the Coordination of Transmission of Electricity
UK	United Kingdom

List of Symbols

In general the symbols are defined locally. This list contains the principal symbols used.

W_{p}	work done to the fluid by the feedwater pump, J
Q_{in}	heat received by the boiler, J
W_{T}	work produced by the expansion of steam in the turbine, J
Q_{out}	heat removed from the steam in the condenser, J
p	working fluid pressure, Pa
v	specific volume, m^3/kg
T	working fluid temperature, K
s	specific entropy, J/(kg·K)
h	specific enthalpy, J/kg
q_A	specific heat added, J/kg
w_T	specific turbine work, J/kg
q_R	specific heat rejected, J/kg
w_P	specific pump work, J/kg
Δw_{net}	specific net work, J/kg
η_{th}	thermal efficiency
p_c	critical pressure of water, Pa
T_c	critical temperature of water, °C

v_c	critical volume of water, m^3/kg
t	time, s
R	speed droop
N_R	rated speed, r/min
N_{PR}	speed at full load, r/min
N_0	speed at no load, r/min
r	flow resistance, 1/(kg·m)
Δp	pressure drop over the pipe resistance, Pa
ζ	flow resistance coefficient
C_m	constant characterizing the medium
$\boldsymbol{\mu}$	solid phase concentration
σ	compressibility coefficient of the fluid
S_0	flow area of the pipe, m^2
ρ_1	flow density, kg/m^3
r_0	flow resistance for a temperature of 0°C, 1/(kg·m)
T_1	fluid temperature at the pipe input, °C
l	valve opening
r_{00}	flow resistance for valve fully open, and temperature 0°C, 1/(kg·m)
f	function depending on the l variable
$\mathbf{H_p}$	pressure gain generated by the height difference, Pa
$\mathbf{h_p}$	height difference between flow points, m
ρ_{env}	density of the environment, kg/m^3

g	gravitational acceleration, m/s^2
T_p	sampling time of the controller, s
u	control signal
N_u	control horizon
y^{sp}	set-point for process output
N	prediction horizon
y	process output
y^0	free process output component
d	unmeasured disturbance
J	cost function
$\underline{\Psi}$	matrix of weights for the predicted process output errors
$\underline{\Lambda}$	matrix of weights for the control input increments
Δy	forced process output component
u_{min}	minimum amplitude of the control signal
u_{max}	maximum amplitude of the control signal
Δu_{max}	maximum rate of change of control inputs
y_{min}	minimum amplitude of the process outputs
y_{max}	maximum amplitude of the process outputs
τ	time delay, s
s_j	step coefficient
D	horizon of the process dynamics
Y^{sp}	set-point matrix

Y^0	free component matrix
ΔY	forced component matrix
ΔU	future control inputs matrix
M^p	matrix used in the calculation of Y^0
Y	matrix of current measurement
ΔU^p	matrix of past control inputs
M	dynamic matrix
ΔU_{max}	matrix of constraints on rate of change
U_{min}	matrix of lower bound constraints on the amplitude of control signal
U_{max}	matrix of upper bound constraints on the amplitude of control signal
$U(k-1)$	matrix of previously implemented control signal
Θ	lower triangular matrix
Y^{pred}	predicted future outputs matrix
Y_{min}	matrix of lower bound constraints on the process outputs
Y_{max}	matrix of upper bound constraints on the process outputs
P_e	electrical power, W
$\mathbf{v_f}$	speed command
$\mathbf{w_{coal}^{set}}$	set-point coal flow rate, kg/s
$\mathbf{w_{coal}}$	total coal flow rate, kg/s
$\mathbf{w_{air}}$	air flow rate, kg/s
P	current load demand, W
$\mathbf{w_{coal}^{pred}}$	predicted coal flow rate, kg/s

G	FOPTD transfer function
k	static gain
θ	time delay
τ	time constant
I	identity matrix
λ	control input weight parameter
$\epsilon(t)$	zero mean white noise
A	polynomial in the backward shift operator z^{-1}
B	polynomial in the backward shift operator z^{-1}
C	polynomial in the backward shift operator z^{-1}
z^{-1}	backward shift operator
a_i	polynomial A parameters
b_i	polynomial B parameters
c_i	polynomial A parameters
na	polynomial A degree
nb	polynomial B degree
nc	polynomial C degree
$\boldsymbol{E_j}$	polynomial of Diophantine equation
$\boldsymbol{F_j}$	polynomial of Diophantine equation
$\boldsymbol{G_j}$	polynomial used to express the output predictions
$\boldsymbol{e_j}$	coefficient of the E_j polynomial
$\boldsymbol{f_j}$	coefficient of the F_j polynomial

$\boldsymbol{g_j}$	coefficient of the G_j polynomial
y	GPC output predictions vector
u	GPC control inputs vector
G	matrix of g_j coefficients
F	vector of F_j polynomial
f	vector of past inputs and outputs
δ	output predictions error weight
W_{sp}	GPC future set-point
W	GPC vector of future reference trajectory
$T_{set,out}$	set-point temperature at the Final SH outlet, °C
T_{in}	temperature at the Final SH inlet, °C
T_{out}	temperature at the Final SH outlet, °C
α	valve position of the attemperator, %

Chapter 1

Introduction

1.1 Background and motivation

The operation and development of the national economies and everyday living rely heavily on the use of electricity. World net electricity generation in 2010 was 20200 TWh and is predicted to reach 39000 TWh by 2040, which means an increase of over 93% [U.S. Energy Information Administration, 2013].

The electricity is generated worldwide by a mix of primary energy sources, among which the largest share is allocated to coal. The percentage of each fuel used in power generation has changed dramatically throughout the past thirty years and will continue to change in the future. The high fossil fuel prices and the increasing environmental concerns due to CO_2 emissions, have generated from the early 2000s an increased interest in developing nuclear power and especially renewable power generation. U.S. Energy Information Administration [2013] predicted an annual increase of 2.8% per year from 2010 to 2040 for the electricity generated from renewable energy sources, which also means the fastest growing rate. The second place in the predicted annual increase is dedicated to natural gas and nuclear power, with a 2.5% per year from 2010 to 2040.

Although electricity generated by coal has the smallest increase rate of 1.8% over the predicted period, it remains the largest source of power generation until 2040. Nonetheless the use of coal might be limited in the future by national policies or

international agreements aimed at reducing the CO_2 emissions [U.S. Energy Information Administration, 2013].

The forecast for the electricity generation by fuel for the period 2010-2040 is presented in Fig. 1.1. The graph illustrates that the electricity provided by coal-fired generation will increase from 8.05×10^3 TWh in 2010 to 13.89×10^3 TWh in 2040.

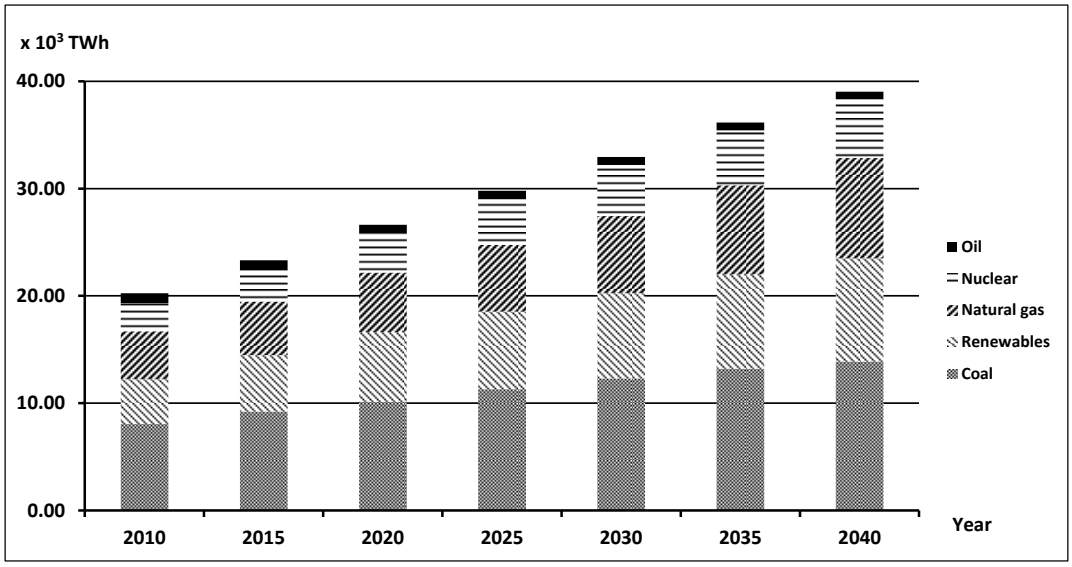

FIGURE 1.1 World electricity generation by fuel for period 2010-2040 [U.S. Energy Information Administration, 2013]

Electricity generation by fuel type in 2012 for member countries of the Organization for Economic Co-operation and Development (OECD) is presented in Fig. 1.2.

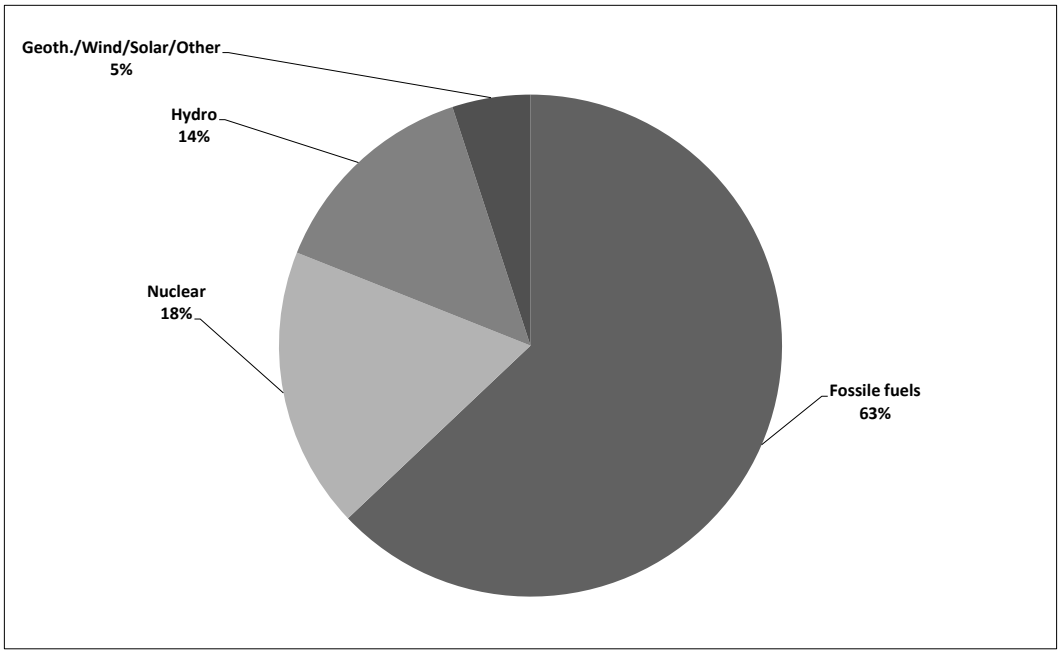

FIGURE 1.2 World electricity supplied by fuel type in 2012 [International Energy Agency, 2013]

It can be seen from Fig. 1.2, that the major part of the electricity around the world (63%) is still generated from fossil fuels, which also includes coal, while the renewable sources stand for only 5% of the generation.

According to the Department of Energy and Climate Change [2013], the electricity consumption in the UK has risen from 264.9 TWh up to 353.9 TWh for the period 1980-2012, which represents an increase of nearly 34% in power demand. This is covered by a mix of power generation sources, which has continually changed through time. The evolution of the electricity generation mix for the analysed period is reflected by the data presented in Table 1.1 and in Fig. 1.3.

TABLE 1.1 Electricity supplied by fuel type in UK [Department of Energy and Climate Change, 2013]

	Year					
	1980	**1990**	**2000**	**2010**	**2011**	**2012**
Fuel type	**TWh**					
Coal	220.8	213.4	114.7	102.3	103.1	135.9
Oil & other fuels	7.9	19.2	7.3	5.6	4.4	4
Gas	0	0.4	138.7	172.5	143.8	98.2
Nuclear	32.3	58.7	78.3	56.4	62.7	63.9
Hydro	3.9	5.2	5.1	3.6	5.7	5.3
Wind & Solar	0	0	0.9	10.2	15.8	20.8
Other renewables	0	0	4.1	10.9	11.8	13.4
Net Imports	0	11.9	14.2	2.7	6.2	12
Total	**264.9**	**308.7**	**371.4**	**364.1**	**353.4**	**353.9**

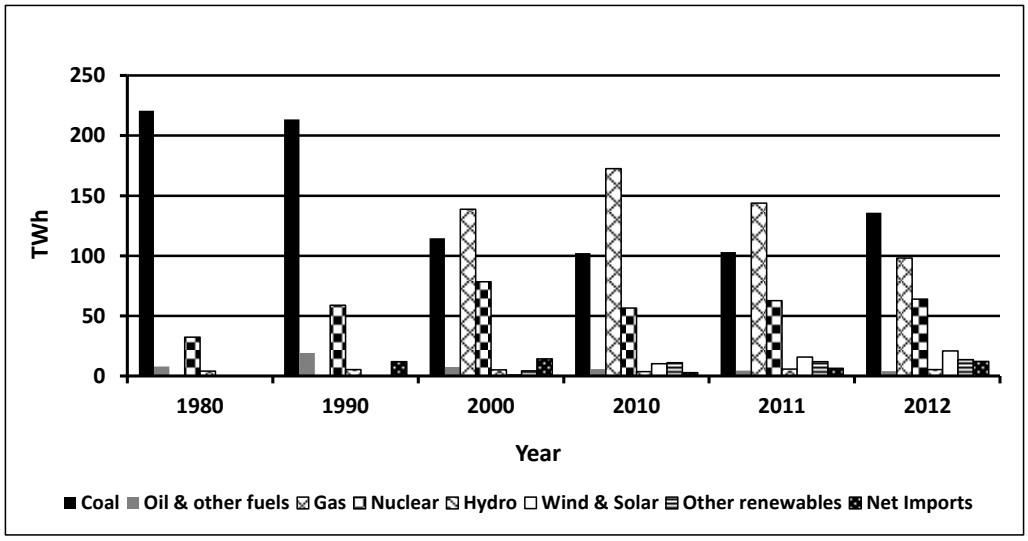

FIGURE 1.3 Electricity supplied by fuel type in UK [Department of Energy and Climate Change, 2013]

As a general characteristic, beginning with 1990s there is a decline in the use of coal and oil, while gas and renewables have registered increasing figures. The fluctuations of the gas prices through time compared to a more stable and smaller price for the coal, have allowed coal fired power plants to generate electricity at a lower cost than gas fired ones, maintaining in this way a significant share in the electricity generation mix. In 2012 to compensate for the decline of 32% in gas use, the coal generation increased with nearly the same percentage compared to 2011. Starting with 2000, more and more electricity was supplied by renewable sources, mainly wind and solar due to yearly increase of the capacity levels. For the analysed period a maximum of 20.8 TWh was achieved in 2012. A more detailed overview of the generation mix for the year 2012 is given in Fig. 1.4.

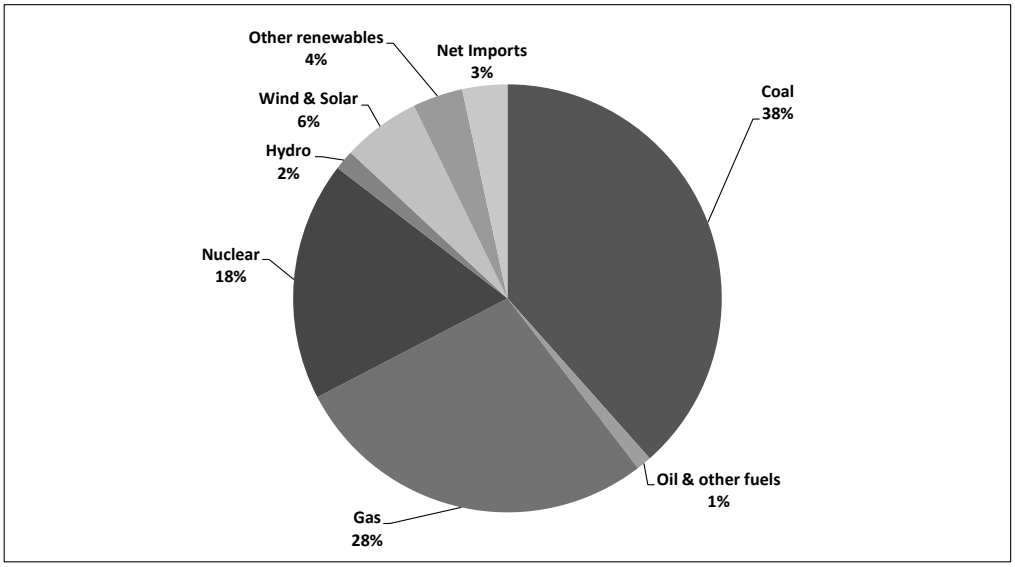

FIGURE 1.4 Electricity supplied by fuel type in 2012, UK [Department of Energy and Climate Change, 2013]

The conclusion which can be drawn from Fig. 1.4 is that coal and gas are still responsible for 38% and 28%, respectively of the generated power, the largest percentage from all the energy sources used for power generation.

The forecast regarding economic growth, an increase in the population number and the end of service life for several power plants, will see UK in the situation of a power shortage of over 20 GW by 2015-2020 [Taylor, 2008]. The solutions to fill this power gap need to be in line as well with the government's commitment to reducing the CO_2 emissions by at least 80% (from the 1990 baseline) by 2050 [Department of Energy & Climate Change, 2008].

The prospective renewable power generation capacity cannot provide only by itself the electricity needed; also if nuclear generation is considered, the closest estimated date for the nuclear power plants being currently under construction to become fully operational is 2018. Although gas power generation still makes 28% of the total generation in UK, its percentage started to decline from 2010 due to high prices and reached its lowest level since 1996 in 2012 [Department of Energy and Climate Change, 2013]. It is unrealistic under this trend to think of increasing the gas power generation for filling the power gap. Compared to gas, coal has had a smaller and more constant price which generated an increase in its use for power generation in 2011 and consequently in 2012, having currently a share of 38% from the total electricity generated. Considering the data available from the statistics and presented above, one of the realistic solutions to fill the future power gap in the UK is the coal power generation.

Total coal production around the globe averages 55 billion tons and 50% of this quantity is used for electricity generation by coal-fired power plants [ETSU coal R&D Programme, 1997]. This makes coal-fired generation responsible for the major part of the global emissions. Through coal combustion process various pollutants such as oxides of carbon (CO_x), oxides of sulphur (SO_x), oxides of nitrogen (NO_x) and others are released. From these pollutants SO_2 and NO_x can cause acid rain, while CO_2 is considered to be responsible for climate changes [Flynn, 2003]. This means that coal-fired power generation requires cleaner technologies. Electrostatic precipitators can remove up to 99% of the particles from the flue gases and a flue gas desulphurization plant can eliminate over 90% of SO_2. The reduction of NO_x still poses technical challenges in developing a practical method, which can achieve a high level of efficiency. Regarding the reduction of CO_2 emissions, the best way to achieve this is to increase power generation efficiency [Flynn, 2003].

A conventional subcritical pulverized coal-fired power plant can achieve an efficiency between 33-35% and having a high level of flue gas emissions. Compared to this technology, the efficiency of a supercritical coal-fired power plant can go up to 46% and hence reduced CO_2 emissions per unit of electricity generated. Also the capital cost is smaller in comparison with other clean coal technologies, which makes it more affordable for implementation [Wang, 2009].

Supercritical boilers were first developed in U.S. in the 1950s and with the development of materials and components, which are better fitted to withstand high pressure/temperature conditions, they are today reliable and operationally flexible. There are more than 430 supercritical power plants worldwide in operation or under

construction, with ratings ranging from 200 MW to 1300 MW and a total capacity of above 330 GW [Susta, 2008]. A distribution of these power plants around the world is presented in Fig. 1.5. At this moment there is no supercritical power plant operating in UK.

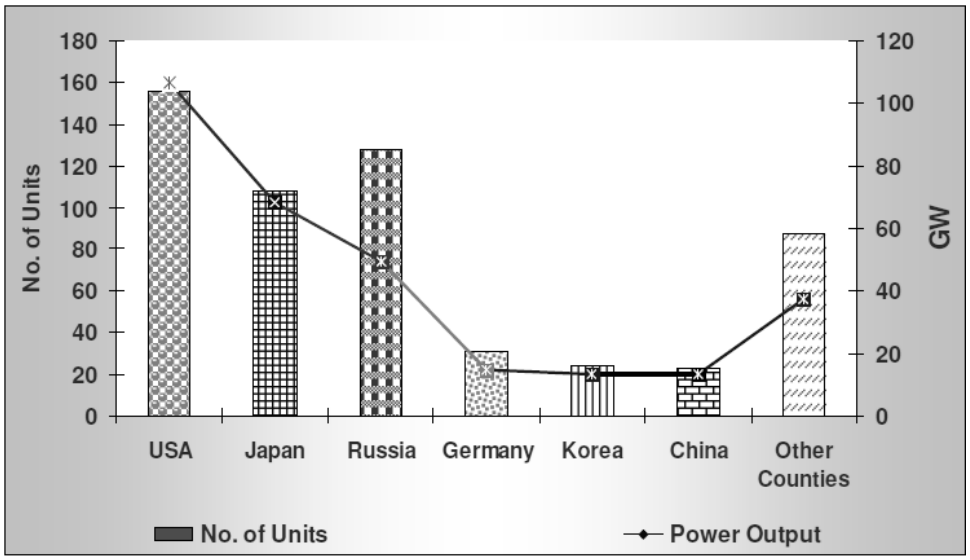

FIGURE 1.5 The number and installed capacity of supercritical power plants worldwide [Susta, 2008]

If coal-fired generation is considered as an option to compensate for the extra electricity needed in UK and its more efficient technology, the supercritical power plant is chosen, then this unit will have to be compliant with the operational requirements specified by GB Grid Code.

Different amounts of power are required at different times in a power system. This generates a power demand curve (see Fig. 1.6), which varies by time of day and season.

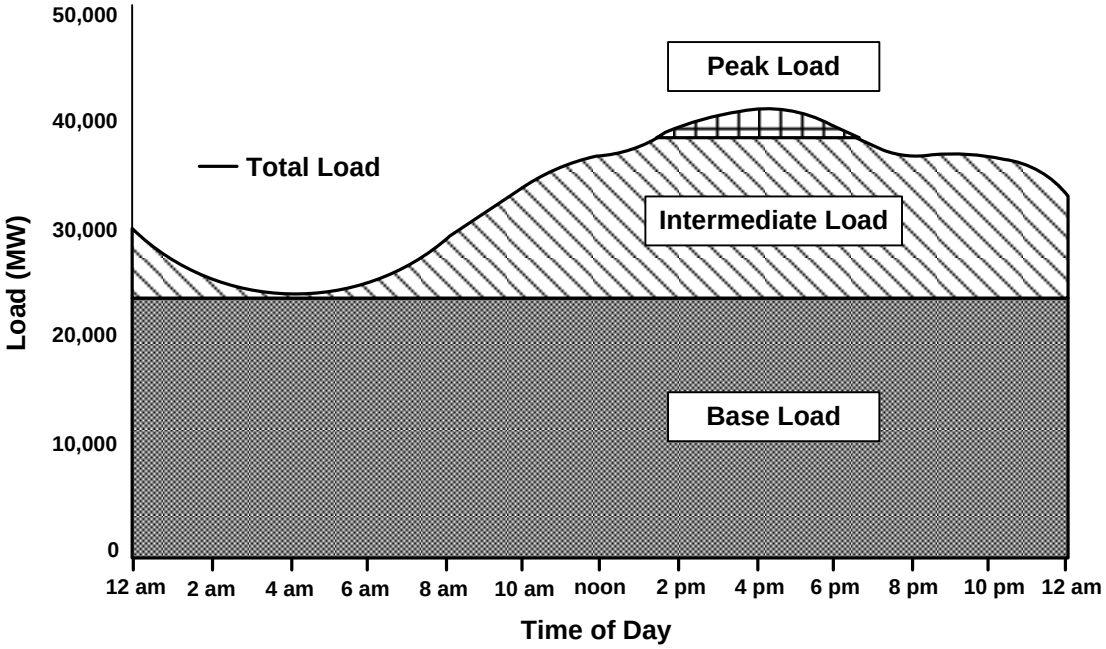

FIGURE 1.6 Typically daily power demand curve

The response from each of the grid connected power plants to a change in the power demand varies in size and ramping time. The response time and marginal operational costs are criteria which determine the dispatch order of the power plants. Some units are designed to operate at almost full power continuously and at low costs, like the nuclear power plants, giving them the name "must-run" plants and supplying the base-load. Some renewable power plants provide power only when the resource is available. Because of their intermittency and of almost zero marginal costs they are categorised as well as "must-run" plants. Predictable changes in the daily power demand are tracked by most fossil-fuelled and hydroelectric units, which can slowly be ramped up and down. These units are supplying the intermediate load. Peak load is supplied by power plants which have the capability to quickly ramp up and down in order to meet sudden increases and decreases in demand. They are expensive to

run and operate only for a few hours at a time. Typically they have natural gas combustion turbines.

The Grid Code specifies that in case of a frequency ramp of 0.5 Hz over 10 seconds, each Generating Unit is required to provide a frequency response at least to the solid boundaries shown in Fig. 1.7, the percentage response capabilities and loading levels being defined on the basis of the Registered Capacity (RC) of the Generating Unit. The black line represents the minimum required level for the Primary and Secondary Frequency Response throughout normal operating range of the Generating Unit. The minimum required level for the High Frequency Response is represented by the dark grey line and this profile should be followed throughout normal operating range of the Generating Unit.

The most demanding requirement for a power plant is the one regarding Primary Frequency Response. The time response specified by GB Grid Code is 10 s during which the power plant needs to increase its power output with 10% RC, according to the graph from Fig. 1.7. This requirement is very strict compared to other national grid codes and the reasons are the geographical isolation of the power system and the lack of strong interconnections with the neighbouring power systems.

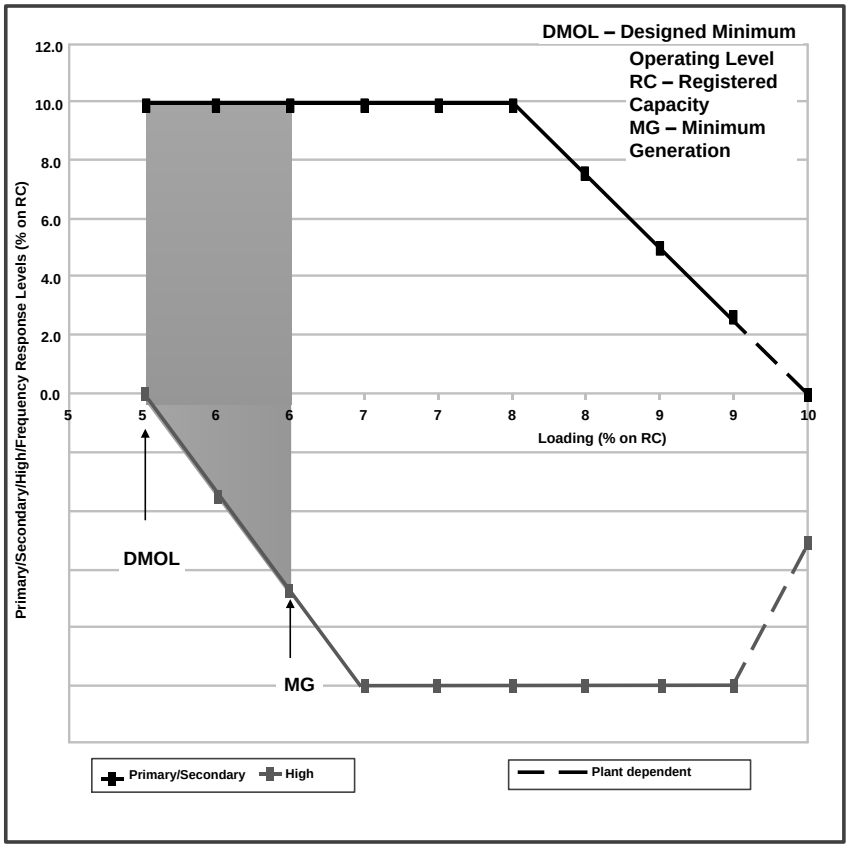

FIGURE 1.7 Minimum frequency response requirement profile for a 0.5 Hz frequency change from target frequency [National Grid Electricity Transmission plc, 2010]

Compared to a subcritical power plant, the supercritical power plant does not have a steam drum, which acts as an energy storage. The steam stored in the drum is released accordingly by opening the governor valve and then through expansion in the turbine is converted into mechanical/electrical energy as required by the change in the load demand.

As a result there are concerns from the power generation companies regarding the ability of a supercritical power plant to fulfil GB Grid Code requirements [Nicholls

et al., 2013]. The adoption of this clean coal technology depends on whether or not it can comply with GB Grid Code requirements and if there can be found ways to improve its dynamic responses.

This research aims at studying the dynamic responses of the coal fired supercritical power plant through modelling and simulations. The conduct of this research requires operating data from real power plants. As it is illustrated in Fig 1.5, around 30 supercritical power plants are already in operation in China, which makes a partnership for this research between the two countries very attractive. Given the above considerations, the research partners of this project were Tsinghua University and North China Electrical Power University, both from Beijing, China. The universities hold an outstanding research record in supercritical process and power plant modelling and simulation.

1.2 Power plant control system

Many processes are undergoing simultaneously during the operation of a power plant, where each action taken by an individual control loop is affecting not only its controlled variable but also variables from other processes regulated by their corresponding control loops. The actions of all the control loops must be coordinated to work together in such a way as to achieve the ultimate objective of the power plant, which is to follow the load demand signal in a safe and efficient manner.

The control system of a power plant is generally comprised by a number of control loops and feedforward compensators, which have the role of keeping the main thermodynamic variables in their designed limits. The advantages of using such a

control structure is that it provides a satisfactory operation for normal operation of the power plant, it is reliable and it allows the intervention of the operator on single components in case of emergency situations.

The control of the power plant refers mainly to the control of two major plant operating units: the boiler and the turbine. The dynamic characteristics of these differ significantly one from the other. The turbine has a quicker response to load changes than the boiler. The boiler's dynamics are slower due to the thermal inertia of its steam and water circuits and also by the type of fuel used for combustion.

The master control signal is represented by the load demand, which sets the firing rate, regulates the combustion air flow so that it matches the fuel input and controls the quantity of feedwater needed for the steam generation.

Depending on the role the power plant is going to play in the power system, there are several control options available.

- **Boiler following mode** In this control mode the turbine main steam governor is regulated such as to meet the load demand, while the boiler systems have the role to keep the steam pressure constant.
- **Turbine following mode** In this control mode the load demand signal is sent directly to boiler's control system, while the role of the turbine governor valve is to maintain a constant steam pressure.
- **Coordinated Control System (CCS)** In this control mode the load demand signal is sent both to boiler and turbine control systems. This control structure allows a fast tracking of the load demand and prevents possible dangerous situations.

- **Sliding pressure mode** In this control mode the pressure set point is allowed to vary between certain limits. The governor valve is fully open, no throttling action being taken. The steam pressure is proportional to the load. In this way the steam pressure has the same value from boiler output, turbine input, inside turbine.

The CCS control philosophy was developed and implemented during 1970s in the supercritical power units. This allowed for a better dynamic performance of the boiler-turbine unit in response to changes in load demand coming from the power system. The manipulated variables were: fuel flow, feedwater flow, air flow and steam flow. The load demand, acting as a feedforward signal, is sent to each of the four feedback control loops regulating the controlled variables: power output, steam pressure, steam temperature and the amount of air. In all the control loops Proportional-Integral-Derivative (PID) controllers are used to minimise the errors [Laubli *et al.,* 1971].

While the performance of PID controllers is fairly adequate when the power plant is operating under steady-state conditions, its performance deteriorates for frequent load changes. This generated the need for more advanced control techniques to be developed [Waddington *et al.,* 1987].

Fuzzy logic is used by Kocaarslan *et al.* [2006] to design the controllers needed to regulate a 765 MW coal fired once through boiler. The model used for the power plant has the coal flow and feedwater flow as input variables, while generated power and steam enthalpy are considered as output variables. As a decoupling system was used to linearise the relationships between outputs and inputs, two controllers are

needed to regulate each one of the system's outputs. In order to assess their performance, three types of controllers are designed in this study: a conventional PID, a Fuzzy Logic (FL) controller and a Fuzzy Gain Scheduling Proportional and Integral (FGPI) controller. The last type of controller is used to adjust the gains of the PI controller according to the disturbances in the system's outputs. The inference mechanism of the fuzzy logic controllers are realised by seven rules. The rules are formed based on the error signal and its time derivative, while triangular membership functions are preferred, since fast response is necessary for the system. The results from the simulations show that the best performance with regard to maximum overshoot and settling time is achieved by the FGPI controllers, followed closely by the FL controllers, while the PID controllers had the worst performance.

A successful attempt of using optimal control in a 500 MW supercritical power plant was realised by Nakamura *et al.* [1981]. With fast and large load demand changes, keeping the steam temperature at the superheater and reheater outlets becomes a challenging problem. Considering the power plant as a mutually interacting multivariable system, it is hard to contain the controlled variables within their specified limits by using a multiple loop feedback system based on PID controllers. As a solution to the problem, the authors propose the design of a linear quadratic controller, which will augment the performance of the existing PID based control system. The manipulated variables are: fuel to feedwater ratio, flow rate of the spray water at the desuperheater and the opening of the gas damper in the rear path of the boiler shell. An Autoregressive model is fitted for a low and a high operating points, from which the state equation is derived afterwards. Subsequently the feedback gain

matrix is calculated by optimizing the cost function using the Dynamic Programming procedure. As the dynamic properties of the power plant vary with the load demand, the state equation and the feedback gain matrix are recalculated for other operating points of the power plant using linear interpolation between the low and high operating points. In this way the control parameters are adjusted accordingly to each new value of the load demand, providing an adaptive feature to the controller. The new control architecture is tested both with a simulator and a field power plant and the results show a significant improvement in the control of both superheater and reheater steam temperature. Although the research proves successful in implementing a new control strategy in a supercritical power plant, there are not given enough details on how both control systems, PIDs and linear quadratic regulator, cooperate together.

One of the advanced control techniques, which proved to be successful in practical applications in recent decades, is Model Predictive Control (MPC). MPC refers to a series of control algorithms, which uses a model of the process to calculate the next control moves by minimizing a cost function. MPC applications are very popular especially in the process industry given to several reasons:

- it can take into account constraints both on process inputs and outputs;
- the control moves are calculated with considerations to the internal interactions within the process, due to the use of a model;
- it can easily deal with a multivariable process;
- it can control processes with complex dynamics;
- its concepts are relatively easy to explain to the operator staff.

One of MPC algorithms, Dynamic Matrix Control (DMC) was used by Rovnak *et al.* [1991] to design a multivariable controller for a supercritical power plant. The system is identified as a ninth-order process model having as inputs the feedwater flow, the fuel firing rate and the governor valve position and as outputs the steam pressure, the steam temperature and the energy of the turbine. The controller uses a matrix equation to calculate the future values of the controlled variables for increments in the manipulated variables. Step tests on the inputs of the identified process model are performed and the resulting step response coefficients are recorded. The coefficients are afterwards used explicitly in the matrix equation. In order to verify the performance of the controller, the power plant was subjected to a ramp up, ramp down change in the load demand signal. The results show a tight control of the steam pressure and temperature during the variations in the load demand. The research does not mention one disadvantage of this algorithm, which is the difficulty in performing the step tests on a real process.

Another MPC algorithm, Generalized Predictive Control (GPC), is used by Hou *et al.* [2011] to design the CCS for a 500 MW power plant. The controlled object is simplified to two inputs, defined by the coal feeder speed and the opening degree of the turbine governor valve and two outputs, represented by generated power and main steam pressure. The controller is using a Controlled Auto-Regressive Integrated Moving Average model, which was identified for the power plant operating at 100 % power output. For comparison a CCS using PID controllers is also designed for the power plant. The performance of the CCS, for each control strategy employed, is tested for a load demand step disturbance and for a pressure step disturbance. A

smaller overshoot and settling time is recorded when using the GPC strategy, compared to when PID is used. The tests are repeated, this time for the power plant operating at 70% power output, without changing the model used by the GPC controller. The simulation results show a good set-point tracking of the controlled variables, which proves the robustness of the controller. The research proved the effectiveness of the GPC controller, although more manipulated variables might need to be included in a practical application.

1.3 Project objectives

The research work covered by this project has the following objectives:

- to study the dynamic responses of the supercritical power plant for different operating scenarios. The capability of the power plant to provide system frequency control services under the requirements specified by the GB Grid Code is verified using the simulator.
- to evaluate the performance of the existing control strategies from the simulator. Advanced control algorithms, like DMC and GPC are used to design new controllers for different subsystems of the power plant and their performance is compared against the existing controllers.
- to investigate the way frequency control is realized at the power plant level. An extensive research into different national grid codes is carried out regarding frequency control requirements needed to be fulfilled by the power plants connected to the grid.

1.4 Thesis outline

The thesis is structured into seven chapters, with the first chapter presenting the background and motivation of the research project and as well as other introductory notions.

Chapter 2 is presenting the general structure and operation of a steam power plant with a focus on the supercritical coal-fired power plant. The basic thermodynamic cycles on which the operation of a power plant is based are illustrated and analysed. It continues with the description of the supercritical power plant and an analysis of its thermodynamic cycle is made.

Chapter 3 defines power system frequency and then describes the way it is controlled at power plant level. Several national grid codes have been researched and the regulations regarding frequency control are tabulated and compared.

Chapter 4 investigates the dynamic responses of the power plant through simulation tests, aiming to determine if the frequency control requirements specified by GB Grid Code are fulfilled. Different control modes for the steam pressure are considered and the data recorded for power output and steam pressure was presented in graphs and tables, which were afterwards used for analysis.

Chapter 5 deals with the control system responsible for the regulation of the fuel flow sent to the furnace by the coal mills. The existing PID based control system architecture is presented and its performance is analysed. In order to optimize this control structure, a DMC controller is proposed to replace the PID controller. Through simulation tests the performance of the DMC controller is compared to the one of the PID and the superiority of the first one is assessed.

Chapter 6 analyses the control system which regulates through the use of the attemperator the steam temperature at the final superheater outlet. This control structure is based on a cascade PID control loop, which is far from being optimal due to various disturbing factors. As an improved solution, a GPC controller is proposed to replace the existing control structure. Simulation tests are run and the results show a better performance of the GPC controller compared to the existing PID based structure.

Chapter 7 ends this thesis with a summary of the research work undertaken, underlying the main contributions brought in this specific research area. Also some future research directions are proposed in this part.

Chapter 2

General Structure and Operation of a Supercritical Coal-Fired Power Plant

2.1 Basic operating principles of a steam power plant

A power plant is a complex facility, which generates electricity through transformation of various types of energy sources. If the electricity generation process requires the conversion of water into steam, the unit is defined as a steam power plant. In this research work the heat required to produce steam comes from the coal burning process.

2.1.1 The Rankine cycle

One of the most used thermodynamic cycles in power plants is the Rankine cycle. A simplified diagram of a power plant using a Rankine cycle is depicted in Fig. 2.1.

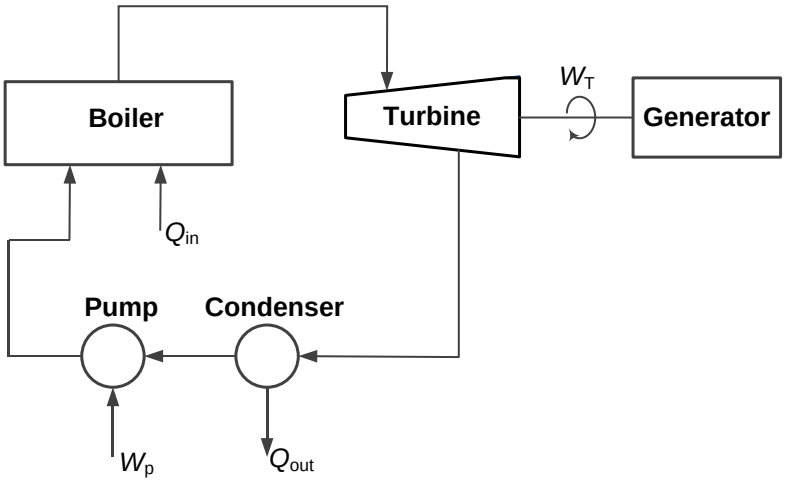

FIGURE 2.1 Schematic diagram of a Rankine cycle [Woodruff *et al.*, 2004]

Feedwater is sent to the boiler after the pump increased its pressure corresponding to the work done W_p. The boiler receives the heat Q_{in}, which is then used to transform the water into dry saturated steam. The steam then expands in the turbine, producing the work W_T, which drives the generator. The outlet steam from the turbine is then directed into condenser, where the heat Q_{out} is removed. The condensed steam is sent back to the boiler and the process is repeated.

The ideal Rankine cycle is presented in Fig. 2.2 (a, b) as pressure-volume, *p*-*v* and temperature-entropy, *T*-*s* diagrams. Cycle 1-2-3-4-*B*-1 is a saturated Rankine cycle and cycle 1′-2′-3-4-*B*-1′ is a superheated Rankine cycle. It is assumed that the cycles are reversible, the processes going on in turbine and pump are adiabatic reversible and there are no pressure losses in the pipes.

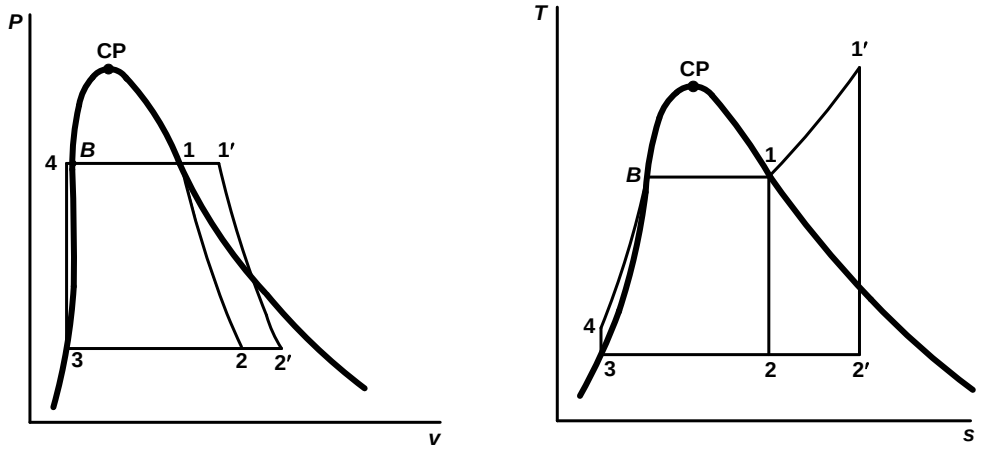

(a) **(b)**

FIGURE 2.2 Ideal Rankine cycle in (a) *p*-*v* and (b) *T*-*s* diagrams; 1-2-3-4-B-1 is a saturated cycle and 1′-2′-3-4-*B*-1′ is a superheated cycle; CP - critical point; B - boiling point [Kiameh, 2002].

During a Rankine cycle the following processes take place:

- 1-2 or 1′-2′ represents an adiabatic reversible expansion of the steam in the turbine; at point 2 or 2′ the working agent is in the two phase-region;
- 2-3 or 2′-3 takes place in condenser, at constant temperature and pressure, with the removal of the heat from the working agent.
- 3-4 is an adiabatic reversible compression by the pump. The saturated liquid from condenser is sent to the boiler with an increased pressure, as required by point 4.
- 4-1 or 4-1′ is a constant pressure heat transfer in the boiler. The subcooled liquid from point 4 is brought to saturation in point *B*. This section is called economizer. Through additional heating, the saturated liquid is brought to saturated vapour in point 1. Portion *B*-1 takes place in the evapourator. For the saturated cycle, the temperature of saturated vapour is further increased from point 1 to point 1′. This process is taking place in the superheater.

For a unit mass of vapour the following thermodynamic relations can be written, where *h* denotes the specific enthalpy of the liquid [Kiameh, 2002]:

- Heat added
$$q_A = h_1 - h_4 \quad J/kg \tag{2.1}$$
- Turbine work
$$w_T = h_1 - h_2 \quad J/kg \tag{2.2}$$
- Heat rejected
$$|q_R| = h_2 - h_3 \quad J/kg \tag{2.3}$$
- Pump work
$$|w_P| = h_4 - h_3 \quad J/kg \tag{2.4}$$

- Net work

$$\Delta w_{net} = (h_1 - h_2) - (h_4 - h_3) \qquad J/kg \tag{2.5}$$

- Thermal efficiency

$$\eta_{th} = \frac{\Delta w_{net}}{q_A} = \frac{(h_1 - h_2) - (h_4 - h_3)}{(h_1 - h_4)} \tag{2.6}$$

If the unit is small, the pressure p_4 can be considered similar to p_3 and so,

$$h_3 \approx h_4 \tag{2.7}$$

which means the pump work can be neglected compared to the turbine work and the thermal efficiency will have the following formula,

$$\eta_{th} = \frac{h_1 - h_2}{h_1 - h_3} \tag{2.8}$$

2.1.2 The Reheat cycle

A schematic diagram for a reversible Rankine cycle with superheater and reheater is presented in Fig. 2.3 and the associated *T-s* diagram is illustrated in Fig. 2.4. The main advantages of reheating the steam are the increased thermal efficiency and the decreased quantity of moisture in the steam at the turbine exhaust, which has the effect the reduction of the erosion on the turbine blades caused by the impact of water drops.

The steam leaving the superheater at point 1 expands through the high-pressure turbine up to point 2. From here it is reheated at constant pressure until it reaches the temperature from point 3, which is close to the one from point 1. It then expands through the low-pressure turbine up to condenser pressure at point 4.

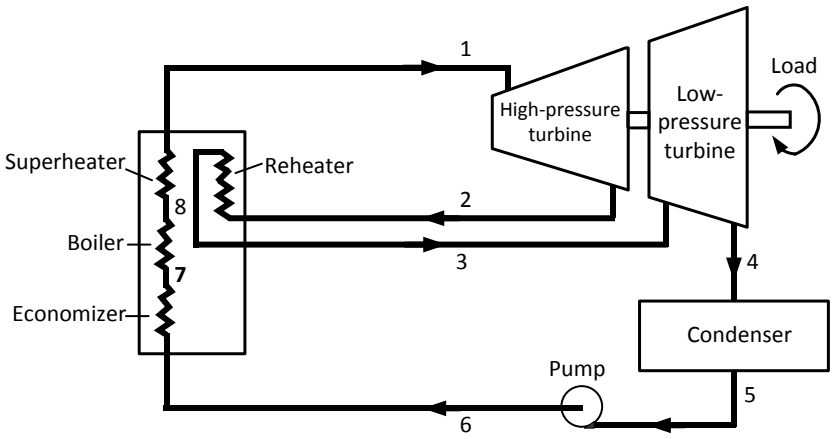

FIGURE 2.3 Schematic diagram of a Rankine cycle with superheater and reheater [Kiameh, 2002]

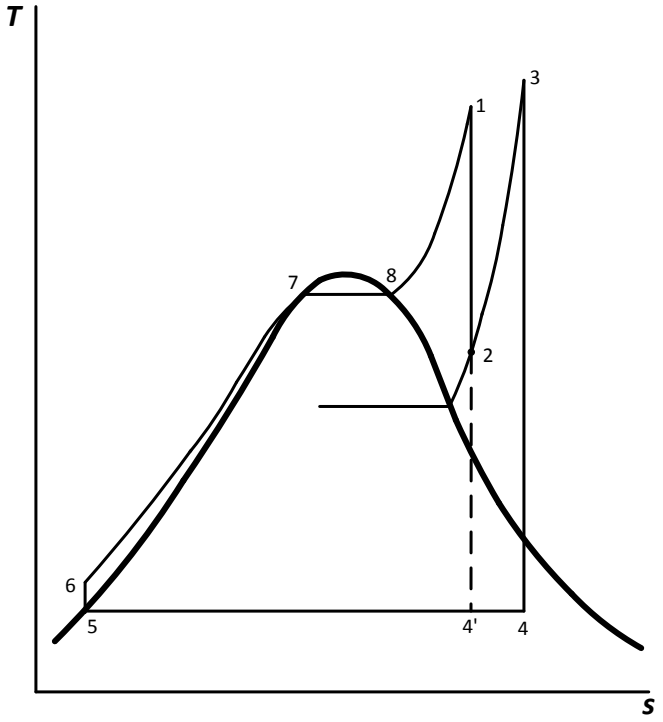

FIGURE 2.4 *T-s* diagram of a Rankine cycle with superheater and reheater [Kiameh, 2002].

In this cycle heat is added twice: one time from point 6 to point 1 and the second time from point 2 to point 3. The supplementary added heat results in low-pressure turbine expansion work. In this way total output work is increased, which increases thermal efficiency.

The moisture in the steam at the turbine exhaust is reduced due to the reheating process. Turbine exit point is shifted from 4 to 4′, which means that the process is moved away from the two-phase region towards the superheat region of the *T*-*s* diagram, thus drying the turbine exhaust.

The net work, Δw_{net}, is represented by the algebraic sum of the work done by the two turbines, w_T, and the pump work, $|w_P|$. Their expressions are [Kiameh, 2002]:

$$w_T = (h_1 - h_2) + (h_3 - h_4) \quad J/kg \tag{2.9}$$

$$|w_P| = h_6 - h_5 \quad J/kg \tag{2.10}$$

$$\Delta w_{net} = (h_1 - h_2) + (h_3 - h_4) - (h_6 - h_5) \quad J/kg \tag{2.11}$$

The total added heat is the sum of the heat added in the feedwater and the heat added in the reheater section. It has the following expression [Kiameh, 2002]:

$$q_A = (h_1 - h_6) + (h_3 - h_2) \quad J/kg \tag{2.12}$$

Considering the net work and total added heat expressions, thermal efficiency of the cycle can be calculated as [Kiameh, 2002],

$$\eta_{th} = \frac{\Delta w_{net}}{q_A} = \frac{(h_1 - h_2) + (h_3 - h_4) - (h_6 - h_5)}{(h_1 - h_6) + (h_3 - h_2)} \tag{2.13}$$

Generally fossil-fuelled power plants have at least one stage of reheat, but no more than two stages, as the improvement in efficiency is not justified by investment costs.

The efficiency of the reheat cycle is affected by the value of the reheat pressure p_2. If this pressure is close to the initial pressure, the heat added at high temperature has a small value, which negatively affects the efficiency. The reheat cycle reaches its maximum efficiency when the ratio p_2/p_1 is between 20 and 25 percent.

2.1.3 Water properties

The working agent in the power plant is water, which changes phases along the thermodynamic cycle from liquid to vapour and vice versa. To better understand the thermodynamic processes undergoing in a power plant, a short description of the phases through which water passes as the pressure and temperature change, is given below.

For a given temperature, the pressure at which water turns into vapour, or vapour condenses is called the *saturation pressure*. Similarly, for a given pressure the temperature at which these phenomena occur is named the *saturation temperature*. For example when the pressure is 1 MPa, the saturation temperature is 179.9 °C.

Water is called a *saturated liquid*, when its phase is liquid for a given saturation pressure and temperature. If from the saturated liquid, the temperature is lowered, keeping during all this time the same saturation pressure, then the water is called *subcooled* or *compressed liquid*. Adding more heat to the saturated liquid, will generate some of the liquid to change into vapour, such as a mixture of liquid and vapour occurs. When all the water turns into vapour for a given saturation temperature and pressure, the phase is called *saturated vapour*. If more heat is added

to the saturated vapour, the temperature increases above the saturation temperature and the water reaches the *superheated vapour* phase.

Fig. 2.5 and Fig. 2.6 illustrate the temperature-volume, *T*-*v* and pressure-volume diagrams, *p*-*v* for water, showing liquid and vapour phases.

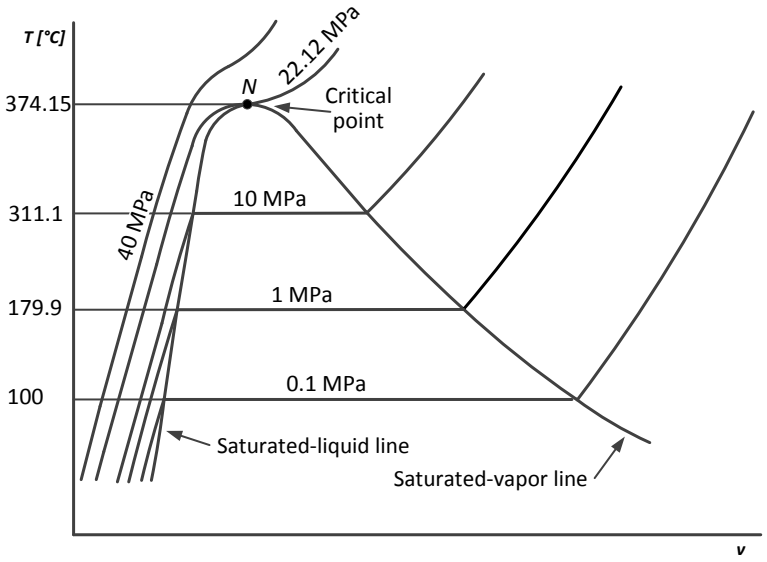

FIGURE 2.5 *T*-*v* diagram for water [Kiameh, 2002]

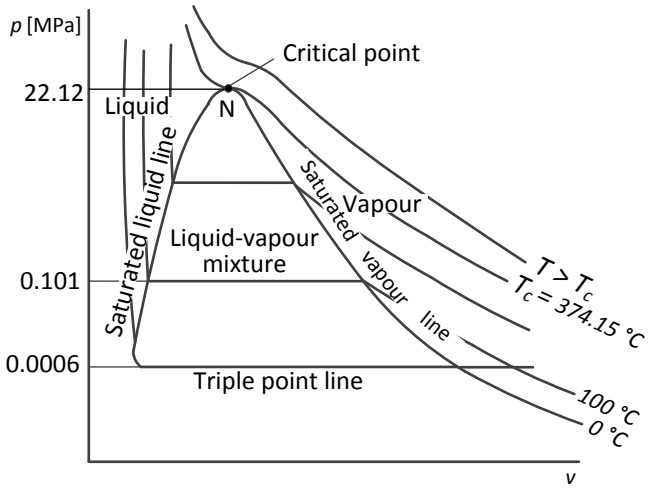

FIGURE 2.6 *p*-*v* diagram for water [Rogers and Mayhew, 1992]

For pressure values above atmospheric pressure (0.1 MPa), the change of volume following the evaporation of the liquid reduces considerably, in such a way that for a specific high pressure, the change of volume is zero, and the isobar line is reduced to a point of inflexion. This is named the *critical point* (CP) and the state properties for water, namely the critical pressure p_c, critical temperature T_c, and critical volume v_c, have the following values [Rogers and Mayhew, 1992]:

$$p_c = 22.12 \text{ MPa}, T_c = 374.15 \text{ °C}, v_c = 0.00317 \text{ m}^3/\text{kg}. \quad (2.14)$$

For pressures above critical, there is no definite transition from liquid to vapour and the two phases cannot be distinguished visually. As a liquid is heated, its density decreases while the pressure and density of the vapour being formed increases. As temperature and pressure increase, the liquid and vapour densities become closer and closer to each other until they are the same. At that point, the CP, the two densities are equal and the liquid becomes a supercritical fluid. Above the CP, the fluid changes volume continuously with the change of pressure.

Diagram *p-T* from Fig. 2.7 gives a spatial representation of the domains of existence for each of the phases of water: ice, liquid and vapour. Along the continuous lines, the two phases existing on each side coexist in thermodynamic equilibrium. From the CP onwards, there is no distinction between liquid and vapour.

If the state values for pressure and temperature follow the curve p-q-r from Fig. 2.7, the phase changes continuously, but at no point there is coexistence between liquid and vapour. The phase is either liquid, supercritical fluid or vapour.

For descriptive purposes, the area above CP, is divided into supercritical liquid ($p>p_c$, $T<T_c$), supercritical vapour ($p<p_c$, $T>T_c$) and supercritical fluid ($p>p_c$, $T>T_c$). However there is no discontinuity in the change of phase between any two domains.

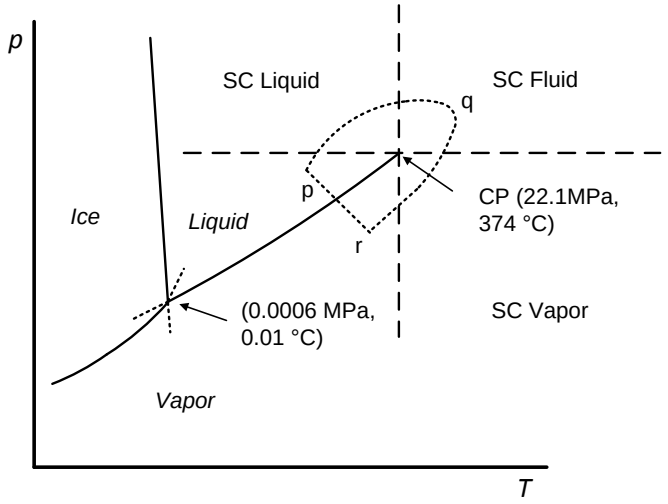

FIGURE 2.7 *p-T* diagram showing phase equilibrium lines, the CP and the domains of the supercritical phases [Ganguly, 2008]

2.1.4 Operation of a typical pulverized coal-fired power plant

Fig. 2.8 illustrates the typical structure of a pulverized coal-fired power plant.

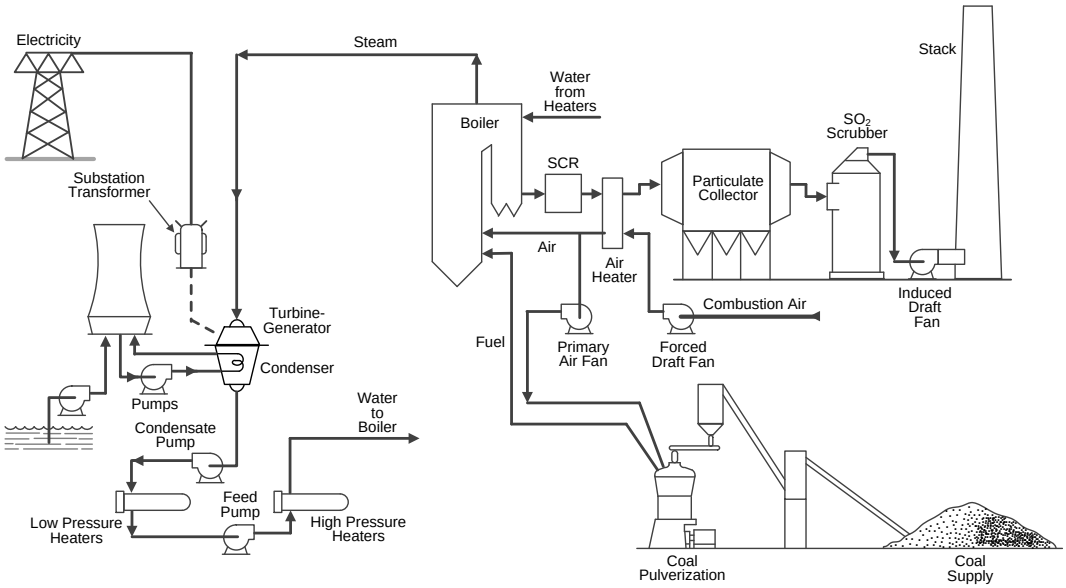

FIGURE 2.8 Schematic of a typical pulverized coal-fired power plant [Kitto and Stultz, 2005].

The structure of a power plant is composed by the following major subsystems:

- coal storage and preparation;
- boiler and combustion;
- environmental protection;
- turbine-generator unit;
- condenser and feedwater system;
- cooling tower.

The coal stored in the bunkers is sent at a controlled rate to the mills, where it is pulverized and passed afterwards to the burners. The forced draft fans draw warm air

from the top of the boiler house, which then picks up more heat in the air heater. Part of this air flow called secondary air, around 80%, is fed to the burners, while the rest 20%, called primary air, is used to transport the pulverized coal from mills to the burners. The heat generated in the combustion process is used in the boiler to generate steam at the required temperature and pressure. In its way out, part of the heat from the combustion gas (flue gas) is recovered in the air heater. The flue gas enters the selective catalytic reduction system (SCR), the particulate collector, the sulfur dioxide (SO_2) scrubbing system, where acid gases are removed and afterwards the resulting cleaned flue gas is sent to the stack by an induced draft fan.

The steam from the boiler, under the controlled values of pressure and temperature, flows into the turbine, which in turn drives a generator. Most part of the electricity produced by the generator is sent to the grid, after its voltage was stepped up by the transformer. A small portion of the generated electricity is used by the power plant internal consumers.

From the turbine, the steam is directed to the condenser, where it is condensed back to water by transferring its remaining heat to the coolant. The cooled water, called feedwater, is then passed through a series of heat exchangers and pumps, which will increase its temperature and pressure before is returned to the boiler. The heat absorbed by the coolant (water) in the condenser is then released in the atmosphere by means of a cooling tower.

2.2 Supercritical power plant

In a subcritical power plant the steam generated in the boiler has its temperature and pressure values situated bellow the ones of the CP (22.12 MPa, 374.15 °C). The main structural particularity of a subcritical boiler is the existence of a drum. This component has the role to separate the saturated steam from the steam-water mixture, which leaves the walls of the furnace and has also the role to supply feedwater to the walls of the furnace, such that they do not overheat. A typical subcritical coal fired power plant can achieve an efficiency between 33-35% [Kitto and Stultz, 2005].

The efficiency of the thermodynamic cycle can be improved, if the mean temperature characterising the heat added in the process is increased. In the Rankine cycle, the saturation temperature is related to the feedwater pressure, which means that in order to increase the temperature, the pressure has to be increased as well. If the pressure is increased above CP (22.12 MPa), the resultant thermodynamic cycle is called supercritical steam cycle. The cycle was first proposed in 1920s and was originally given the name Benson Super Pressure Plant [Kitto and Stultz, 2005].

The first supercritical unit started its service in 1957 and continued until 1979. The unit installed at Philo Plant, had a power output of 125 MW and operated at a pressure of 31 MPa and a temperature of 621°C [Smith, 1998].

Supercritical boilers are also called once-through boilers, as the feedwater passes just one time through the boiler in each steam cycle. For pressure values above the CP, the resulting fluid can be treated as a single phase, as it changes from the liquid phase to the vapour phase without an interface. As a consequence, the separation between

water and steam, usually done by the drum is no longer needed. This structural difference between a subcritical and a supercritical boiler is illustrated in Fig. 2.9.

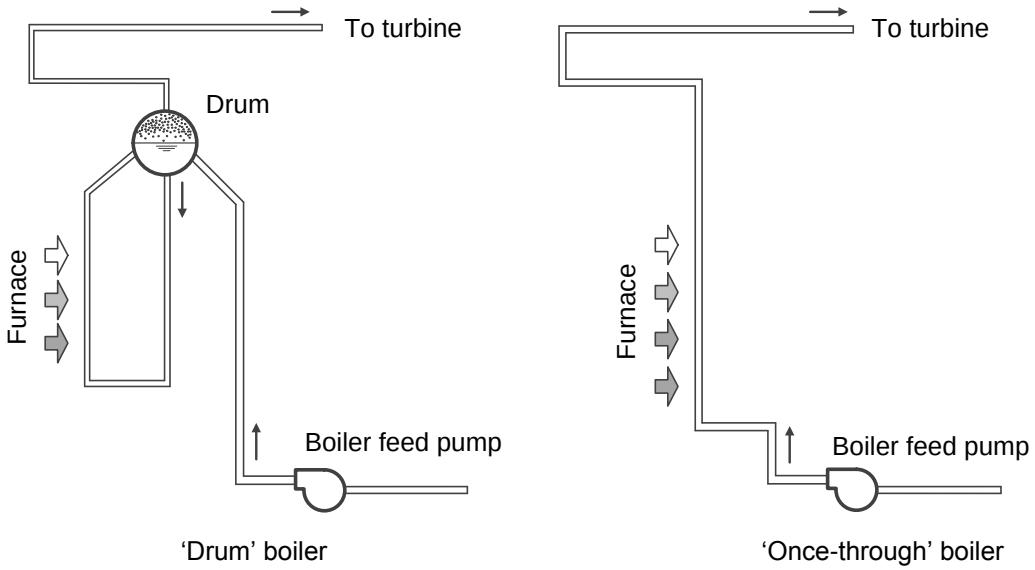

FIGURE 2.9 Steam-water circulation in a subcritical/supercritical boiler [Flynn, 2003]

The efficiency of a supercritical coal fired power plant can reach 46% [Wang, 2009].

2.2.1 Typical supercritical steam cycle

A steam cycle for a typical supercritical power plant is shown in a *T-s* diagram in Fig. 2.10. The water leaving the condensate pump at point *a* increases its temperature up to point *b* by passing through the low pressure heater and adding in its way the heat transferred by the steam extracted from turbines. Point *b* corresponds to the input of the high pressure feedwater pump. The feedwater pressure is increased by the pump up to a value of 28.96 MPa, represented as point *c* in the diagram. Between points *c* and *d* more heat is added to the feedwater on its way through the heat

exchangers, which are supplied with steam extracted from high and low pressure turbines. At point *d* the feedwater has the right temperature and pressure, before entering the evaporation section of the boiler. The heat provided by the combustion process in the furnace is added to the fluid and when it reaches point *e*, corresponding to the boiler outlet and high pressure turbine inlet, the supercritical steam has a pressure of 24.1 MPa and a temperature of 566 °C. The steam expands in the turbine up to point *f*, which corresponds to the superheated steam phase. It is then reheated in the boiler up to a temperature of 560 °C and having a pressure of 3.7 MPa, enters the low pressure turbine at point *g*. It expands in the turbine from point *g* to point *h*. The mixture of steam and water from point *h*, enters the condenser where it is transformed in a slightly subcooled liquid. The liquid is then recirculated by the condensate pump up to point *a*, which corresponds to the inlet of the low pressure heater. In this way the cycle is completed.

In order to achieve the required high pressure values for the feedwater, the power needed to drive the feedwater pump is increased to 3% of the turbine output in a supercritical cycle, compared to 2% in a typical saturated Rankine cycle with a steam pressure of 16.55 MPa [Kitto and Stultz, 2005].

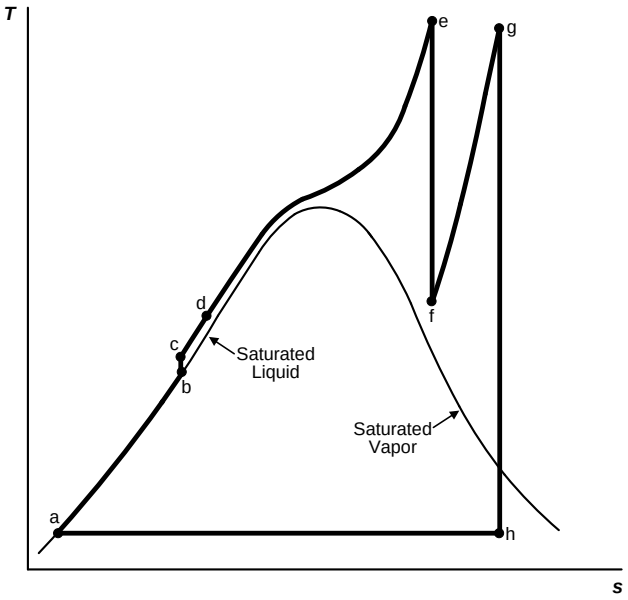

FIGURE 2.10 Steam cycle for a typical supercritical power plant [Kitto and Stultz, 2005]

2.3 Summary

The chapter gives a presentation over the structure and operation of a steam power plant, with an emphasis on supercritical coal-fired power plant.

In the first part, the basic thermodynamic cycles Rankine and Reheat, which govern the operation of a steam power plant, are described by following the evolution of the working fluid along the main points of the cycles illustrated in *T-s* and *p-V* diagrams. The thermodynamic properties of water are detailed, with an accent on its behaviour for parameters situated above the CP. The first part ends with the description of a typical pulverized coal-fired power plant, its structure being illustrated by a schematic diagram. The pathways for water, steam, coal and flue gases are followed along the operation of the power plant.

The second part focuses on supercritical coal-fired power plant. A short history of its development is given and it is explained what defines a supercritical power plant and also why the term of once-through boiler is associated with it. The absence of the drum, as the major structural difference between a subcritical and supercritical power plant is illustrated by a schematic diagram and the advantages and disadvantages of using pulverized coal as fuel are given. The increased net efficiency places the supercritical plant above the subcritical one. Using the steam cycle for a typical supercritical power plant, the main working points are followed along the cycle path, underlining the values of the parameters for the water/steam (pressure and temperature) and showing in what section of the plant the process is taking place.

Chapter 3

Power System Frequency Control and Grid Code

3.1 Introduction

The frequency of AC power is associated with the rotation speed of the synchronized generators at the power plant. Its value is kept constant as long as the generated active power is balanced simultaneously with the electrical energy usage/consumption. Power demand in a power system is constantly changing. Figure 3.1 illustrates the daily power demand curves in a power system for different seasons: summer and winter. The task of matching power generation with power demand is challenging, since the latter is constantly changing and an exact balance can only be maintained for a short period of time.

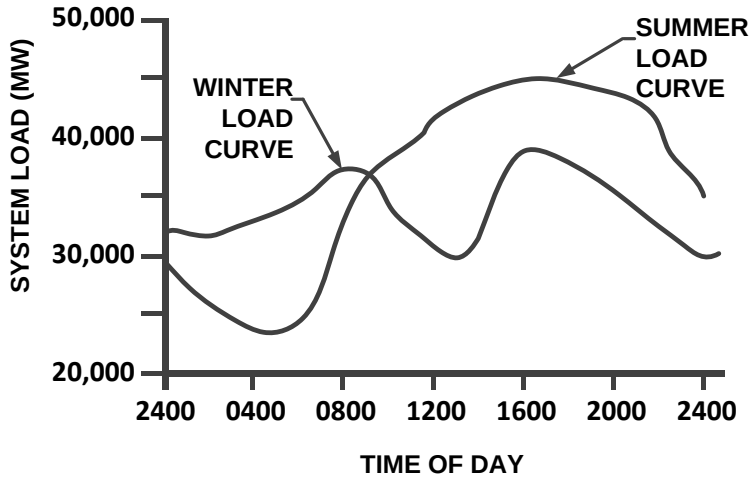

FIGURE 3.1 Daily power demand curves for summer and winter [Bucciero and Terbrueggen, 1998]

If the balance between power generation and power demand is lost, a power deviation occurs, which will cause a frequency deviation from its set-point value. When the load demand increases and the generation unit cannot respond simultaneously, the system frequency might drop and when the load demand decreases, the system frequency might increase accordingly.

The level of the power imbalance and the capacity size of the power system determine the dimension and the speed of the frequency deviation. This deviation will be initially offset by the rotating masses of the generators and the rotating machines connected to the system. Power system inertia represents the resistance which the masses of the generators and the rotating machines synchronized to the system oppose to a change in system frequency. For large interconnected power systems, frequency is easier to retain than in reduced size ones. This is due to the higher inertia of the systems, which results in a relatively slow rate of change of frequency.

The consequences of the frequency deviations from the operating value of the power system frequency can have varied effects and also different degrees of importance. Small frequency deviations do not have a serious impact on the operation of the power system, while large frequency deviations can pose serious threat to its security and reliability. The effects of a generating plant outage, transmission line trip or loss of large load block can generate large frequency deviations, which can drag the power system into instability. If this instability is not addressed properly, it can lead to a total outage (blackout).

The power system frequency is maintained between its operating limits first by the low level control hierarchy in the power plants, which is represented by the speed governor control system and second by the high level supervisory control system.

3.2 Frequency control at the power plant

A governor control system is used to control the shaft speed of an electric generator. The speed deviations of the shaft are monitored by the governor and it adjusts the mechanical power delivered to the generator, in such a way as to increase or decrease the generator's speed.

In case of a steam turbine, the mechanical power input is controlled by the opening or closing of the valves regulating the steam flow into the turbine.

For the description of the governor operation the simple diagram of the turbine-generator system from Fig. 3.2 is used.

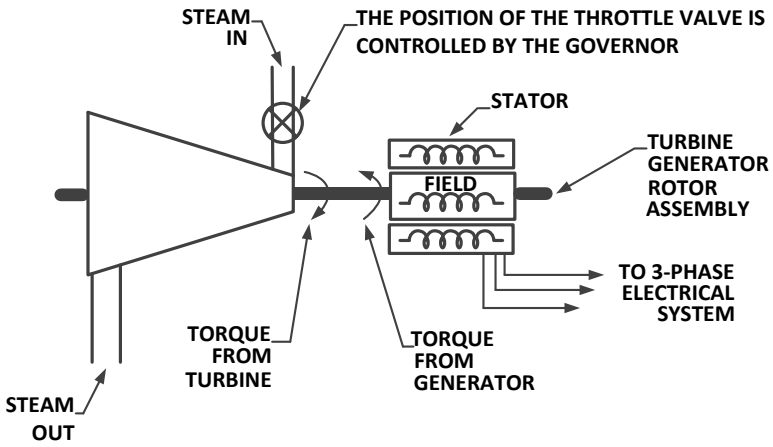

FIGURE 3.2 Simple diagram of turbine-generator system [Bucciero and Terbrueggen, 1998]

Consider that the turbine-generator system from Figure 3.2 undergoes a large increase in the load demand. The counter torque of the generator is higher than the mechanical torque produced by the turbine. Because of this imbalance the generator shaft speed starts to decrease. The governor senses this speed deviation and sends the signal to open the steam valve for the turbine. In this way the steam flow to the turbine is increased and this added rotational energy will increase the shaft speed. The process will continue until the desired shaft speed is reached.

3.2.1 Governor Droop Characteristics

The capability of a generator to handle a full-load rejection due to an electrical fault in the system, to contribute to the frequency regulation and to work in parallel with other generators is only possible if it operates with a speed-droop characteristic.

The speed-droop characteristic represents the expected response of a generator's power output to changes in system frequency. This is the main characteristic of a governing system and an illustration of this characteristic is given in Fig. 3.3.

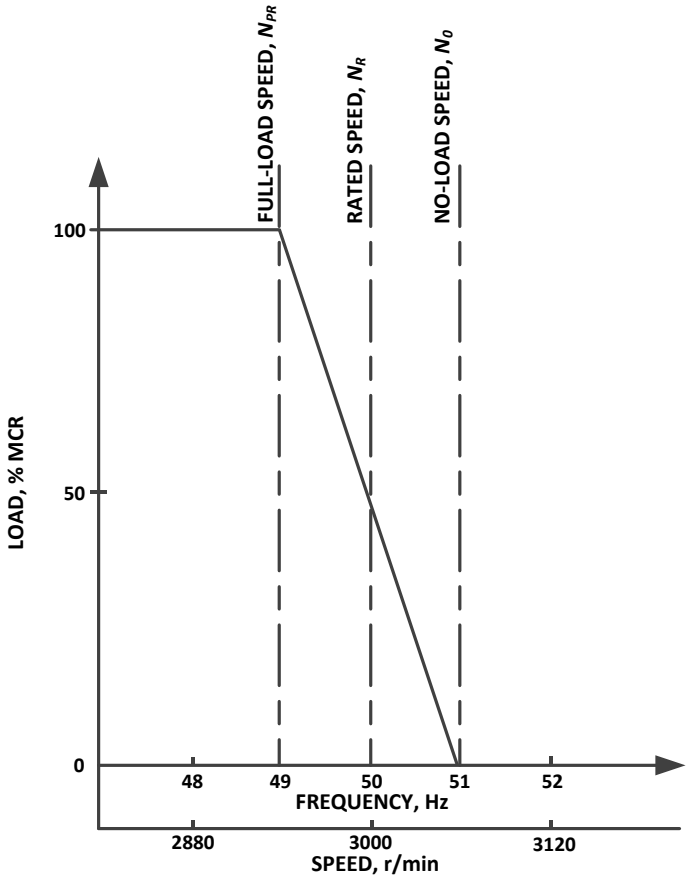

FIGURE 3.3 Governor speed droop characteristic [Kiameh, 2002]

The formula defining the speed droop has the following expression [Kiameh, 2002]:

$$R = \frac{\mathrm{N_0} - \mathrm{N_{PR}}}{\mathrm{N_R}} \times 100\% \tag{3.1}$$

where $\mathrm{N_R}$ – rated speed

$\mathrm{N_{PR}}$ – speed at full load

$\mathrm{N_0}$ – speed at no load

A generator operating with a speed droop can share load with other generators in the system and its power output can be adjusted according to the operator's command. A

better illustration for how changes of the speed set-point affect the power output is given in Fig. 3.4.

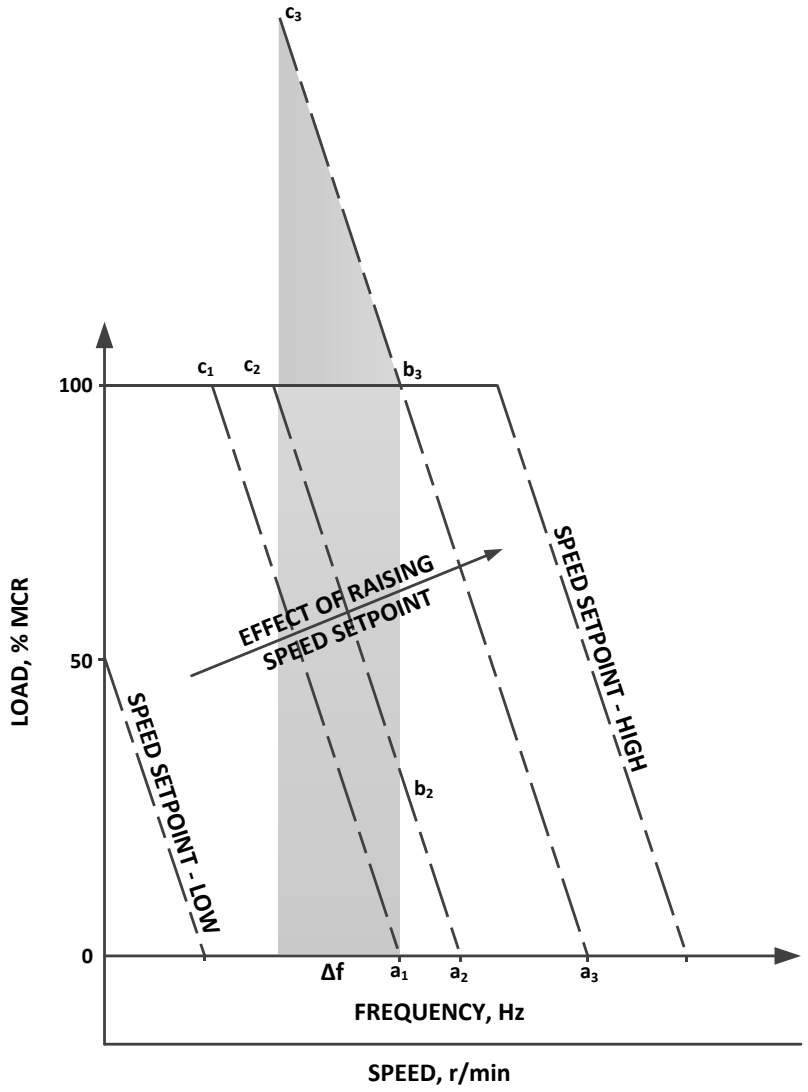

FIGURE 3.4 The effect of changes in the speed set-points on the power output of the generator [Kiameh, 2002]

For a generator which is not connected to the power system, a change in the no load speed set-point from a_1 to a_3 will generate an increase in the frequency from a_1 to a_3. If the generator is synchronized to a power system operating at the scheduled

frequency a_1, a change in no load speed set-point from a_1 to a_2 and then a_3 will increase the power output to b_2 and then b_3. The generator operates with speed a_1 at no load and with speed a_3 at full load. The values used by the industry for the speed droop range between 3% and 7%.

The phenomenon of *overwound* speed set-point is also illustrated in Fig. 3.4. If the generator is operating at full load at a frequency f following the a_3b_3 speed droop characteristic then a decrease in the system's frequency should move the operating point of the generator to c_3. Since the turbine is already operating at full power, the power output will not increase beyond b_3. In this case the speed set-point is called *overwound*. In this situation the generator is unable to reduce its power output immediately. In order to do this the speed set-point needs to be lowered to the line given by c_2a_2.

3.3 Frequency regulations defined by grid codes

To ensure the power network's operation stability and reliability, a set of technical specifications are defined to specify the technical parameters/boundary requirements, that power generation plants must meet; this is normally named Grid Code. Grid Code varies from country to country.

This section provides an overview and a comparison for the current frequency control practices across several European (Great Britain, Northern Ireland, Ireland, France, Italy, Austria, Romania, Poland) and non-European (Australia, China) countries at the end of which a clearer picture of the present Grid Code specifications can be drawn across different regions worldwide.

Each country adopts a standardized frequency value called nominal frequency. This value represents a technical and economic compromise for the design and operating characteristics of the main components in the power system. The standardized values of the nominal frequency are 50 Hz in Europe and most of the Asian countries and 60 Hz for the majority of the American continent.

To maintain power system frequency, a certain amount of active power is kept to be available especially for this purpose. In case of a frequency disturbance, the deployment of the active power is required to restore the balance between generation and demand which is usually done in three stages [UCTE, 2004]. The names given to these stages may differ from one country to another. The chapter adopts the terms and definitions used in the Union for the Coordination of Transmission of Electricity (UCTE) interconnected system. The three frequency control stages in UCTE are: primary control, secondary control and tertiary control, which is depicted by the diagram in Fig. 3.5.

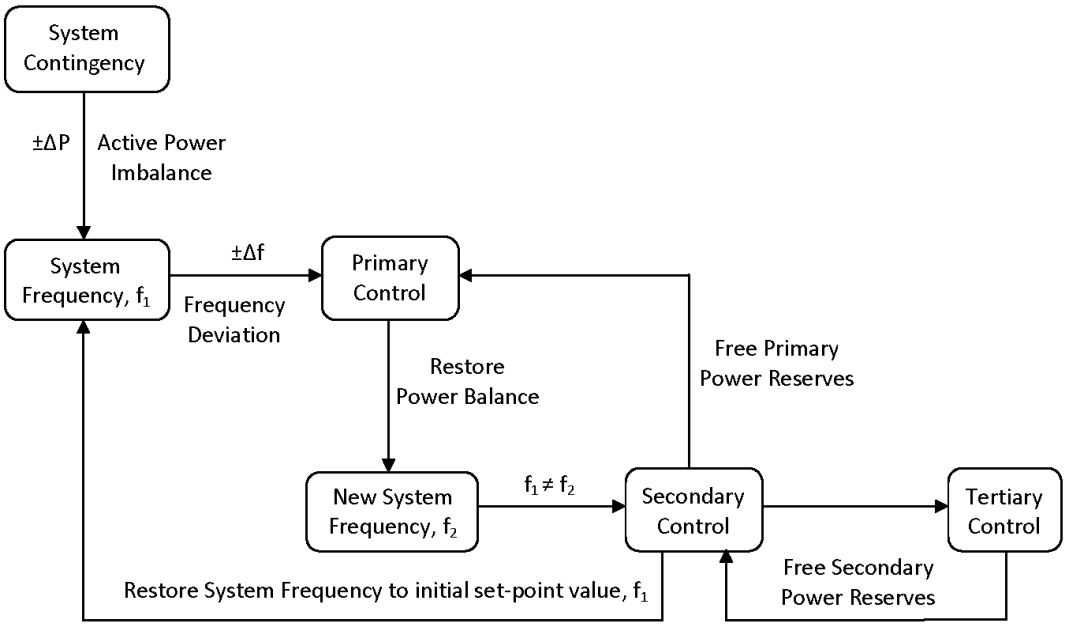

FIGURE 3.5 Frequency control stages in a power system [UCTE, 2004]

Primary control is performed as soon as a frequency deviation occurs. The controllers for generators involved in primary control, will take actions within a few seconds after the occurrence of the contingency by modifying the power delivered into the grid. The actions will continue until the balance between generation and demand is re-established. As a result of the re-established balance, the frequency will be stabilised at a quasi-steady-state value, which is different from the frequency set-point value existing in the grid before the contingency took place. This is due to the speed droops of the generators which set out their contribution for the correction of the disturbance. As a result, the power exchanges between interconnected power systems will differ from the initially agreed values.

Secondary control is a centralised automatic control and has the purpose to restore the power exchanges between power systems to their planned values and also to restore the frequency to its initial set-point value. In this way, the primary control power reserve will be available again. Secondary control will be performed only by those generators designated for this action. The controllers of the generators involved in secondary control need to be set such that, only the controller in the area affected by the contingency will respond and initiate the deployment of the necessary active power secondary reserve.

Tertiary control is defined as an automatic or manual change in the operating points of the generators in order to restore the secondary control reserves when it is needed. Tertiary control will operate in succession as an addition to the secondary control and has the same effect on the power system responses as secondary control does.

Figure 3.6 presents the evolution through time of the frequency in a power system which suffers from a serious contingency, such as the disconnection from the grid of a large power plant. From the figure, the activation of the three frequency control measures can be observed, which are described in the above paragraphs and how they contribute towards frequency regulation.

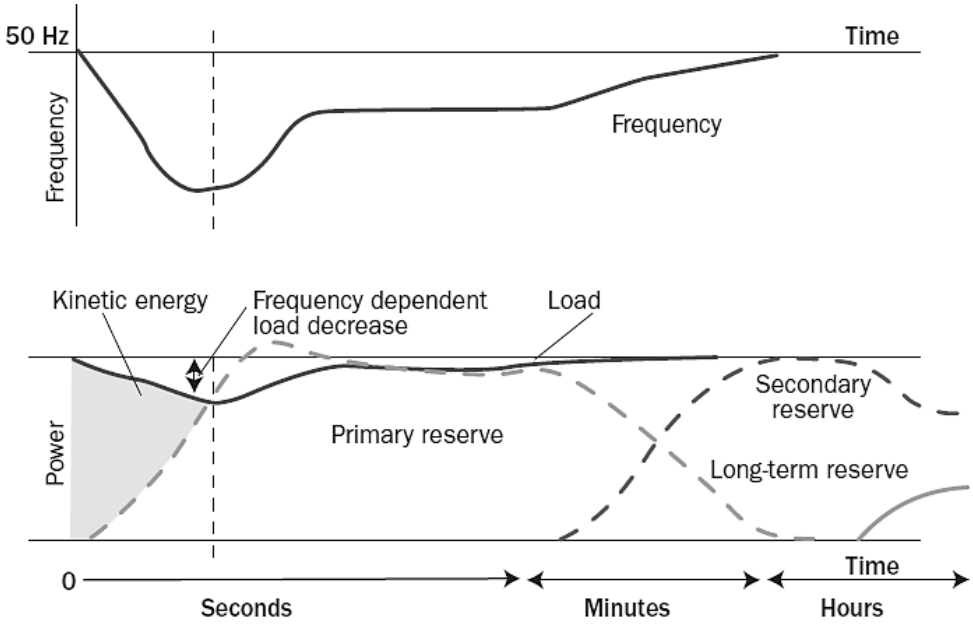

FIGURE 3.6 Frequency evolution through time, after the disconnection of a large power plant and the activation of power reserves [EWEA, December 2005]

The Grid Code normally specifies the particular figures for those responses and set the limits for the variations. As results from the national grid codes, the nominal frequency for all the national power systems analysed here is 50 Hz. Having the same nominal frequency represents a mandatory condition for the interconnected countries like France, Italy, Austria, Romania and Poland, which are members of UCTE, allowing the power exchanges between them and keeping national power systems more secure and stable against different contingencies.

During normal operation, the frequency is allowed to vary between a restricted interval, which has been defined by every Transmission System Operator (TSO). These intervals for allowed variations are shown in Table 3.1 [National Grid Electricity Transmission plc, 2010; System Operator for Northern Ireland, 2011; EirGrid, 2009; Réseau de Transport d'électricité, 2009; Terna, 2011; Energie -

Control Austria, 2008; CN Transelectrica SA, 2004; AEMC, 2001; National Development and Reform Commission, 2007; PSE Operator S.A., 2006].

TABLE 3.1 Normal operation frequency variation interval

Country	**Frequency variation interval**
	[Hz]
Great Britain	49.5 - 50.5
Northern Ireland	49.5 - 50.5
Ireland	49.8 - 50.2
France	49.5 - 50.5
Italy	49.9 - 50.1 49.5 - 50.5(1)
Austria	49.5 - 50.5
Romania	49.5 - 50.5
Poland	49.5 - 50.5
Australia	49.75 - 50.25
China	49.8 - 50.2

(1) Sicily and Sardinia

In the case of a serious contingency event, frequency will deviate considerably over the range of the normal operating conditions. The highest and the lowest limit allowed for the frequency to vary are presented in Table 3.2 [National Grid Electricity Transmission plc, 2010; System Operator for Northern Ireland, 2011; EirGrid, 2009; Réseau de Transport d'électricité, 2009; Terna, 2011; Energie - Control Austria, 2008; CN Transelectrica SA, 2004; AEMC, 2001; National Development and Reform Commission, 2007; PSE Operator S.A., 2006].

TABLE 3.2 Critical situations frequency variation interval

Country	**Frequency variation interval**
	[Hz]
Great Britain	47.0 - 52.0
Northern Ireland	47.0 - 52.0
Ireland	47.0 - 52.0
France	47.0 - 52.0
Italy	47.5 - 51.5
Austria	47.5 - 51.5
Romania	47.0 - 52.0
Poland	47.0 - 52.0
Australia	47.0 - 52.0 47.0 - 55(1)
China	48.0 - 51.0

(1) Tasmania

As observed from the tables above, the limits of frequency variations for normal/extreme operation are similar for the majority of the power systems analysed. During normal operation, a frequency deviation of ±0.5 Hz from the nominal value of 50 Hz is allowed in the majority of cases. The exceptions are Ireland, Italy, Australia and China, where the interval of allowed frequency variation for normal operation is smaller, which may be justified by power quality or interconnection problems that may arise.

In the case of serious contingencies, the frequency variation interval is usually 47.0 - 52.0 Hz for most power systems analysed in the paper. But Italy, Austria, Australia and China have different specified ranges. The smaller frequency variation interval is

motivated by the small value of the power system inertia, which means that in case of a contingency the rate of change for the frequency is high and the frequency will decrease fast. If this value is too low, the low frequency protection relays will disconnect the generators from the grid. Tasmania has a broader interval for allowed frequency variation in the case of extreme operation conditions and this is owed to the smaller size of the Tasmanian power system and its predominantly hydro-power nature. The smaller size of the power system results in a small value of the power system inertia and also the use of hydro power plants for primary frequency control, allow a considerable frequency decay before the system is brought back to the steady-state frequency.

The strategies adopted for frequency control for the power systems analyzed are summarized in Table 3.3 [National Grid Electricity Transmission plc, 2010; System Operator for Northern Ireland, 2011; EirGrid, 2009; Réseau de Transport d'électricité, 2009; Terna, 2011; Energie - Control Austria, 2008; CN Transelectrica SA, 2004; AEMO, 2010; National Development and Reform Commission, 2007; PSE Operator S.A., 2006].

As can be seen from Table 3.3 presented below, different strategies/regulations/specifications for frequency control are applied. Although the definitions may vary, it can be observed that there are generally three levels of control to maintain the balance between generation vs. load demand: primary, secondary and tertiary frequency control. As primary frequency control is the first

action taken in the case of a serious frequency deviation happening, a brief analysis based on the data given in Table 3.3 is described below.

TABLE 3.3 Frequency control strategies as implemented by each country

Country	Type of frequency control strategy		Response time
Great Britain	Primary Frequency Response		active power increase within ***10 s*** and maintained for another ***30 s***
	Seconday Frequency Response		active power increase within ***30 s*** and maintained for another ***30 min***
	High Frequency Response		active power decrease within ***10 s*** and maintained ***thereafter***
Northern Ireland & Ireland	Operating Reserve	Primary Operating Reserve	active power increase within ***5 s*** and maintained for another ***15 s***
		Secondary Operating Reserve	active power increase within ***15 s*** and maintained for another ***90 s***
		Tertiary Operating Reserve band 1	active power increase within ***90 s*** and maintained for another ***5 min***
		Tertiary Operating Reserve band 2	active power increase within ***5 min*** and maintained for another ***20 min***
France, Italy, Austria, Romania, Poland (UCTE members)	Primary Control		• 50% of the active power increase within ***15 s***; • 100% of the active power increase within ***30 s***; • 100% of the active power increase supplied for at least ***15 min***. *The quantum of active power required for Primary Control is regulated by the TSO, for each Generating Unit apart.*
	Secondary Control		activated no later than ***30 s*** after the incident and its operation must end within ***15 min*** at the latest
	Tertiary Control		activated during Secondary Control and maintained for no longer than ***15'***.

Country	Type of frequency control strategy	Response time
Australia	**Contingency service**	
	Fast Raise Service	active power increase within ***6 s***
	Fast Lower Service	active power decrease within ***6 s***
	Slow Raise Service	active power increase within ***60 s***
	Slow Lower Service	active power decrease within ***60 s***
	Delayed Raise Service	active power increase within ***5 min.***
	Delayed Lower Service	active power decrease within ***5 min.***
	Regulating service	
	Regulating Raise Service	active power increase needed for ***5 min.*** dispatch interval
	Regulating Lower Service	active power decrease needed for ***5 min.*** dispatch interval
China	Primary Frequency Control	active power increase within ***15 s***
	Secondary Frequency Control	N/A

Primary frequency control, responsible for the increase/decrease of the active power output from the generators, meant to quickly restore the balance between load changes and power output. There are different regulations to specify the allowed time interval taken for stabilizing frequency for each power system analysed here. The shortest time for activation is 5 seconds in Ireland and Northern Ireland and 6 seconds in Australia. This means that in case of a serious contingency, the rate of change of frequency can be high, so if countermeasures are not taken in a short time, frequency can decay to a low value jeopardizing the stability and security of the entire power system.

Being part of an interconnected system with a high inertia, which results in a low rate of change of frequency in case of a serious contingency, the UCTE members have

much slower activation times for primary frequency control: 15 seconds for 50% of the active power reserve and 30 seconds for the entire reserve. Given the size of the Chinese power system and the high inertia associated with it, the grid code specifies a time interval of 15 seconds for the generating units to provide the entire active power reserve. Great Britain, which can be considered as an island power system in nature, has also a reduced time of only 10 seconds available for the active power reserve designated for primary frequency control, to be fully activated.

3.4 Summary

This chapter gives an overview of the frequency control strategies and frequency regulations for power system operation.

The importance of having a constant frequency in the power system is given and the consequences resulting for the cases when the frequency deviations are out of their normal operation boundaries are presented as well. Frequency emerges as an indicator of the system's stability, providing information about system generation and load imbalance.

Frequency control strategies are divided into local control at the power plant level and into supervisory control at the power system level. The local control is ensured by the speed governor control system, while the response of the generator to a frequency deviation depends on its speed-droop characteristic.

All the participants in the power system operation must comply with the rules defined in a national document entitled Grid Code. Frequency regulations are also stipulated in it. As frequency control practices differ from one country to another, a

review of the national Grid Codes for several European countries and two non-European ones has been made. The results from this review are presented in a tabulated format. The differences between the normal frequency variation interval and the emergency one are compared and possible reasons for these values are presented. Also the frequency control strategies implemented in each national power system are presented and comments upon their differences are made.

Chapter 4

Simulation Study of Supercritical Power Plant Dynamic Performance

4.1 Supercritical power plant simulator software

The power plant simulator used in this research, was developed by the researchers from Tsinghua University, Beijing, China and is based on more than 20 years of research experience in the field of thermodynamic simulations of steam power plant process. This section makes an introduction to the software using the information made available by Institute of Thermal Dynamic Simulation and Control - Tsinghua University [2012].

4.1.1 Description of the operational power plant

The mathematical model used behind the simulator software was developed by using the technical parameters and sets of operational data obtained from field tests of a supercritical coal-fired power plant in China.

The power plant has a nominal power output of 600 MW and the diagram from Fig. 4.1 presents its structure and the main paths used by the water and steam flows.

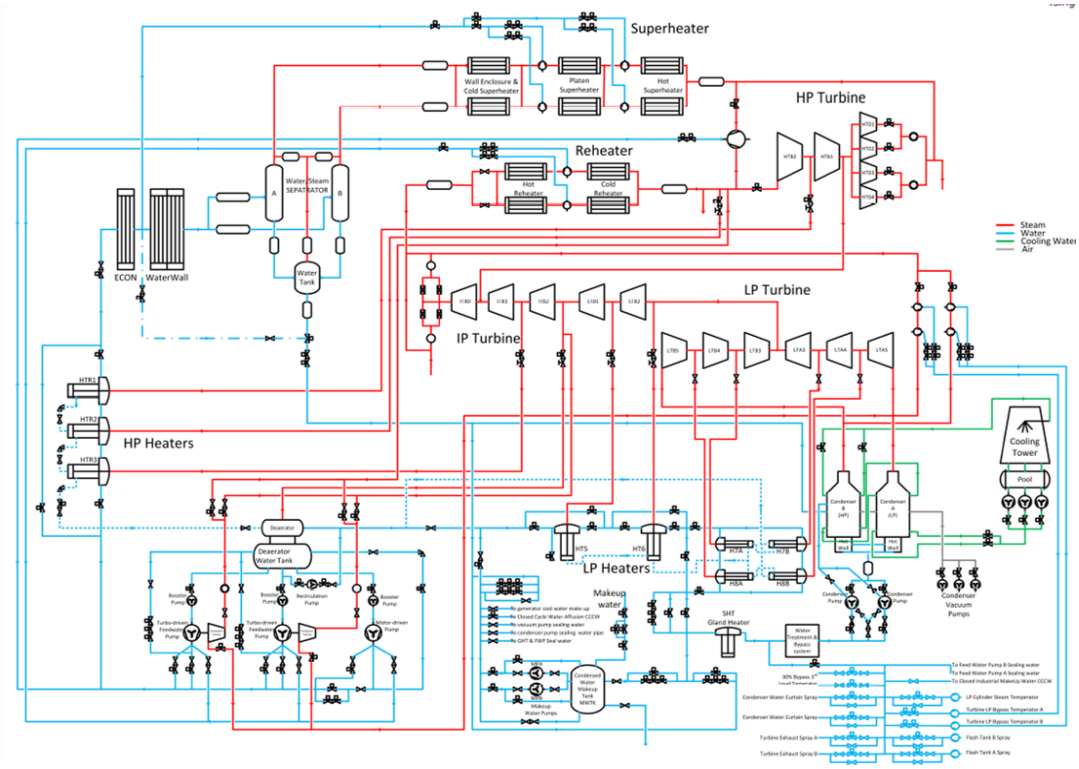

FIGURE 4.1 Schematic diagram of the operational power plant [Institute of Thermal Dynamic Simulation and Control - Tsinghua University, 2012]

4.1.2 Structure of the simulator software

All the components of the power plant mathematical model and the control loops have been converted into source code files by using FORTRAN 95 programming language. The mathematical models have been derived and refined by the researchers from Tsinghua University, who used appropriate sets of operational data for models parameters identification.

The software platform used to compile, generate the executable files and run the simulations is SimuEngine. SimuEngine is a visual simulation support system between simulation systems and computer operating systems, which can run on a PC

using a Windows operating system. It provides real-time network database and complete simulation running support functions, data visualisation, online testing, collaborative development, multitask parallel running, multiple processes and distributed simulation and other functions.

The supervisory control system installed in the real power plant, namely the Distributed Control System was also modelled and implemented in the simulator. The control system can be communicated through the Boiler Menu and the Turbine Menu and the menus lead to the process diagrams depicting the main components of the power plant and the network of pipes connecting them can be accessed. In each process diagram, parameters like temperature, pressure, flow rate of the fluid can be monitored at different points and the status of the flow control devices, like valves, can be observed and manually changed if required. The overall operation of the power plant and the decision of the level of power generation and the selection of the control system can be done by accessing the screen entitled Load Control Centre. Some screenshots of the Distributed Control System are illustrated in Fig 4.2.

All the processes undergoing in the real power plant, starting from fuel processing and to the electricity generation are modelled in the power plant simulator. The values of the key operating parameters of the simulator for the power plant running at rated load are described in Table 4.1. The simulator was designed to run with a steady-state error of less than ±1% for key parameters and an error of less than ±5% for power plant dynamic response.

FIGURE 4.2 Illustration of the Distributed Control System

TABLE 4.1 Power plant simulator specifications

Name	Value	Unit
Generated power	600	MW
Fuel flow	276	t/h
Water flow	1913	t/h
Main steam pressure	25.4	MPa
Reheat steam pressure	4.16	MPa
Main steam temperature	571	°C
Reheat steam temperature	569	°C
Load ramping	72	MW/min
Pressure rate of change	0.3	MPa/min
Governor droop	5	%

4.1.3 Calculation of a fluid network model

A power plant model can be considered as being composed of the models for different components and a network of different fluid flows connecting these components in between. The fluids circulating through this network can be incompressible, like water and compressible, like air, combustion gases and steam.

The complex fluid network of the power plant can be divided into small networks formed of nodes and branches. After the calculation of pressures and flow rates for these small networks is conducted, connecting them together will provide the pressures and the flow rates for the entire fluid network of the power plant.

The method used in this software to calculate the pressure and flow rate values is the Node Pressure Method and makes use of the basic relationships, known as Kirchhoff's Laws, applicable to electric circuits but also to fluid networks. Kirchhoff's first law states that the mass flow entering a node equals the mass flow leaving that node. The statement of Kirchhoff's second law is that the algebraic sum of all pressure drops around a closed path in the network must be zero, having taken into account the effects of fans and pumps. A fluid network model consists of models of flow resistance inside pipes, of fans, of pumps, of source nodes and of sink nodes.

4.1.3.1 Flow resistance model

Flow resistance r is defined as:

$$r = \frac{\Delta p}{\dot{m}^2} \tag{4.1}$$

where r is the resistance factor in $[1/(kg \cdot m)]$, Δp is the pressure drop over the pipe resistance in $[Pa]$ and $\dot{m}$ is the mass flow through the pipe resistance in $[kg/s]$.

Equation (4.1) can be further detailed into (4.2) by using the characteristics of the pipe and fluid.

$$r = \frac{\zeta(1 + \mathrm{C_m}\boldsymbol{\mu})}{2\sigma^2 S_0^2 \rho_1} \tag{4.2}$$

The terms used in (4.2) denote the following: ζ is the flow resistance coefficient, $\mathrm{C_m}$ is a constant characterizing the medium, $\boldsymbol{\mu}$ represents the solid phase concentration of gas-solid two phase flow, σ is the compressibility coefficient of the fluid, S_0 is the flow area of the pipe in $[m^2]$, ρ_1 marks the flow density in $[kg/m^3]$. σ is a function of S_0 and $\Delta p/p_1$, with $p_1$being the pipe input pressure and can be considered constant for a small enough pressure ratio, $\Delta p/p_1$.

If the area of the pipe, S_0 and the flow rate are considered constant, the resistance is found to depend only on the fluid temperature at the pipe input, as presented by the formula below,

$$r = r(r_0, T_1) = r_0 \cdot (1 + \frac{T_1}{273}) \tag{4.3}$$

where r_0 is the value of the resistance for a temperature of 0°C and T_1 is the fluid temperature at the pipe input.

4.1.3.2 Valve model

The control of the fluid flow through pipes is achieved by the use of valves. A valve can be considered a resistance in the fluid flow, but for which the changing area of the flow has to be taken into account. Expression (4.3) is still valid for the calculation of the resistance, with the only amendment that now r_0 is no longer constant, but its value depends on the valve opening.

$$r_0 = r_0(l) = \frac{r_{00}}{[l \cdot f(l)]^2} \tag{4.4}$$

where the following notations have been used:

- l is the valve opening, $l \in [0,1]$;
- r_{00} is the resistance for $l = 1$, valve fully open, and temperature 0°C, $[1/(kg \cdot m)]$.
- f is a function depending on the l variable, according to the formula,

$$f(l) = a_2 l^2 + a_1 l + a_0$$

4.1.3.3 Fan and pump model

A pump or a fan can be modelled by its equivalent resistance to which is added the desired outlet pressure.

4.1.3.4 Gravitational potential energy

The difference in height between two points in the fluid flow path, represented by the potential energy, is modeled as a pressure difference expressed by the equation,

$$\mathbf{H_p} = \mathbf{h_p}(\rho_{env} - \rho)g \tag{4.5}$$

where $\mathbf{H_p}$ represents the pressure gain generated by the height difference in $[Pa]$, $\mathbf{h_p}$ is the height difference between flow points in $[m]$, ρ_{env} is the density of the environment in $[kg/m^3]$, ρ represents the fluid density in $[kg/m^3]$ and g symbolises the gravitational acceleration in $[m/s^2]$.

4.1.3.5 Resistance flow equation

The relationship between the fluid flow rate and the pressure difference between two points on a pipe can be described as,

$$\Delta p = r \cdot \dot{m}^2 \tag{4.6}$$

where Δp symbolizes the pressure drop between the two points of the pipe in $[Pa]$, $\dot{m}$ is the flow rate through the pipe in $[kg/s]$ and r is the resistance factor.

4.1.3.6 Source and sink nodes

In the fluid network model there are some branches, where the resistance flow equation cannot be applied for the calculation of the flow rate. It is assumed that one of these branches is connected between a source node and a sink node. The node where fluid flows are entering is considered a source and the node where the fluid flows are leaving is considered a sink.

4.2 Power plant dynamic responses related to GB Grid Code requirements

The main target of this research project is to verify through simulation study the compliance of a coal fired supercritical power plant to GB Grid Code frequency control requirements. The power plant must be able to provide three frequency control services: Primary, Secondary and High Frequency Response. The definition for these services is given below for the case of a frequency ramp of 0.5 Hz over 10s.

The Primary Frequency Response capability of a Generating Unit is defined as the minimum increase in active power provided within 10 s and maintained for another 30 s, as it is illustrated in Fig. 4.3.

The Secondary Frequency Response capability of a Generating Unit is defined as the minimum increase in active power output provided within 30 seconds and maintained for 30 minutes, as it is illustrated in Fig. 4.3.

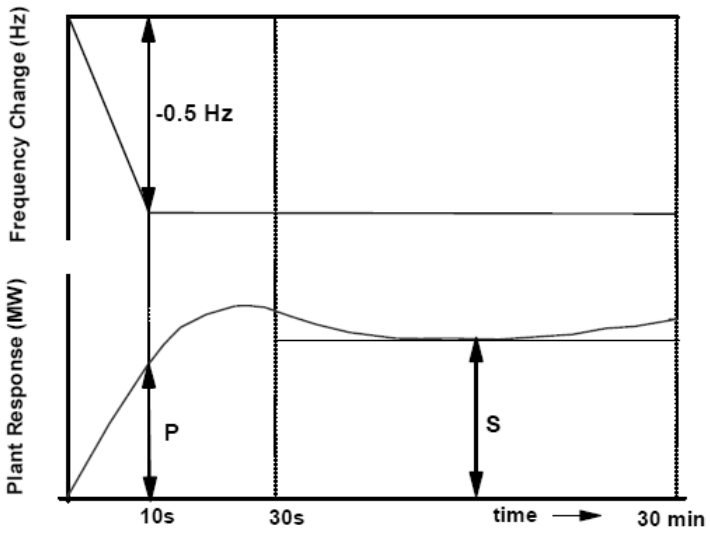

FIGURE 4.3 Interpretation of Primary and Secondary Frequency Response values [National Grid Electricity Transmission plc, 2010]

The High Frequency Response capability of a Generating Unit is the decrease in active power output provided within 10 seconds and maintained thereafter as illustrated in Fig. 4.4.

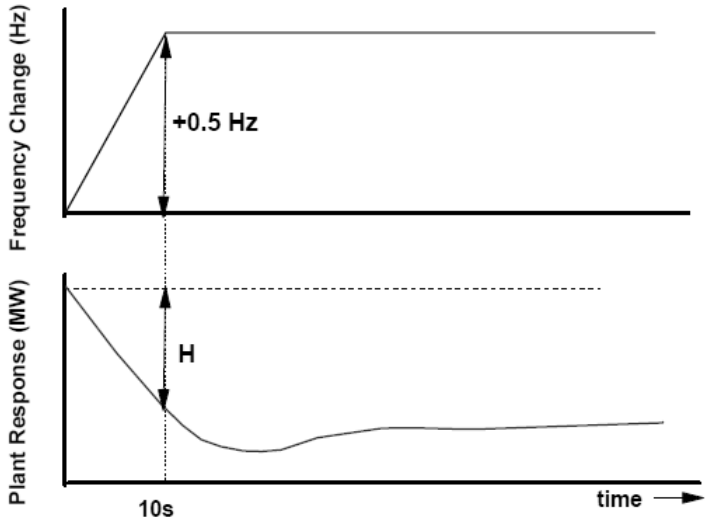

FIGURE 4.4 Interpretation of High Frequency Response values [National Grid Electricity Transmission plc, 2010]

The increase/decrease of the active power output by the power plant is required to be at least to the solid boundaries, as it is shown in Fig. 1.7 (Chapter 1). Considering that the supercritical power plant simulator has a RC of 600 MW, Fig. 1.7 can be converted to Fig. 4.5.

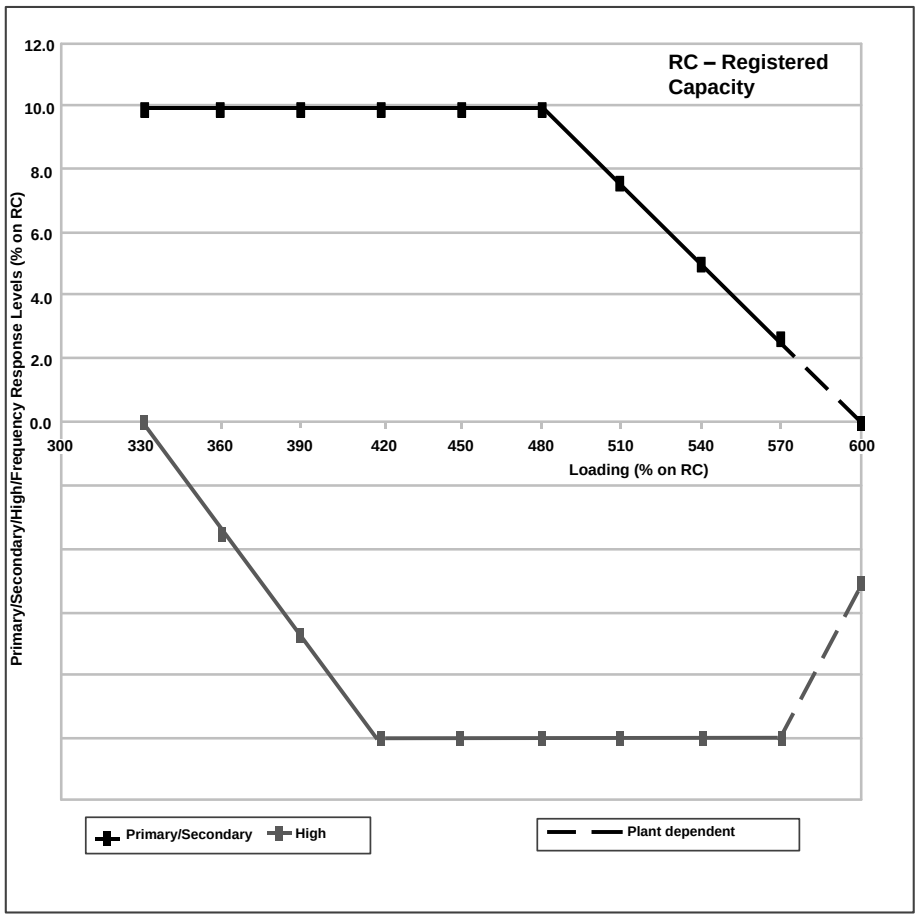

FIGURE 4.5 Minimum frequency response requirement profile for a 0.5 Hz frequency change from target frequency

Among frequency control services, Primary Frequency Response is the most demanding for the power plant generating capabilities and very important for the operation of the power system, as it is the first measure taken in case of a frequency deviation. According to Fig. 4.5, the power plant needs to increase within 10 s its power output with 10% of RC, for operation between 330 MW (55% RC) and 480 MW (80% RC) and then the necessary power increment decreases linearly towards zero for power plant operating at 600 MW (100% RC). For High Frequency Response, the power plant needs to decrease its power output linearly for operation

between 330 MW (55% RC) and 420 MW (70% RC) loading capacity and then a constant 10% RC decrement for loadings between 420 MW (70% RC) and 570 MW (95% RC).

The load ramping capability of a supercritical power plant is between 8-12% RC/min. The power plant simulator has been set to the maximum 12% RC/min. Since the requirement for Primary Frequency Response for most operating loading levels of the power plant is 10% RC within 10 s, it follows that the load ramping should be 60% RC/min. The requirements of the Grid Code expressed in load ramping capability are illustrated in Fig. 4.6.

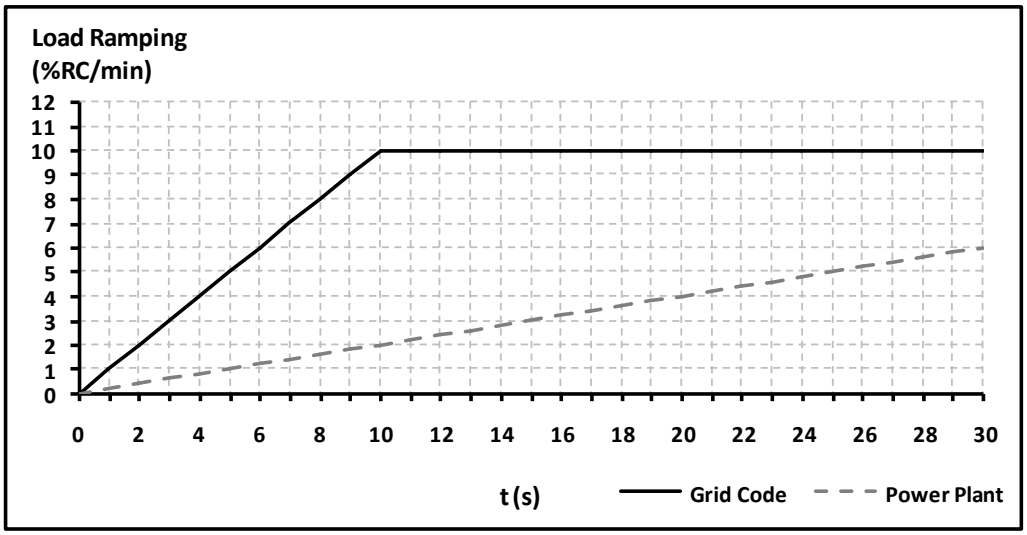

FIGURE 4.6 Load ramping required by Grid Code and power plant capability

It appears from Fig. 4.6 that the Grid Code requirements are too stringent for the supercritical power plant technical capabilities.

The dynamic response of the power plant is very much influenced by the relation existing between the steam pressure set point and the loading of the unit. One way is

to consider the steam pressure set point to have a constant value, regardless of whether the unit is at full load or partial load. This is called fixed pressure control mode and one negative aspect is that it leads to high thermal gradients during steam throttling, between control valve and the first stage of the high pressure (HP) turbine. In the case of the power plant simulator, the pressure set point for this control mode is 25.2 MPa. The second way considers steam pressure set point to be proportional to the load demand. The set point is allowed to slide within a range of admissible values. This is called sliding pressure control mode and it involves having the control valve kept almost entirely open, which minimises the temperature and pressure gradients between control valve and the first stage of HP turbine. The rate of change for steam pressure implemented in the simulator is 0.3 MPa/min. Fig. 4.7 presents the map of the pressure set points for different loading levels together with the fixed pressure set point values, as they are implemented in the power plant simulator.

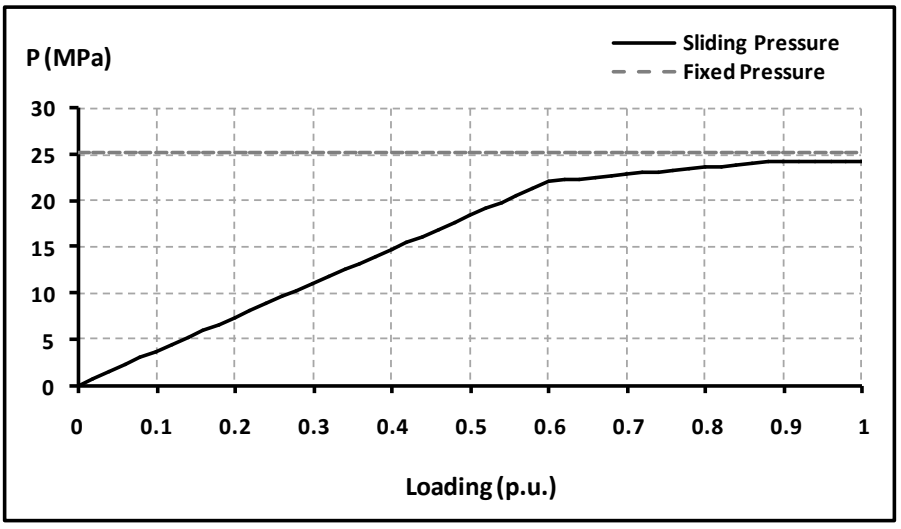

FIGURE 4.7 Steam pressure set point for fixed and sliding pressure control modes

Although beneficial for the service life of the power plant, operating in sliding pressure control mode means a limited ability to use the stored energy of the boiler in meeting the quick changes of the load demand. In this aspect using fixed pressure control mode gives the fastest response time of the power plant needed for Primary Frequency Response service.

4.2.1 Simulation tests for Primary Frequency Response requirements

Using the requirements of Grid Code for Primary Frequency Response regarding the increase in power output by the power plant, several simulations for different operating loading levels were conducted, with steam pressure considered to be in fixed pressure control mode. Having the power plant operating at steady state, a step change was applied to the load demand signal at time t = 60 s. The simulation data was processed in Fig. 4.8 – Fig. 4.12 presented below.

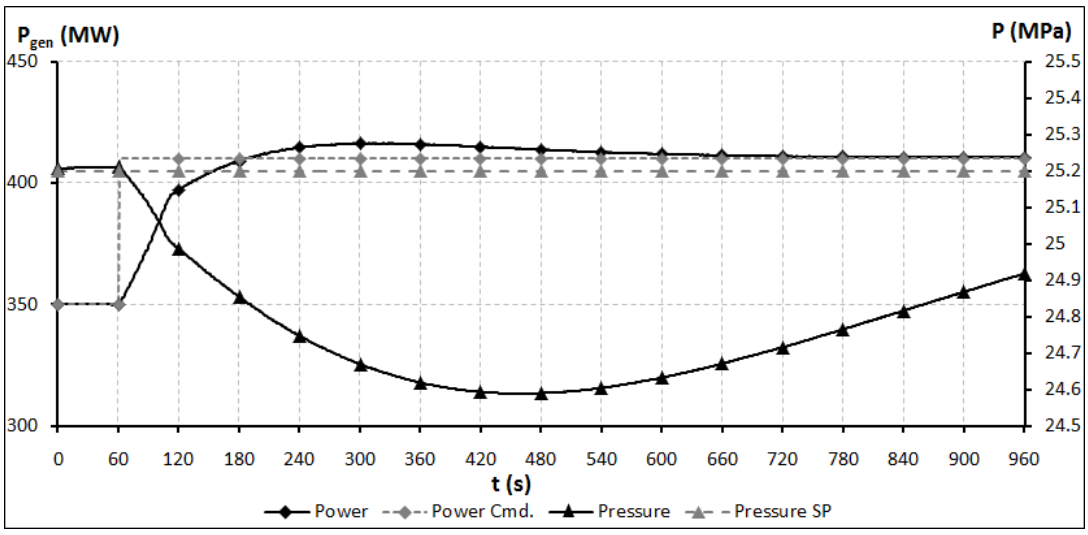

FIGURE 4.8 Power output response and steam pressure evolution for 60 MW load demand step increase from the power plant loading level of 350 MW

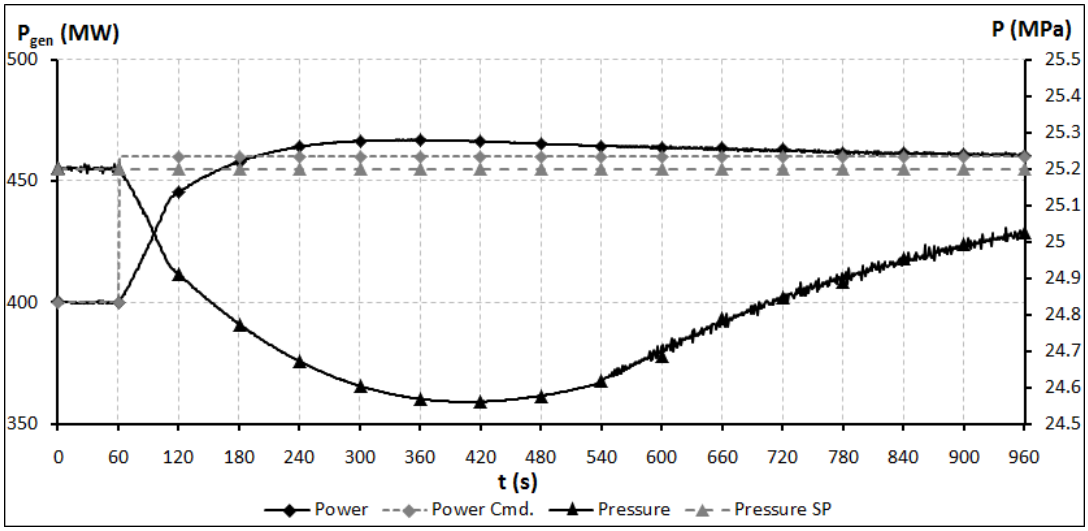

FIGURE 4.9 Power output response and steam pressure evolution for 60 MW load demand step increase from the power plant loading level of 400 MW

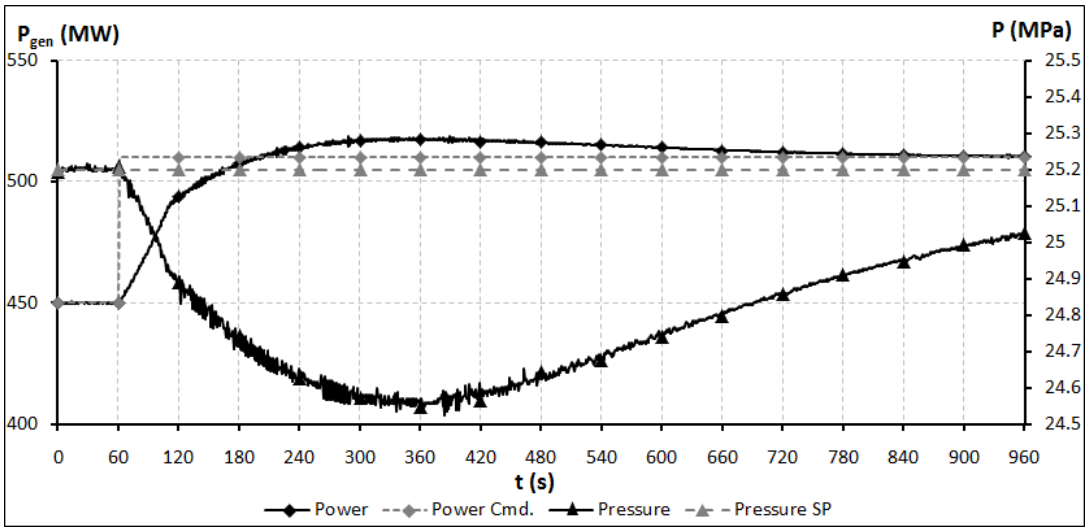

FIGURE 4.10 Power output response and steam pressure evolution for 60 MW load demand step increase from the power plant loading level of 450 MW

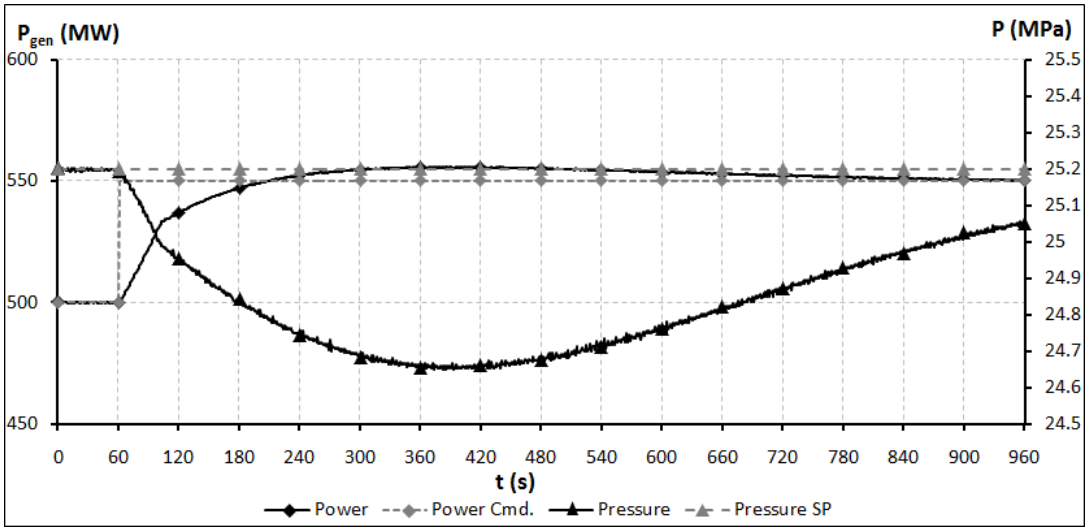

FIGURE 4.11 Power output response and steam pressure evolution for 50 MW load demand step increase from the power plant loading level of 500 MW

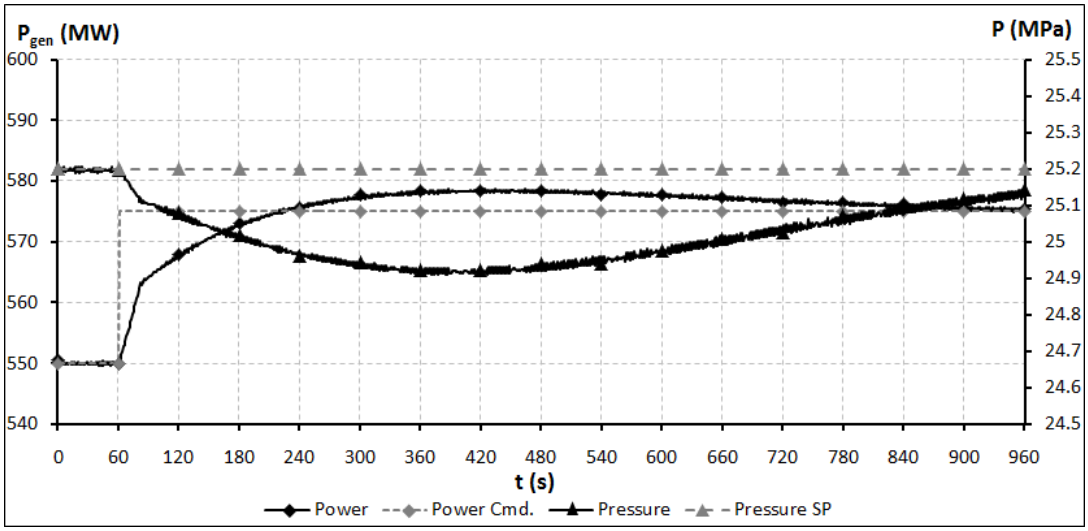

FIGURE 4.12 Power output response and steam pressure evolution for 25 MW load demand step increase from the power plant loading level of 550 MW

The response time, power output overshoot and pressure drop values obtained for each simulation test are presented in Table 4.2.

TABLE 4.2 Results obtained from the simulation tests for Primary Frequency Response requirements with the plant operating in fixed pressure control mode

Loading level		**Fixed Pressure Control Mode**						
		Load demand step increase		**Response time**	**Power output overshoot**		**Steam pressure drop**	
%RC	MW	%RC	MW	s	%	MW	%	MPa
58.33	350	10	60	128	1.56	6.41	2.43	0.61
66.66	400	10	60	136	1.50	6.90	2.54	0.64
75	450	10	60	136	1.68	8.56	2.68	0.68
83.33	500	8.33	50	147	1.08	5.91	2.19	0.55
91.66	550	4.17	25	160	0.66	3.78	1.15	0.29

The response time is defined as the time elapsed between the moment when the load demand step change signal was applied (t = 60 s) and the first time instance when the increase in the power output matches the load demand.

Looking at the simulation response time values from Table 4.2, it shows that the time required by the power plant to increase its power output according to specified load demand step changes is increasing with the increase of the operating loading level.

All the results show that the power plant cannot fulfil the Primary Frequency Response regulations specified by the Grid Code, being far more than the required response time of 10 s. By analysing Fig. 4.8 – Fig. 4.12, it results that after a new load demand signal is given to the power plant, there follows an immediate linear increase of the power output, with a high rate of change, which is due to the fast opening of the control valve, allowing more steam to flow into turbine. As the stored energy of the boiler is limited, this high rate of change of the power output comes to

an end after a certain time. The rest of the necessary power increase is delivered at a smaller rate, as there is a time delay until the new fuel demand signal is reflected by the coal mills' output and then a further delay is added by the combustion and steam generation process in the boiler.

The fast opening of the control valve generates an increase in the steam flow going through turbine, which means as well a steam pressure drop from its set point. These values and the ones of the power output overshoot obtained from the simulation tests are presented in Table 4.2. The power output overshoot expressed in MWs represents the maximum power generated minus the load demand step change value. This result can be expressed in percentages if it is further divided by the load demand step change value and multiplied with one hundred. The steam pressure drop is calculated as the difference between the minimum value of the steam pressure and its set point value. By dividing this result with the set point value and then multiplying it with one hundred, it can also be expressed in percentages.

It can be observed from Table 4.2 that when the same load demand step signal (60 MW) is sent to the power plant, operating at three different loading levels, the overshoot of the generated power (expressed in MW) is increasing with the increase of the loading level. This can be justified by the initial fuel demand signal given to the coal mills, which increases with the operating loading level. As power output reaches the set point setting, the fuel demand signal is decreased, but there will continue to be an increase in generated power due to the thermal inertia constant of the boiler.

The pressure drop values (expressed in MPa) for all the simulation tests are of small value, but it can be observed a slight increase with the increase of the operating load level. This is due to the wider opening of the control valve.

Although operating with sliding pressure control mode is not suitable for achieving a fast power plant response, simulation tests were run considering the same Primary Frequency Response requirements specified by the Grid Code. The results were processed in the graphs presented in Fig. 4.13 to Fig. 4.17.

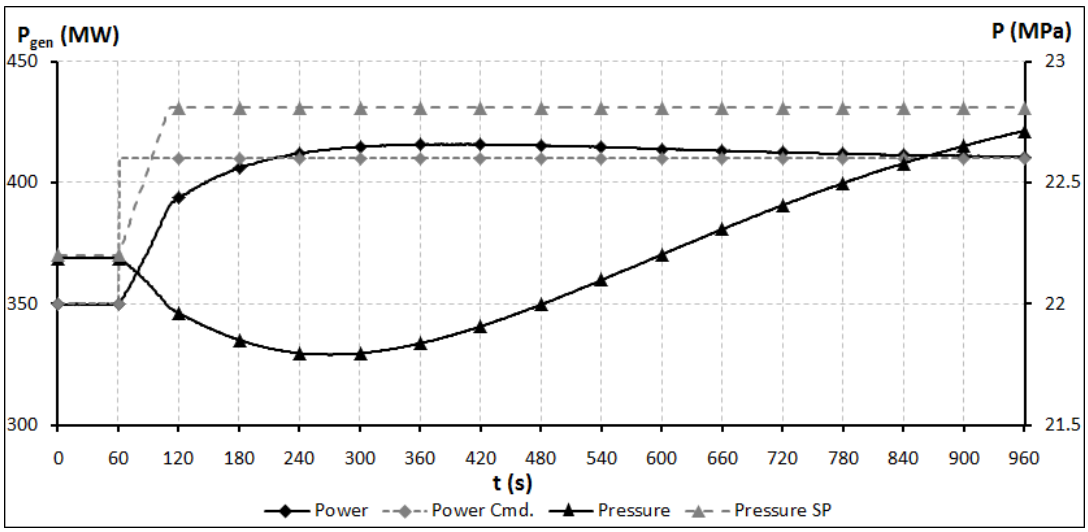

FIGURE 4.13 Power output response and steam pressure evolution for 60 MW load demand step increase from the power plant loading level of 350 MW

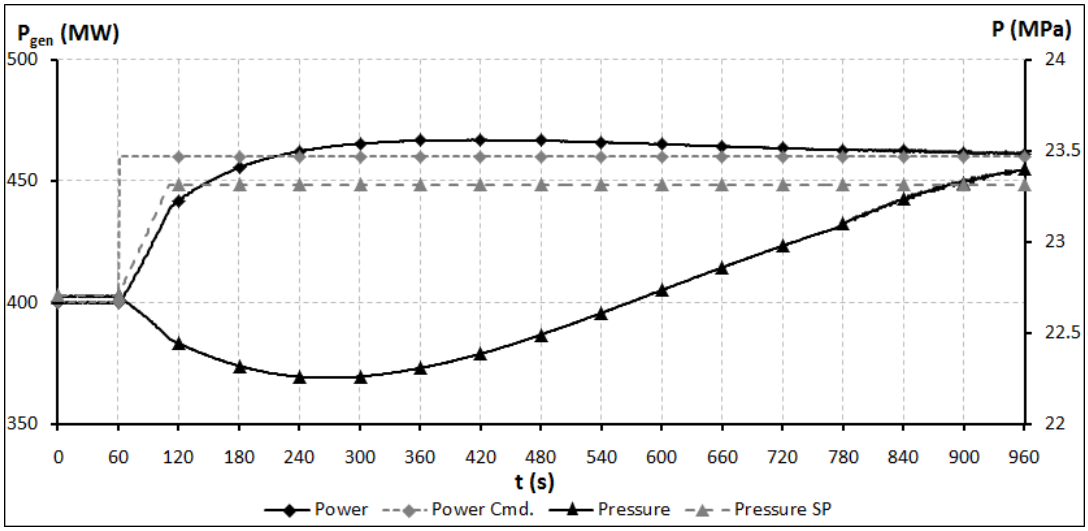

FIGURE 4.14 Power output response and steam pressure evolution for 60 MW load demand step increase from the power plant loading level of 400 MW

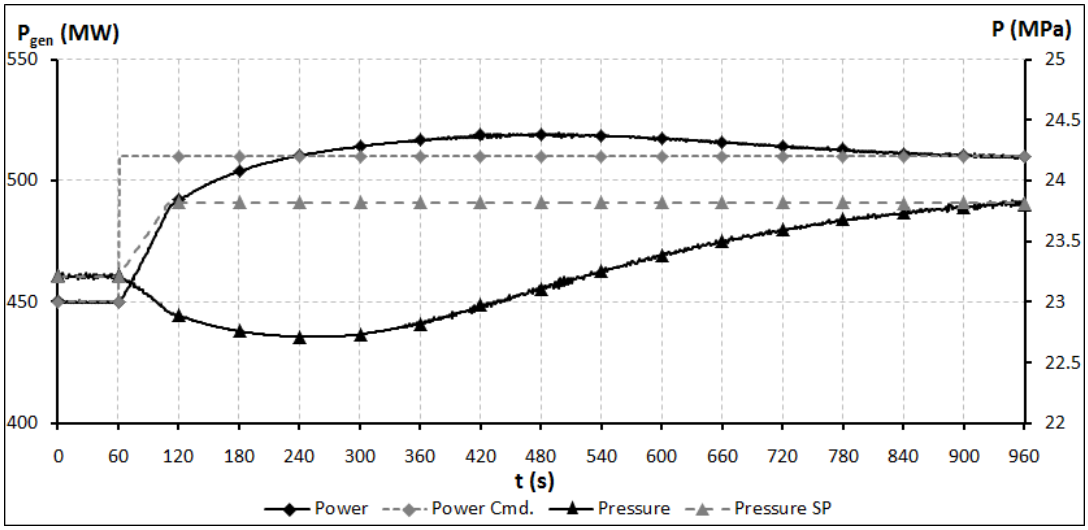

FIGURE 4.15 Power output response and steam pressure evolution for 60 MW load demand step increase from the power plant loading level of 450 MW

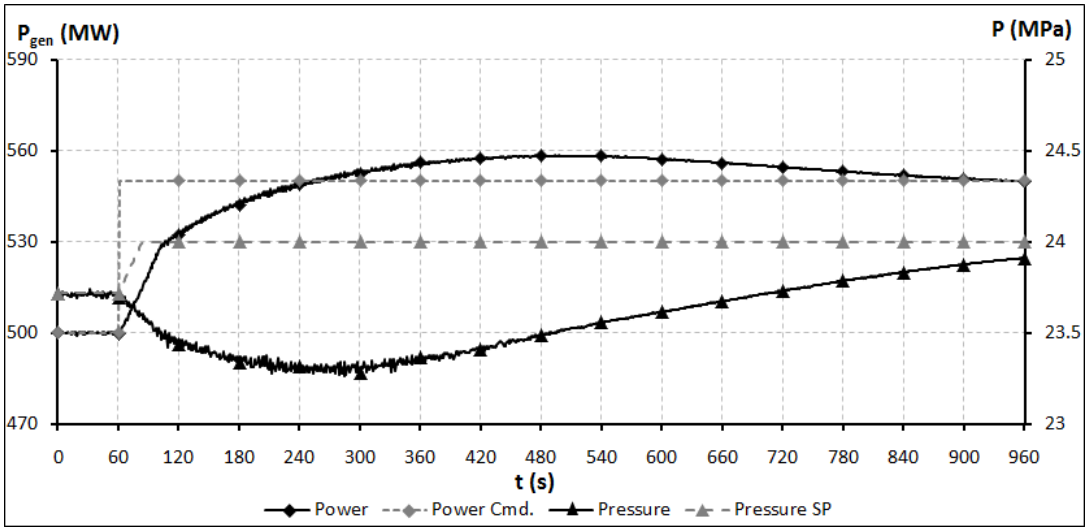

FIGURE 4.16 Power output response and steam pressure evolution for 50 MW load demand step increase from the power plant loading level of 500 MW

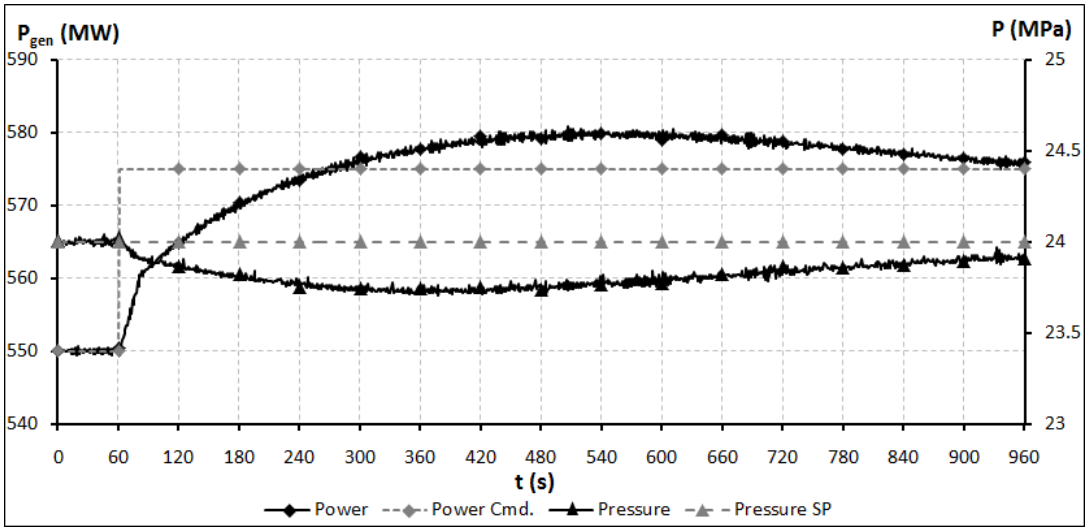

FIGURE 4.17 Power output response and steam pressure evolution for 25 MW load demand step increase from the power plant loading level of 550 MW

It can visually be observed from the figures above, that the response times of the power plant are longer than the ones obtained when operating in fixed pressure control mode. This is expected, considering that the control valve is kept more than

90% opened, which means that the boiler has no stored energy to use for fast changes in the load demand. The response time, power output overshoot and pressure drop values obtained for each simulation test are presented in Table 4.3.

TABLE 4.3 Results obtained from the simulation tests for Primary Frequency Response requirements with the plant operating in sliding pressure control mode

Loading level		**Sliding Pressure Control Mode**						
		Load demand step increase		**Response time**	**Power output overshoot**		**Steam pressure drop**	
%RC	MW	%RC	MW	s	%	MW	%	MPa
58.33	350	10	60	153	1.44	5.89	4.43	1.01
66.66	400	10	60	155	1.50	6.89	4.49	1.05
75	450	10	60	175	1.93	9.82	4.57	1.09
83.33	500	8.33	50	189	1.52	8.37	3.08	0.74
91.66	550	4.17	25	202	1.01	5.80	1.21	0.29

Similar with the case of power plant operating with fixed pressure control mode, it can be noticed from Table 4.3, that the response time is increasing with the increase of the operating loading level. Analysing the figures in Table 4.3 for power output overshoot, it can be observed that for the same load demand step increase (60 MW), the overshoot of the power output (expressed in MW) is increasing for operating at a higher operating loading level. The values are higher than when the power plant was operating in fixed pressure control mode. The same conclusion can be drawn for the values of the pressure drop. The response time values obtained during simulation tests, for the power plant operating under fixed pressure and sliding pressure control mode are plotted together in Fig. 4.18.

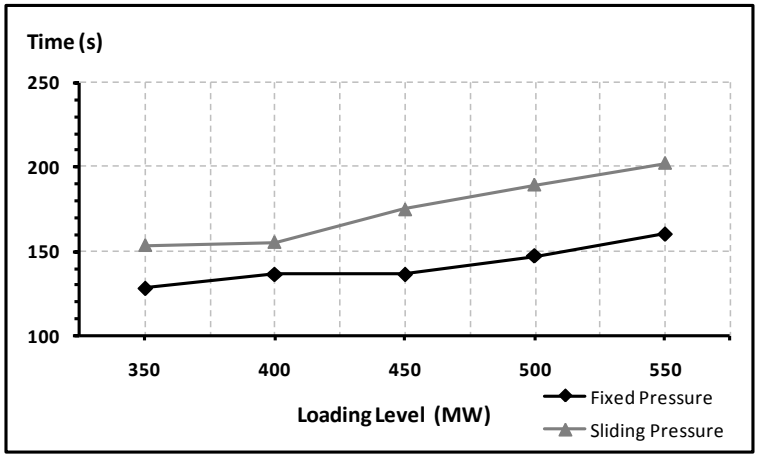

FIGURE 4.18 Power plant response times for the boiler operating in fixed pressure and sliding pressure control mode

It can be observed from Fig. 4.18 that the difference between response times for different pressure control mode is even more consistent for operating loading levels situated above 400 MW (~ 65% RC). The numerical comparison is summarised in Table 4.4.

TABLE 4.4 Power plant response times for boiler operating in fixed/sliding pressure control mode

Loading level		**Response time**			
		Fixed Pressure Control Mode	**Sliding Pressure Control Mode**	**Time difference**	
%RC	MW	s	s	s	%
58.33	350	128	153	25	19.53
66.66	400	136	155	19	13.97
75	450	136	175	39	28.67
83.33	500	147	189	42	28.57
91.66	550	160	202	42	26.25

Table 4.4 shows that the difference in response times is quite consistent, being between 19 s and up to 42 s. The simulation results prove that the fastest response of the power plant is obtained when steam pressure is controlled in fixed pressure control mode.

4.2.2 Simulation tests for High Frequency Response requirements

In case power system frequency is increasing, the power plant needs to decrease its power output. Using the requirements of the High Frequency Response specified in the Grid Code, some simulation tests were conducted for different operating loading levels and the results were shown in Fig. 4.19 to Fig. 4.23. The steam pressure control was considered to be in fixed pressure control mode.

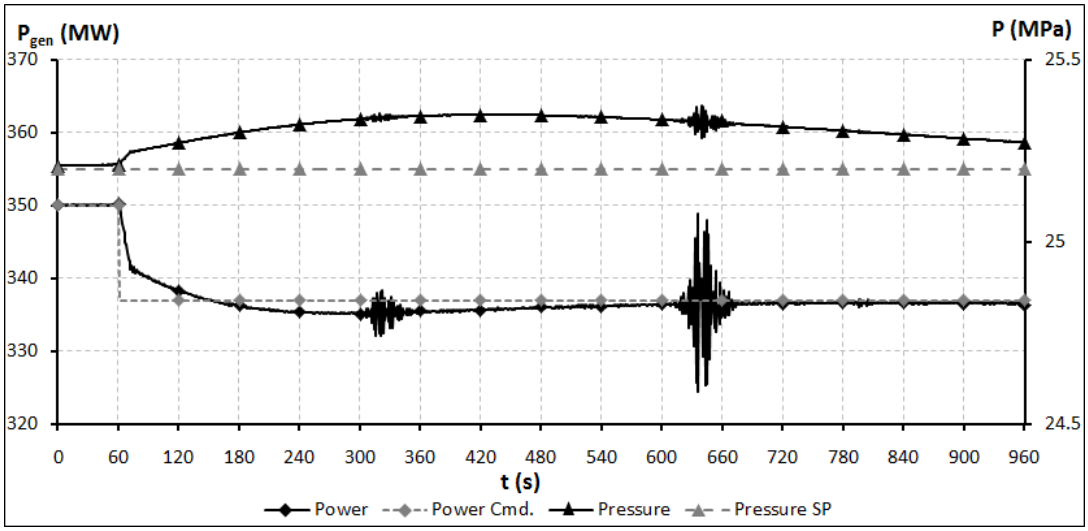

FIGURE 4.19 Power output response and steam pressure evolution for 13.33 MW load demand step decrease from the power plant loading level of 350 MW

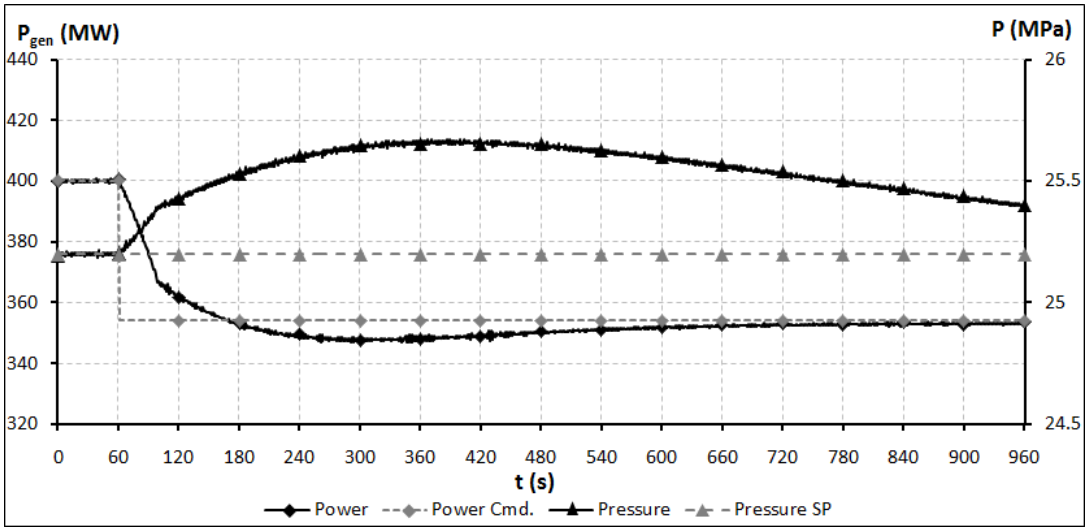

FIGURE 4.20 Power output response and steam pressure evolution for 46.66 MW load demand step decrease from the power plant loading level of 400 MW

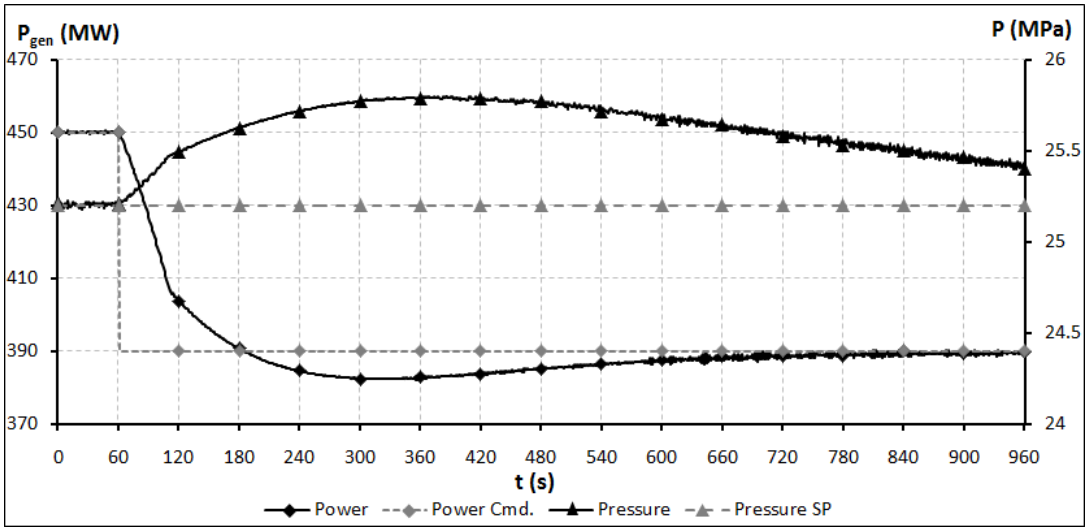

FIGURE 4.21 Power output response and steam pressure evolution for 60 MW load demand step decrease from the power plant loading level of 450 MW

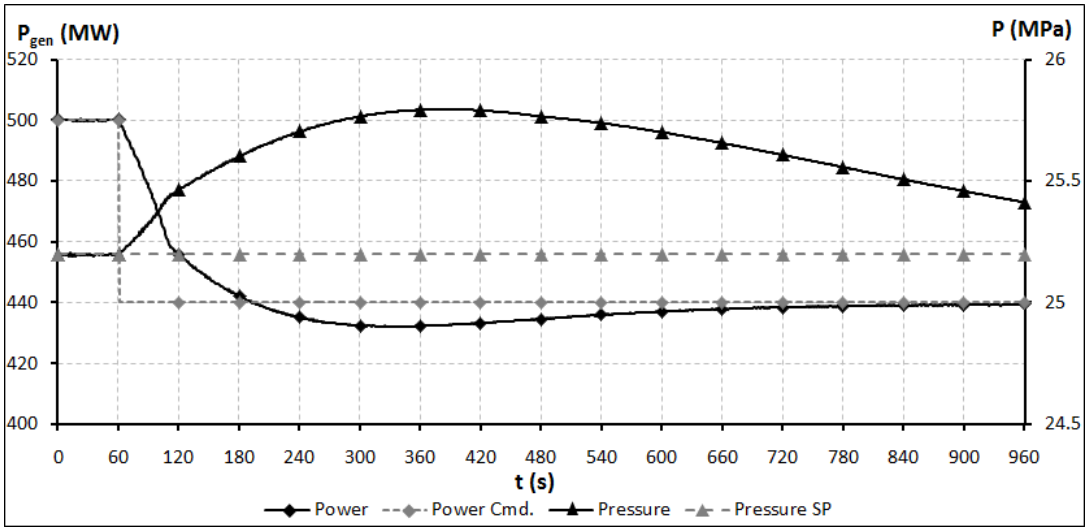

FIGURE 4.22 Power output response and steam pressure evolution for 60 MW load demand step decrease from the power plant loading level of 500 MW

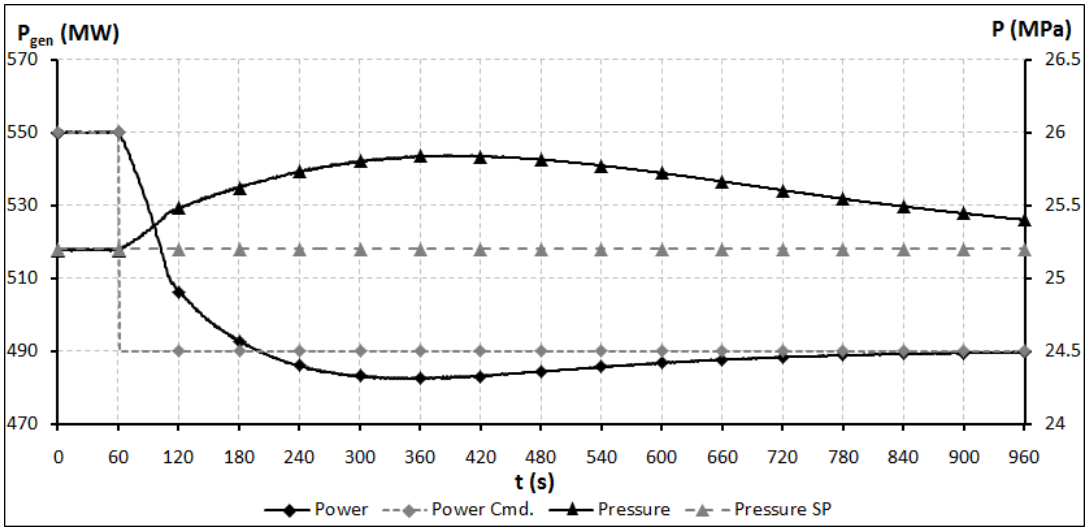

FIGURE 4.23 Power output response and steam pressure evolution for 60 MW load demand step decrease from the power plant loading level of 550 MW

Looking at the figures above, it can be observed that after the initiation of the step decrease load demand signal, the power output starts decreasing, having an undershoot until the new set point setting is reached. At the same time, as the control

valve is closing, the steam pressure is increasing, having an overshoot until it reaches its set point value again. The response times of the power plant for different operating loading levels and different load demand step decrements are tabulated in Table 4.5.

TABLE 4.5 Results obtained from the simulation tests for High Frequency Response requirements with the plant operating in fixed pressure control mode

Loading level		**Fixed Pressure Control Mode**						
		Load demand step decrease		**Response time**	**Power output drop**		**Steam pressure overshoot**	
%RC	MW	%RC	MW	s	%	MW	%	MPa
58.33	350	2.22	13.33	101	3.63	12.20	0.69	0.17
66.66	400	7.78	46.66	115	1.87	6.61	1.88	0.47
75	450	10	60	125	2.01	7.84	2.37	0.60
83.33	500	10	60	133	1.80	7.93	2.36	0.59
91.66	550	10	60	140	1.56	7.62	2.56	0.64

Observing the data from Table 4.5, it can be noticed that the response time is increasing with the operating loading level, as well as with the load demand step decrements. This is due to the fact, that although the closing of the control valve is fast, the turbine's rotor has its own spinning inertia, which will cause a delay until its rotational speed will decrease accordingly and the power output will reach the required level.

The fast closing of the control valve produces an increase of the steam pressure and a decrease of the power output. Analysing the data from Table 4.5, it results that the steam pressure is well controlled, with small values of overshoot. For the same

reduction of the power (60 MW), these have similar values with the increase of the operating loading values. When operating loading levels and step down power demand signals are increased, the pressure overshoot is also increased. This is due to closing of the control valve, which minimises the opening area and increases in this way the steam pressure. There is a consistent amount of power drop for power plant operating at 350 MW and this is due to the fact that it hasn't reached yet its full stable operating level. For the same reduction of power output, the values of the power drop are similar.

4.2.3 Data analysis from an operating power plant

With the help of data collected from an operating power plant, a comparative analysis between the real dynamic responses and the ones obtained through simulation tests was carried out.

The power plant from which the data was recorded is a 600 MW supercritical coal-fired unit, connected to grid and operated in a sliding pressure control mode. The collected data represents the daily normal operation of the power plant, so its performance does not replicate the test conditions from the power plant simulator. The most representative dynamic responses for load demand step increase are plotted in the graph below.

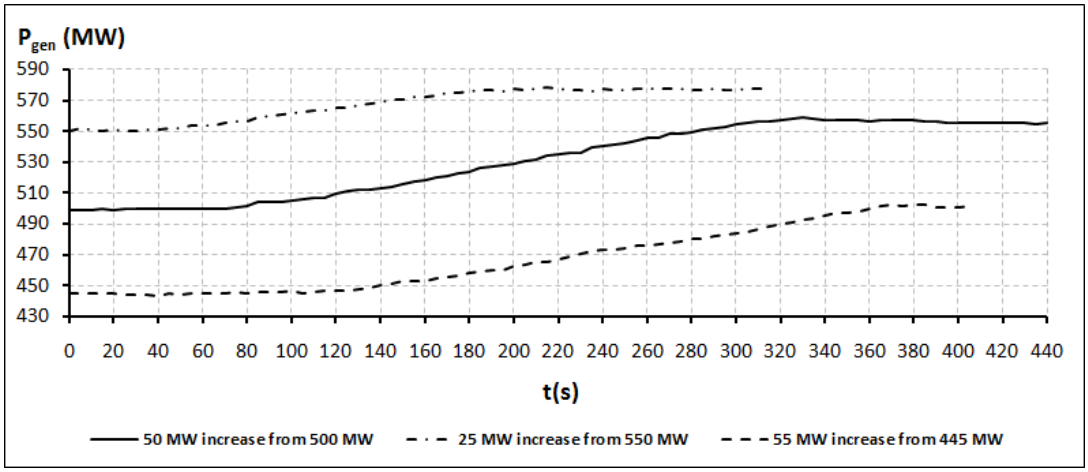

FIGURE 4.24 Power output responses for: 55 MW load demand step increase from the power plant loading level of 445 MW; 50 MW load demand step increase from the power plant loading level of 500 MW; 25 MW load demand step increase from the power plant loading level of 550 MW.

The response times derived from the operating power plant data and from the simulations tests for different load demand step increments are gathered in Table 4.6.

TABLE 4.6 Power plant response times from real and simulation tests data

Loading level	**Sliding Pressure Control Mode**		
	Load demand step increase	**Response time**	
MW	MW	Simulation	Real
		s	
450 445*	60 55*	175	250
500	50	189	210
550	25	202	140

* real power plant case

Analysing the response times from Table 4.6, it can be observed that the real power plant requires longer times to increase power than the ones resulted from the simulation tests. This is assumed to be due to different initial conditions and also to other factors which might deteriorate the performance of a real power plant and which cannot be considered in a simulation environment.

To compare the simulation results obtained for the high frequency response requirements, a set of data collected from the operating power plant and representing a decrease in power output from 600 MW to 350 MW was used. This dynamic response of the power plant is plotted in Fig. 4.25.

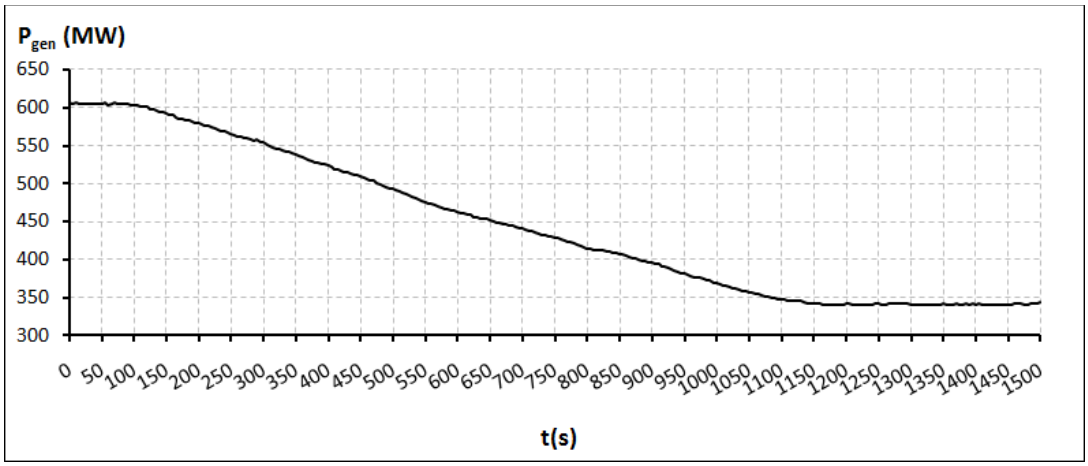

FIGURE 4.25 Power output response for 250 MW load demand step decrease from the power plant loading level of 600 MW

The data plotted in Fig. 4.25 was used to determine the response time of the power plant for different load demand step decrease values from various power output operating levels. These results are presented in Table 4.7 together with the results obtained through simulation tests.

TABLE 4.7 Power plant response times from real and simulation tests data

Loading level	**Load demand step decrease**	**Response time**	
MW	MW	Simulation	Real
		s	
400	46.66	115	195
450	60	125	260
500	60	133	225
550	60	140	200

The results extracted from the real power plant operation differ significantly in comparison with the ones obtained through simulation tests. The real response times are longer and this is first of all due to the operation in sliding pressure control mode, which slows down the responses of the power plant. The differences can as well be justified by the initial conditions, settings of the control system, coal quality and other conditions encountered in real operation and which cannot be replicated in a simulation environment.

4.3 Summary

The chapter presents and analyses the results gathered from the simulation tests conducted by the mean of the power plant simulator, in order to asses if its dynamic performance can comply with the frequency control requirements specified by GB Grid Code.

The chapter begins with a description of the power plant simulator software, emphasising its technical characteristics. The Grid Code frequency control services and the dynamic responses required from a grid connected power plant are defined.

The first set of simulations is considering the Primary Frequency Response requirements, with the power plant operating in fixed pressure control mode. According to the results, the power output increase conditions necessary to fulfil Primary Frequency Response regulations are too demanding for the coal fired supercritical power plant operating capabilities.

Although is not providing a fast response, sliding pressure control mode was also considered and the results were presented and compared with the ones when operating in fixed pressure control mode. This control mode is preferred by power plant operators for its advantage of ensuring a longer service life of the power plants.

Further simulation tests were conducted to verify if the power plant dynamic responses comply with the requirements of the High Frequency Response. The results show that the power plant has a faster response in decreasing its power output, but still not enough to comply with the Grid Code regulations.

Chapter 5

Development of a New Coal Flow Rate Control Strategy Based on Dynamic Matrix Control Algorithm

5.1 Introduction to Model Predictive Control

Model Predictive Control (MPC) is part of the advanced control techniques, originating in the seventies and with many successful practical applications in diverse industrial areas [Gomez Ortega and Camacho, 1996; Linkers and Mahfonf, 1994; Clarke, 1988; Richalet, 1993; Lee and Cooley, 1996]. MPC defines a class of control algorithms, which make use of an explicit model of the process to predict the future process behaviour, needed to calculate the control signal by minimizing an objective function.

Among the advantages of MPC over other methods the following present more interest [Camacho, 2007]:

- it takes into account constraints on control variables and on process outputs;
- due to the use of a model to generate control inputs, the internal interactions within the process are also considered;
- it can be applied to processes with complex dynamics;
- multivariable control strategies can be developed;
- its concepts are very intuitive and tuning is relatively easy;
- it is very useful for processes with known future reference trajectories.

5.1.1 The principle of MPC

All controllers belonging to MPC family make use of the same strategy. The following presentation references the detailed description of Tatjewski [2007].

If T_p is considered to be the sampling time of the controller, then at each sampling k the future control signals $u(k|k), u(k+1|k), \cdots, u(k+N_u|k)$ are calculated, with the assumption that after a time window N_u, named control horizon, the control inputs are constant, that is $u(k+p|k) = u(k+N_u-1|k)$ for $p \geq N_u$. The calculation is made having the following prerequisite information:

- a process model, a disturbance model and a model of constraints;
- known values up to instant k of process outputs and inputs;
- trajectories of set-points, $y^{sp}(k+p|k)$ for the controlled variables for the prediction horizon N $(p = 1,2, \cdots, N)$.

The future control inputs are calculated by optimizing a determined criterion to keep the predicted process outputs $y(k+p|k)$ as close as possible to the future set-points $y^{sp}(k+p|k)$ over the prediction horizon N. The first element of the sequence of control signals, $u(k) = u(k|k)$ is sent to the process, while the rest is rejected. At the next sampling instant $(k+1)$, the process output $y(k+1)$ is measured and the entire calculation procedure is repeated, considering the same prediction horizon, but shifted one step forward. This is called the principle of a receding horizon.

The simplified structure of an MPC controller is presented in Fig. 5.1.

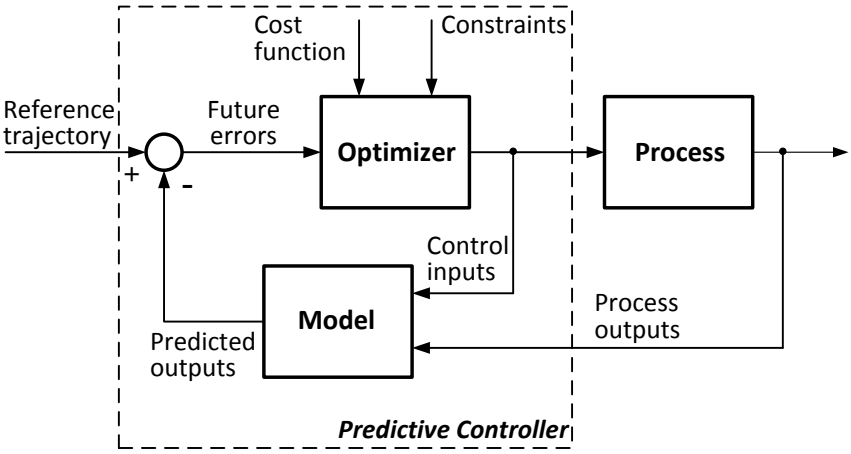

FIGURE 5.1 Simplified structure of an MPC controller [Camacho, 2007]

According to Fig. 5.1 a model is used to predict the future process outputs, based on the values of past control moves and process outputs and the optimal future control inputs. The optimal future control actions are calculated by the optimizer, considering the cost function, where the future errors are considered, and the constraints.

Fig. 5.2 illustrates the principle of MPC for the case of a SISO (Single Input Single Output) process.

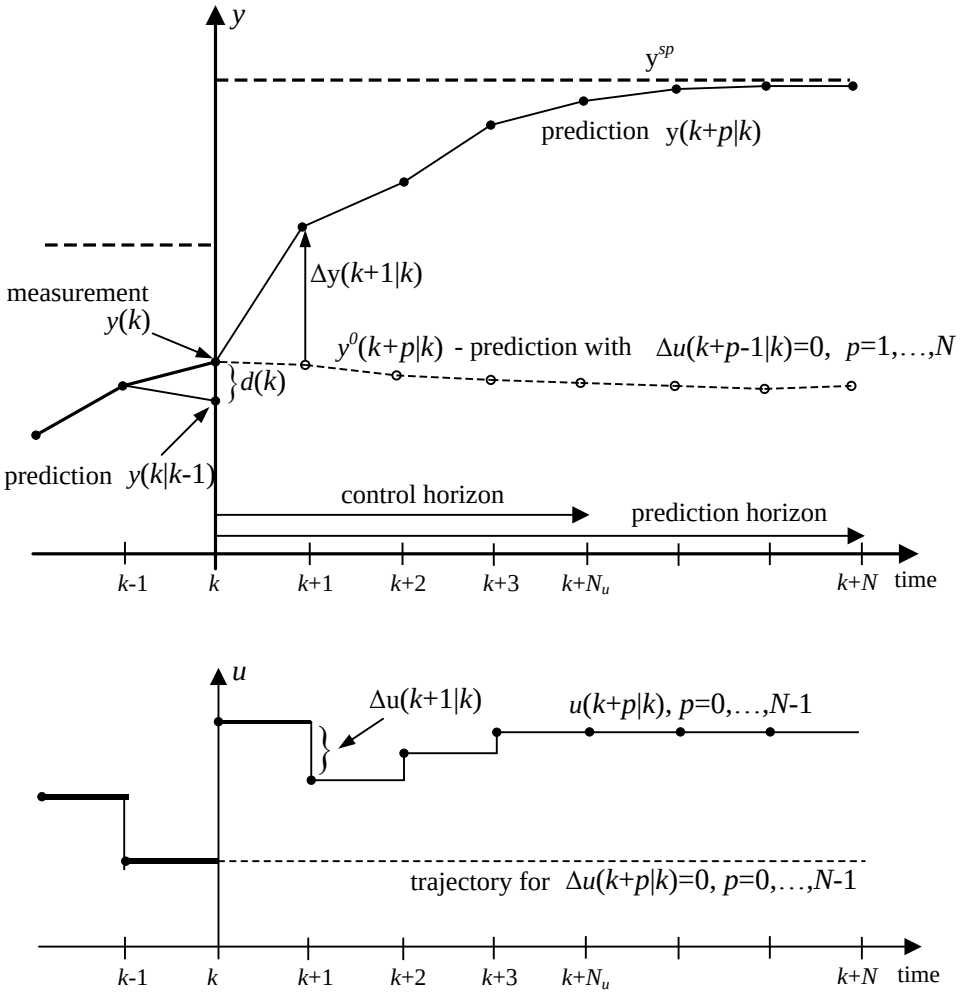

FIGURE 5.2 Illustration of the MPC strategy for the case of a SISO process [Tatjewski, 2007]

The horizontal axis represents the discrete time, the process being at current sampling instant k, when the current control move $u(k) = u(k|k)$ has to be calculated. The variables of the control input and process output, needed for calculation of the next control move $u(k)$, are presented as trajectories. There can be distinguished two process output trajectories, two control input trajectories and a set-point trajectory. The explanation for each trajectory is as follows:

- If the previous calculated control input, $u(k-1)$ is kept constant over the entire prediction horizon, which means $u(k+p-1) = u(k-1)$ for $p = 1, \dots, N$, then the predicted controlled output trajectory, $y^0(k+p|k), p = 1,2, \dots, N$ is illustrated by the dashed line from the first graph. The trajectory of the control input is presented by the dashed line in the second graph. As the trajectory $y^0(k+p|k)$ depends only on the previous control inputs, not being influenced by future control inputs calculated at time sampling k, it is also called a free output trajectory.
- If both past control inputs, up to $u(k-1)$ and future control inputs $u(k+p|k), p = 1,2, \dots, N-1$, are applied to the process then the predicted output trajectory $y(k+p|k)$ is obtained, represented by a continuous curve. The thin parts of the trajectory symbolize predicted values, whereas the thick parts represent the real past evolution of the process. The continuous line from the second graph has the same significance this time applied to control inputs trajectory, with the last thick segment being the control move applied to the process at the current sampling instant.
- The set-points trajectory $y^{sp} = y^{sp}(k+p|k), p = 1,2, \dots, N$ is presented with a thicker dashed line. In this example, the set-points trajectory presents a step change at time sampling k and then remains constant. In general the set-points might vary accordingly along the prediction horizon.

Because the process model used to calculate the predicted future behaviour of the process is an approximation of reality, there are differences between the output predictions and the measured values. This is represented in Fig. 5.2 as an

unmeasured disturbance $d(k)$, calculated as $d(k) = y(k) - y(k|k-1)$, where $y(k)$ is the currently measured process value and $y(k|k-1)$ is the predicted value of process output for time sample k calculated at the previous time sample $k-1$.

The future control inputs $u(k+p|k), p = 1,2,\dots,N-1$ are determined at sampling instant k by minimizing a cost function. This generally consists of two terms. The first term represents the predicted control errors between the predicted output values and the set-points values and the second term represents penalties for control moves. Considering these two terms, the cost function has the shape of a quadratic cost function described by the expression below:

$$J(k) = \sum_{p=N_1}^{N} \left(y^{sp}(k+p|k) - y(k+p|k)\right)^T \underline{\Psi}(p) \left(y^{sp}(k+p|k) - y(k+p|k)\right) + \\ + \sum_{p=0}^{N_u} \Delta u(k+p|k)^T \underline{\Lambda}(\mathrm{p}) \Delta u(k+p|k)$$

$$J(k) = \sum_{p=N_1}^{N} \|y^{sp}(k+p|k) - y(k+p|k)\|^2_{\underline{\Psi}(p)} + \sum_{p=0}^{N_u-1} \|\Delta u(k+p|k)\|^2_{\underline{\Lambda}(p)} \qquad (5.1)$$

The predicted errors are calculated starting from $k+N_1$ and end at $k+N$, where $1 \le N_1 \le N$. A value $N_1 > 1$ is chosen if there is a delay in the process output for a change in the control input at time k. The control horizon N_u can have values in the interval $0 < N_u \le N$, but usually is chosen $N_u < N$, as this reduces the computational load of the optimization problem.

The expression (5.1) of the cost function contains the following terms:

- $y^{sp}(k+p|k)$ are the set-points for the controlled variables;

- $\Delta u(k+p|k)$ represent calculated future control increments, the solution of the optimization problem;
- $y(k+p|k)$ are the values of the predicted future process output variables, dependent on previous control inputs and process outputs and on the calculated future control increments;
- $\underline{\Psi}(p)$ is a matrix of weights used to determine the influence of the predicted process output errors;
- $\underline{\Lambda}(\mathrm{p})$ is a matrix of weights used to scale the control input increments.

In order to calculate the values of the predicted controlled variables $y(k+p|k)$, MPC algorithms use a process model. Although this model can be nonlinear as well, for this research work, there were considered only algorithms which make use of linear process models.

Using a linear model means that the principle of superposition can be applied. Using this, the evolution of the predicted controlled variable $y(k+p|k)$ can be presented as a sum of a first term dependent only on past control inputs and a second term dependent only on current and future control inputs. The first term, $y^0(k+p|k)$ is called free trajectory component and the second term, $\Delta y(k+p|k)$ is called forced output trajectory component. Thus the trajectory of predicted process outputs, $y(k+p|k)$ can be expressed in the following form:

$$y(k+p|k) = y^0(k+p|k) + \Delta y(k+p|k), \quad p = N_1, \dots, N. \tag{5.2}$$

Considering the relation (5.2), the cost function (5.1) can be expressed in the following form:

$$J(k) = \sum_{p=N_1}^{N} \|[y^{sp}(k+p|k) - y^0(k+p|k)] - \Delta y(k+p|k)\|^2_{\underline{\Psi}(p)} +$$

$$+ \sum_{p=0}^{N_u-1} \|\Delta u(k+p|k)\|^2_{\underline{\Lambda}(p)} \quad (5.3)$$

In reality all processes are subject to constraints. Due to constructive reasons, safety operation regulations, environmental reasons or economic ones, the process needs to be controlled under certain constraints.

The constraints which can be included in the MPC algorithms may refer to:

- constraints on the amplitude of the control signal

$$u_{min} \leq u(k+p|k) \leq u_{max}, \ \ p = 0,1,\dots,N_u - 1 \quad (5.4)$$

- constraints on the rate of change of control inputs

$$-\Delta u_{max} \leq \Delta u(k+p|k) \leq \Delta u_{max}, \ \ p = 0,1,\dots,N_u - 1 \quad (5.5)$$

- constraints on the amplitude of the process outputs

$$y_{min} \leq y(k+p|k) \leq y_{max}, \ \ p = N_1, N_1+1,\dots,N \quad (5.6)$$

The minimisation of the cost function from (5.3) is a minimisation of a convex quadratic function, strictly convex if $\underline{\Psi}(p) \geq 0$ and $\underline{\Lambda}(\mathrm{p}) > 0$,. If the inequality constraints on values of control inputs and controlled outputs (5.4), (5.5), (5.6) are added, then an analytic solution is not possible and numerical optimisation is necessary.

5.1.2 Historical perspective over MPC algorithms

Richalet *et al.* [1976, 1978] created an algorithm called Model Predictive Heuristic Control (MPHC), also known as Model Algorithmic Control (MAC) and presented

the successful industrial applications, where it was implemented. The algorithm uses a model in the form of a finite impulse response to predict the controlled outputs.

Another algorithm, Dynamic Matrix Control (DMC) was developed in the early 1970s by the engineers from Shell Oil and was used in an industrial application in 1973, as mentioned in Cutler and Ramaker [1980], Prett and Gillette [1980]. In this case the model used to calculate the predictions of the process outputs has the shape of a step response.

The algorithm of Generalized Predictive Control was developed by Clarke *et al.* [1987] and reported applications followed in Clarke [1988], Clarke and Mohtadi [1989]. This algorithm uses a discrete transfer function as a model to calculate the predicted process outputs. In 1988 was presented by Marquis and Broustail [1988] the first algorithm named Shell Multivariable Optimizing Controller (SMOC), which uses a process model in the form of state equations.

5.2 DMC algorithm

As was mentioned earlier, DMC was developed in the 1970s and successfully implemented in industrial applications by C.E. Garcia and Morshedi [1986], Prett and Gillette [1980], Cutler and Ramaker [1980], Dougherty and Cooper [2003], Aurora *et al.* [2004, Moon and Lee [2005], Kim *et al.* [2010], Li *et al.* [2006]. The structure of the DMC algorithm is presented below for a Single-Input Single-Output (SISO) process, for which the presentation of Tatjewski [2007] was used as a reference.

The process model used to make the predictions of process outputs is represented by a discrete step response. This model describes the output change for a unit step change of control input. In Fig. 5.3 it is illustrated the response of a SISO first order system to a unit step change in the control input. The process has a delay $\tau = 2T_p$, where T_p is the sampling period.

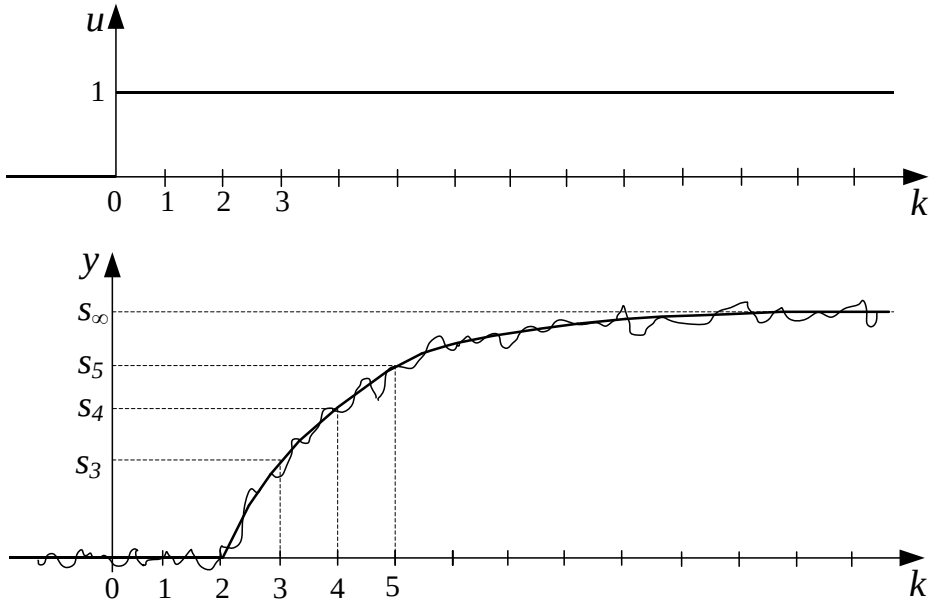

FIGURE 5.3 The process output response y of a system for a unit step change in the control input u [Tatjewski, 2007]

The discrete step response of the process is given in the form of a set of coefficients $\{s_1, s_2, s_3, \cdots, s_D, s_{D+1}, \cdots\}$. For an asymptotically stable process, the output stabilises, after a step change in the input at a certain value. The number of discrete time samplings after which the step response stays constant is denoted **D** and called the horizon of the process dynamics. The step response $\{s_1, s_2, s_3, \cdots, s_D\}$ represents

a complete model of the system, which allows to calculate the discrete process output for any control input sequence.

The step response model and the principle of superposition are used to derive the following formula

$$y(k+p|k) = \sum_{j=1}^{p} s_j \Delta u(k+p-j|k) + y(k) + \sum_{j=1}^{k} s_{j+p} \Delta u(k-j) - \\ - \sum_{j=1}^{k} s_j \Delta u(k-j) \tag{5.7}$$

where $y(k+p|k)$ is the output prediction at the current sampling instant k for a future instant $k+p$, $\Delta u(k+p-j|k)$ is used to define the current and future control input changes, as calculated at the current time k, $\Delta u(k-j)$ are the control input changes determined at previous instants and applied to the process and $y(k)$ is the measured output value at the current time k

It can be noticed that the first sum from the right hand side depends only on current and future control input changes, which will result as a solution of the optimization problem. This part is called the forced component of the predicted output trajectory.

$$\Delta y(k+p|k) = \sum_{j=1}^{p} s_j \Delta u(k+p-j|k), \;\; p = 1,2,\dots,N \tag{5.8}$$

As the remaining part is only dependent on already implemented control input changes, this is called the free component of the predicted output trajectory.

$$y^0(k+p|k) = y(k) + \sum_{j=1}^{k} (s_{j+p} - s_j) \Delta u(k-j), \qquad p = 1,2,\dots,N \tag{5.9}$$

Using the notations given by (5.8) and (5.9), the predicted output for the future time instant $k+p$ calculated at sampling instant k has the following formula:

$$y(k+p|k) = y^0(k+p|k) + \Delta y(k+p|k),\ p = 1,2,\dots,N \tag{5.10}$$

The cost function (5.3) can be expressed in the matrix format, as follows:

$$J(k) = \|[Y^{sp}(k) - Y^0(k)] - \Delta Y(k)\|^2_{\underline{\Psi}} + \|\Delta U(k)\|^2_{\underline{\Lambda}} \tag{5.11}$$

where the matrices involved in its expression are defined as,

$Y^{sp}(k)$ – set-point matrix, dimension $(N - N_1 + 1) \times 1$; $Y^0(k)$ – free component matrix, dimension $(N - N_1 + 1) \times 1$; $\Delta Y(k)$ - forced component matrix, dimension $(N - N_1 + 1) \times 1$, $\Delta U(k)$ - future control inputs matrix, dimension $N_u \times 1$, $\underline{\Psi}$ - predicted output weights matrix, dimension $(N - N_1 + 1) \times (N - N_1 + 1)$; $\underline{\Lambda}$ - predicted control input weights matrix, dimension $N_u \times N_u$.

Using (5.9) the matrix form of the free component of the predicted output trajectory, $Y^0(k)$ can be expressed as,

$$Y^0(k) = Y(k) + M^p \Delta U^p(k) \tag{5.12}$$

where $Y(k)$ is the matrix of current measurement, dimension $(N - N_1 + 1) \times 1$, $\Delta U^p(k)$ is a matrix of past control inputs, dimension $(D-1) \times 1$ and matrix M^p, dimension $(N - N_1 + 1) \times (D-1)$, has the following shape

$$M^p = \begin{bmatrix} s_{1+N_1} - s_1 & s_{2+N_1} - s_2 & s_{3+N_1} - s_3 & \cdots & s_{D-1+N_1} - s_{D-1} \\ s_{2+N_1} - s_1 & s_{3+N_1} - s_2 & s_{4+N_1} - s_3 & \cdots & s_{D+N_1} - s_{D-1} \\ \vdots & \vdots & \vdots & \ddots & \vdots \\ s_{N+1} - s_1 & s_{N+2} - s_2 & s_{N+3} - s_3 & \cdots & s_{N+D-1} - s_{D-1} \end{bmatrix} \tag{5.13}$$

Knowing (5.8), the matrix form of the forced component of the predicted output trajectory can be written as

$$\Delta Y(k) = M\Delta U(k) \tag{5.14}$$

where M is called the dynamic matrix and has the dimension $(N - N_1 + 1) \times N_u$.

$$M = \begin{bmatrix} s_{N_1} & s_{N_1-1} & \cdots & s_1 & 0 & \cdots & 0 \\ s_{N_1}+1 & s_{N_1} & \cdots & s_2 & s_1 & \cdots & 0 \\ \vdots & \vdots & \vdots & \vdots & \vdots & \ddots & \vdots \\ s_{N_u} & s_{N_u-1} & \cdots & s_{N_u-N_1+1} & s_{N_u-N_1} & \cdots & s_1 \\ s_{N_u+1} & s_{N_u} & \cdots & s_{N_u-N_1+2} & s_{N_u-N_1+1} & \cdots & s_2 \\ \vdots & \vdots & \vdots & \vdots & \vdots & \ddots & \vdots \\ s_N & s_{N-1} & \cdots & s_{N-N_1+1} & s_{N-N_1} & \cdots & s_{N-N_u+1} \end{bmatrix} \tag{5.15}$$

Introducing the relations (5.12) and (5.14) into the expression (5.11) of the cost function the optimization problem can be written as

$$\min_{\Delta U(k)} J(k) = \|[Y^{sp}(k) - Y(k) - M^p \Delta U^p(k)] - M\Delta U(k)\|^2_{\underline{\Psi}} + \\ + \|\Delta U(k)\|^2_{\underline{\Lambda}} \tag{5.16}$$

If to the optimization problem (5.16), there are added the linear inequality constraints (5.4)-(5.6), then the resulting optimization problem is a quadratic programming (QP) problem. The constraints need to be formulated in an adequate way, as to be functions of the future control inputs matrix, $\Delta U(k)$. The constraints on rate of change can be written in the following form:

$$-\Delta U_{max} \leq \Delta U(k) \leq \Delta U_{max} \tag{5.17}$$

where matrix ΔU_{max} has a dimension $N_u \times 1$.

To derive the relation for the constraints on the amplitude of control signal, each control signal can be expressed as the sum of the previous control signal and the calculated future control increments.

$$u(k+p|k) = u(k-1) + \sum_{j=0}^{p} \Delta u(k+j|k)\,,\ \ p = 0,1,\dots,N_u - 1 \quad (5.18)$$

Using (5.18), the constraints on the amplitude of control signal can be written in the matrix form.

$$U_{min} \le U(k-1) + \Theta \Delta U(k) \le U_{max} \quad (5.19)$$

The terms from (5.19) are defined as: U_{min} is the matrix of lower bound, dimension $N_u \times 1$, U_{max} is the matrix of upper bound, dimension $N_u \times 1$, $U(k-1)$ is the matrix of previously implemented control signal, at sampling instant $k-1$, dimension $N_u \times 1$ and Θ is a unit lower triangular matrix of dimension $N_u \times N_u$

The relation (5.10), concerning the predicted future outputs $Y^{pred}(k)$, is expressed in matrix form, where $\Delta Y(k)$ is replace by its definition from (5.14) as following,

$$Y^{pred}(k) = Y^0(k) + M\Delta U(k) \quad (5.20)$$

The constraints on the amplitude of the predicted future process outputs, $Y^{pred}(k)$ can be written in the following matrix form,

$$Y_{min} \le Y^0(k) + M\Delta U(k) \le Y_{max} \quad (5.21)$$

Where all the terms have been defined before, except Y_{min} which is the matrix of lower bound, dimension $(N - N_1 + 1) \times 1$, and Y_{max} which is the matrix of upper bound, dimension $(N - N_1 + 1) \times 1$.

It can be concluded that at every sampling instant the following QP problem is solved:

$$\min_{\Delta U(K)} \left\{ \| [Y^{sp}(k) - Y(k) - M^p \Delta U^p(k)] - M\Delta U(k) \|^2_{\underline{\Psi}} + \| \Delta U(k) \|^2_{\underline{\Lambda}} \right\}$$

subject to: $-\Delta U_{max} \le \Delta U(k) \le \Delta U_{max}$ (5.22)

$$U_{min} \leq U(k-1) + J\Delta U(k) \leq U_{max}$$

$$Y_{min} \leq Y^0(k) + M\Delta U(k) \leq Y_{max}$$

5.3 Quadratic Programming

QP is a special case of Nonlinear Programming, which consists of a quadratic objective function and a set of linear constraints. The definition of the QP problem and the description of the active set methods for solving it are presented below, where the reference for this presentation can be found in Wang [2009]. If the objective function is J and the decision variable is x, then the general form of a QP problem is:

$$J(x) = \frac{1}{2}x^T Ex + x^T F \tag{5.23}$$

$$Mx \leq \gamma$$

where,

- F is an n-dimensional column vector describing the coefficients of the linear terms in the objective function
- E is an $(n \times n)$ symmetric matrix describing the coefficients of the quadratic terms
- x is an n-dimensional column vector containing the decision variables
- M is a size $(m \times n)$ matrix defining the constraints.
- γ is an m dimensional column vector defining the right-hand side coefficients.

If the objective function $J(x)$ is strictly convex for all feasible points, then there is a unique local minimum which is also the global minimum. The sufficient condition for $J(x)$ to be strictly convex is that E to be positive definite. The QP problem can be solved iteratively by active set strategies or interior point methods.

The Lagrangian function for the quadratic function $J(x)$ is

$$L(x,\lambda) = \frac{1}{2}x^T Ex + x^T F + \lambda^T(Mx - \gamma) \tag{5.24}$$

where the coefficients stored in the column vector λ of dimension m, are known as the Lagrange multipliers.

The necessary conditions for a minimum of the function $J(x)$ in x are given by the Karush-Kuhn-Tucker conditions:

$$\begin{aligned} &\frac{\partial L}{\partial x} = 0 \longrightarrow Ex + F + M^T\lambda = 0 \\ &\frac{\partial L}{\partial \lambda} = 0 \longrightarrow \lambda^T(Mx - \gamma) = 0 \\ &Mx - \gamma \leq 0 \\ &\lambda \geq 0 \end{aligned} \tag{5.25}$$

The set of constraints $Mx - \gamma \leq 0$ can be divided into active constraints and inactive constraints. The inequality $M_i x - \gamma_i \leq 0$ is defined by the coefficients of the i-th row of the matrix M and the i-th element of the column vector γ. If the design variables x, determine a solution on the boundary of the constraint, then the constraint behaves like and equality constraint,$M_i x - \gamma_i = 0$ and is called and active constraint. If the solution determined by the design variable lies inside the region of the constraint, $M_i x - \gamma_i < 0$ then it is considered an inactive constraint.

Using the definition of the set of active constraints, the necessary conditions (5.25) can be expressed as

$$
\begin{aligned}
&Ex + F + \sum_{i \in S_{act}} \lambda_i M_i^T = 0 \\
&M_i x - \gamma_i = 0 \quad i \in S_{act} \\
&M_i x - \gamma_i < 0 \quad i \notin S_{act} \\
&\lambda_i \geq 0 \quad i \in S_{act} \\
&\lambda_i = 0 \quad i \notin S_{act}
\end{aligned}
\tag{5.26}
$$

where, S_{act} represents the index for the set of active constraints. From (5.26) it results that the Lagrange multiplier is non-negative, if the constraint is active and zero if the constraint is inactive.

The original problem could be simplified if the set of active constraints are known, meaning that only the equality constraints would be considered. If this would be the case, the optimal solution is given by

$$
\begin{aligned}
&\lambda_{act} = -(M_{act} E^{-1} M_{act}^T)^{-1} (\gamma_{act} + M_{act} E^{-1} F) \\
&x = -E^{-1}(F + M_{act}^T \lambda_{act})
\end{aligned}
\tag{5.27}
$$

where, M_{act} and λ_{act} refers to the elements of the matrices M and λ, defining the set of active constraints.

5.3.1 Active set methods

The algorithms belonging to the active set strategies, define at each step a set of active constraints. This set is a subset of the constraints, which are active for the current point. The algorithm searches then for an optimized point on the area defined

by the active constraints. At every step an optimization problem with equality constraints is solved. If the Lagrange multipliers are non-negative, $\lambda_i \geq 0$ it means that the point represents a local solution to the problem. If any of the Lagrange multipliers is negative, $\lambda_i < 0$ then the objective function can be further minimized by relaxing the constraint i.

5.3.1.1 Primal-Dual method

The decision variables are also called primal variables. The algorithms named primal methods use the original definition of the problem to search the feasible region for an optimal solution. Every point found along the process is feasible and the value of the objective function is decreased with each iteration.

The disadvantage of primal methods is that the computational load is quite large, especially if the number of primal variables is more than the number of constraints.

A dual method is used to identify the inactive constraints and eliminate them from the solution. The Lagrange multipliers, λ are called dual variables.

The original primal problem is converted to the dual problem by using the Lagrangian function from (5.24).

$$\max_{\lambda \geq 0} \min_{x} [\frac{1}{2} x^T E x + x^T F + \lambda^T (Mx - \gamma)] \tag{5.28}$$

Because of the convexity of the Lagrangian function, the optimal x must be a stationary point of the Lagrangian function:

$$\nabla_x L(x, \lambda) = 0 \longrightarrow x = -E^{-1}(F + M^T \lambda) \tag{5.29}$$

If the expression for x from (5.29) is substituted in (5.28), the dual problem becomes

$$\max_{\lambda \geq 0}(-\frac{1}{2}\lambda^T H\lambda - \lambda^T K - \frac{1}{2}F^T E^{-1}F) \tag{5.30}$$

where the matrices H and K are defined as

$$H = ME^{-1}M^T \tag{5.31}$$

$$K = \gamma + ME^{-1}F \tag{5.32}$$

The Lagrangian dual of the QP problem is another QP problem with λ as the decision variable and with only nonnegative constraints. Expression (5.30) can be transformed into a minimization problem as follows,

$$\min_{\lambda \geq 0}(\frac{1}{2}\lambda^T H\lambda + \lambda^T K + \frac{1}{2}F^T E^{-1}F) \tag{5.33}$$

It can be noticed that the primal optimization problem had n variables and m inequality constraints, while the dual optimization problem has m variables and m nonnegative constraints. This makes the dual QP more computationally attractive, especially for the case when there are more primal variables, n than the number of constraints, m.

5.3.1.2 Hildreth's algorithm

The algorithm used in this research to solve the QP optimisation problem related to the implementation of the MPC controllers was elaborated by Hildreth [Hildreth, 1957]. It is a simple algorithm, based on a row-action method and proved to be very efficient in solving large sparse quadratic programs [Herman and Lent, 1978]. Other references to the algorithm can be found in Wismer and Chattergy [1978] and Luenberger [1969]. The QP problem has the same definition as in (5.23) and all other variables used in the description of the algorithm have the same meaning as they

were previously defined. The description of the method below is based on the one given in Wang [2009].

The direction vectors are chosen to be equal to the basis vectors $e_i = [0\ 0\ ...\ 1\ ...\ 0\ 0]^T$. At each step of the algorithm, after a vector $\lambda \geq 0$ is calculated, the objective function in a single component λ_i is considered. The value of λ_i is adjusted as to minimise the objective function. If a negative λ_i is required, then it is set $\lambda_i = 0$. The procedure is repeated for the next component λ_{i+1}. If the λ vector for the m-th iteration is written as λ^m, then for the next iteration, the components of the vector λ^{m+1} can be calculated as,

$$\lambda_i^{m+1} = \max(0, w_i^{m+1}) \tag{5.34}$$

with w_i^{m+1} calculated as

$$w_i^{m+1} = -\frac{1}{h_{ii}}[k_i + \sum_{j=1}^{i-1} h_{ij}\lambda_j^{m+1} + \sum_{j=i+1}^{n} h_{ij}\lambda_j^m] \tag{5.35}$$

In expression (5.35), h_{ij} defines the ij-th element in the matrix H from (5.31) and k_i is the i-th element in the vector K from (5.32). Substituting the converged vector, λ^* in (5.29) it results

$$x = -E^{-1}(F + M^T\lambda^*) \tag{5.36}$$

There is no need for any matrix inversion, as Hildreth's algorithm performs an element by element search. If the number of the active constraints is less than or equal to the number of decision variables and they are linearly independent, then there will be a solution for the dual problem. If any or all of the two conditions above are violated, then the algorithm will not converge to a set of dual variables. The

algorithm will stop when the iteration counter will reach its maximum value. The advantage is that the algorithm will provide a near-optimal solution, even for the case when not all the constraints can be satisfied. So even when the QP problem is ill-conditioned and the end of the iterations, the algorithm will provide a control input value, which will allow the safety operation of the process. When there is no conflict situation, the algorithm will converge to the set of λ^*. The vector λ^* contains zeros for inactive constraints and non-negative values for active constraints. λ^*_{act} is a vector containing all the positive components, which is defined by

$$\lambda^*_{act} = -(M_{act}E^{-1}M^T_{act})^{-1}(\gamma_{act} + M_{act}E^{-1}F) \tag{5.37}$$

where M_{act} and γ_{act} are obtained from the constraints matrices M and γ, from which the rows corresponding to the zero elements in λ^* have been deleted.

The Hildreth's algorithm was coded using FORTRAN 95 programming language, which was later attached to the main routine of the DMC controller.

5.4 The control system architecture implemented in the supercritical power plant simulator

Fig. 5.4 represents the existing control structure of the CCS implemented in the power plant. The controlled variables are: the main steam pressure, p_{ms}, the main steam temperature, T_{ms}, and the electrical power, P_e. The CCS unit receives the load demand signal from the grid, calculates the deviations from the set-point values for the controlled variables and sends the turbine and boiler commands, which then reach the appropriate control systems. The turbine command is sent to the HP turbine valve control system and this decides the valve position of the turbine. The boiler

command is sent to the coal mill and feedwater pump control system. These control systems decide the required values for the coal flow rate and for the feedwater flow rate. The turbine valve position, coal flow rate and feedwater flow rate are input variables for the boiler-turbine-generator model.

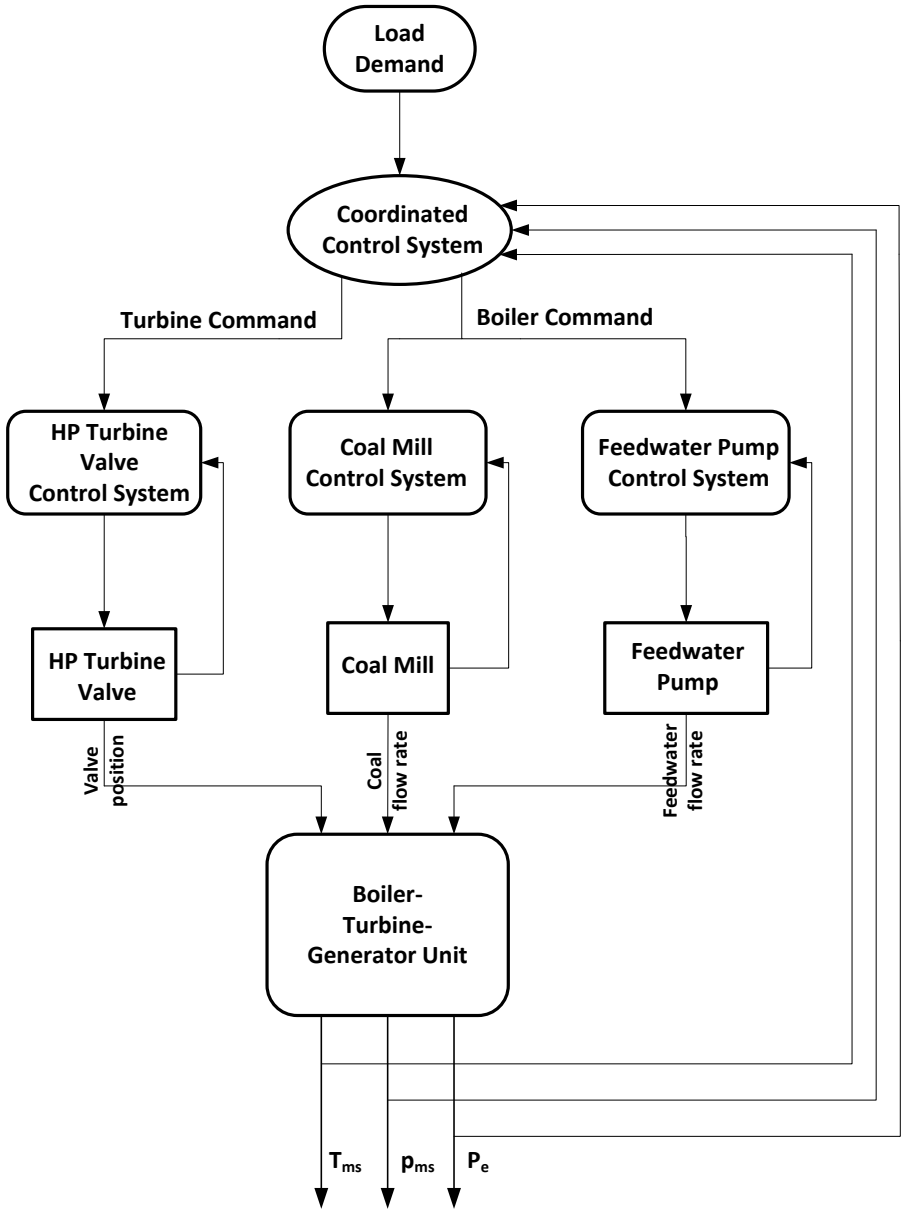

FIGURE 5.4 Existing power plant control system architecture

5.4.1 Coal mill control strategy implemented in the simulator

The control system of a supercritical power plant needs to be well designed and well tuned in such a way, that it allows the power plant to provide fast responses to changes in load demand [Mohamed *et al.*, 2012]. Coal preparation is the first step in the power generation process and the pulverized coal flow rate sent to the boiler determines the total power generation. An increase of the power generation means an increase of the steam flow rate and this in turn means an increase of the coal flow rate sent to the boiler by the coal mills. As a result, an adequate control of the coal mills is one of the key factors to achieve the desired overall power plant performance. This is challenging due to the fact that mill's response depends on the coal quality and wetness, mill wear and on its working principle [Waddington and Maples, 1987].

The necessary coal for the operation of the power plant is provided by six pulverizing coal mills, five of them in continuous operation and one being in stand-by as a reserve. More or less pulverized coal is sent to burners by the coal mills, by adjusting accordingly the speed of the coal feeders. The existing control loop of the coal mill is based on a PID controller.

The speed command, $\mathbf{v_f}$, is generated by the PID controller, which minimizes the error between the set-point value for the coal flow rate, $\mathbf{w_{coal}^{set}}$, and the process value represented by the total coal flow rate, $\mathbf{w_{coal}}$, sent to the furnace at the current time sampling. The set-point value for $\mathbf{w_{coal}^{set}}$ iscalculated as a function of the air flow rate, $\mathbf{w_{air}}$, and the current load demand, P.

The control strategy presented above is better illustrated by the control diagram shown in Fig. 5.5.

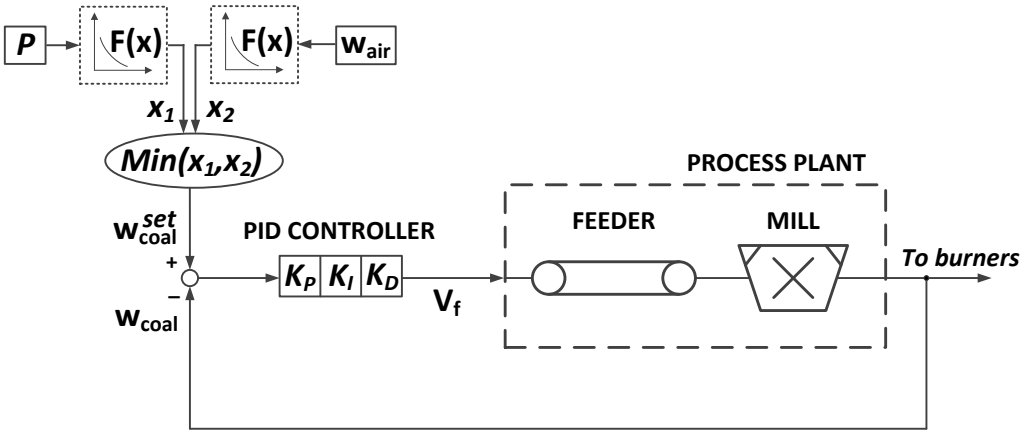

FIGURE 5.5 PID based control loop of the coal mill

PID controllers are currently the most used controllers in industry, due to their good control performance, simplicity in design and control structure, technology maturity and relatively good robustness [Sung *et al.*, 2009]. However PID controller has its limitations, namely it is tuned without taking into account the constraints on the process input signal [Tatjewski, 2007], it doesn't consider the future implications of current control actions [Rossiter, 2004] and it is very difficult to tune PID controllers to achieve the satisfactory or desired performance for Multi Input Multi Output (MIMO) systems [Rossiter, 2004; Gawthrop and Nomikos, 1990].

5.5 Development of the DMC controller

Due to development of computing technology in recent years, advanced control techniques, such as MPC, which has the capability to address previously mentioned disadvantages of PID controller, can now be easily implemented.

Given the importance of the coal flow control in the power generation process, it is proposed to replace the existing Coal Mill Control System, as it is presented in Fig. 5.4 with a DMC controller. This controller will have the structure illustrated in Fig. 5.6, where $\mathbf{w}_{\mathbf{coal}}^{\mathbf{pred}}$ is the predicted coal flow rate and the rest of the variables have the same definitions as the ones used for the variables from Fig. 5.5.

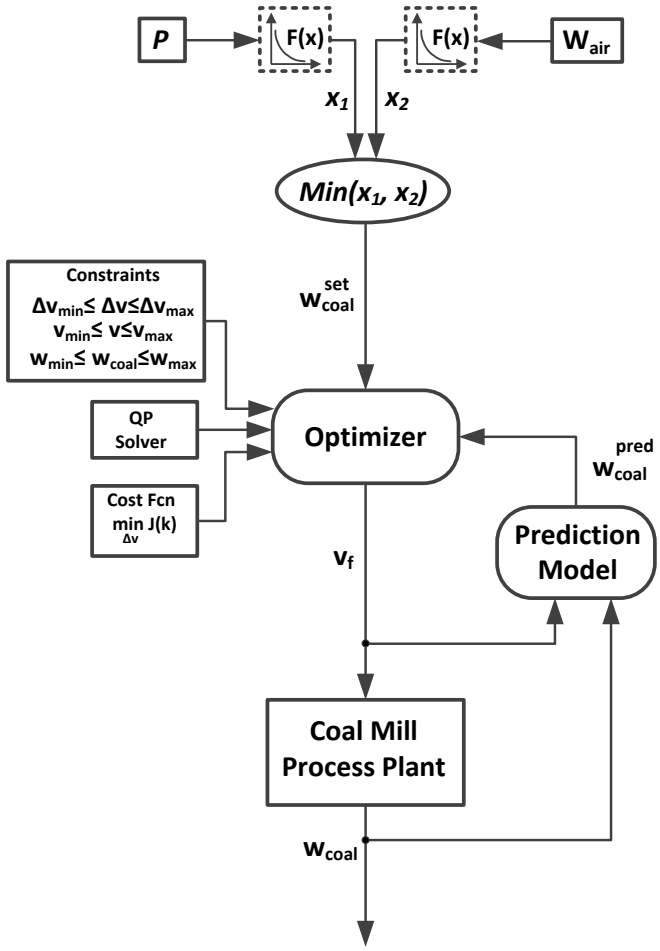

FIGURE 5.6 Structure of the coal mill control loop based on the DMC controller

Following the implementation of the DMC controller, the control system architecture of the power plant simulator changes as it is illustrated in Fig. 5.7.

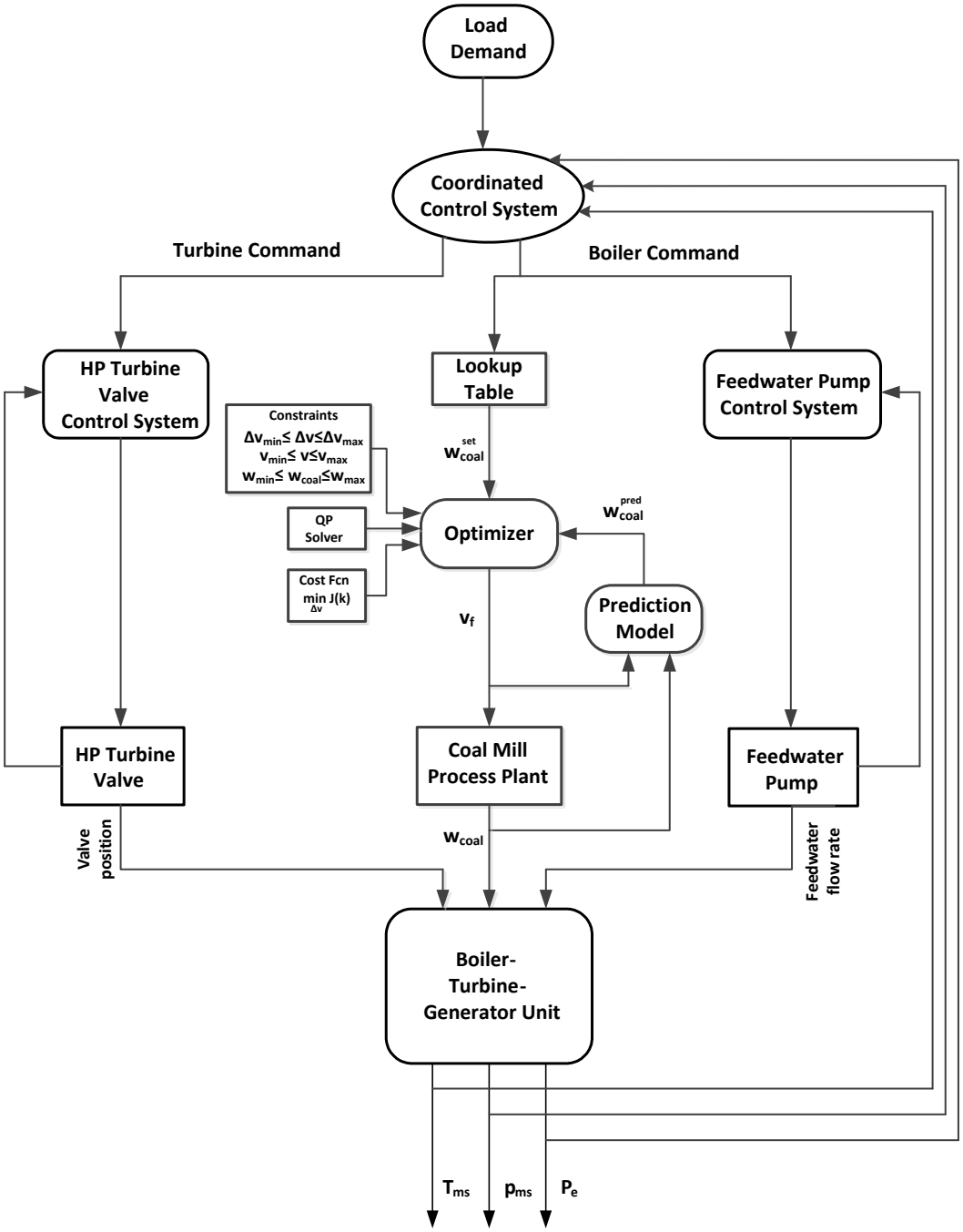

FIGURE 5.7 Power plant control system architecture with the DMC controller integrated in it

5.5.1 Identification of the unit step response model

To calculate the predictions of process outputs, the DMC algorithm uses a process model in the form of a unit step response model.

Two methods can be used to obtain this model [Moon and Lee, 2005].

- The first one assumes that the nonlinear mathematical model of the process is known. Thus one can simulate the response of the system to a step input change and obtain a step response model.
- In the second approach, a step change to the input signal is applied to the real process and the model is identified from the experimental data collected.

In this research the second approach was used for model identification.

Particular attention must be paid to the choice of the amplitude of the step change signal. If it is too large the process output might get into a nonlinear region and if it is too small the output might be affected by disturbances and noise [Moon and Lee, 2005].

The process plant has the speed command, $\mathbf{v_f}$ sent from the PID as input and the coal flowrate, $\mathbf{w_{coal}}$ as output.

From the steady state operation of the power plant simulator at 550 MW power generated, a 20% step increase of the speed command sent to the coal mills was considered the best for model identification. It needs to be mentioned that this step change test was performed with the power plant simulator control system operating in manual mode. This means that all the control variables had a constant value before the test started. Referring to the coal mill control system, this implies that the speed

command, $\mathbf{v_f}$ as the PID controller output variable, was stepped with 20% for the identification test.

The output response was then normalized by dividing the output with the amplitude of the corresponding input. The processed output response represents the unit step response of the process plant as it is illustrated in Fig. 5.8.

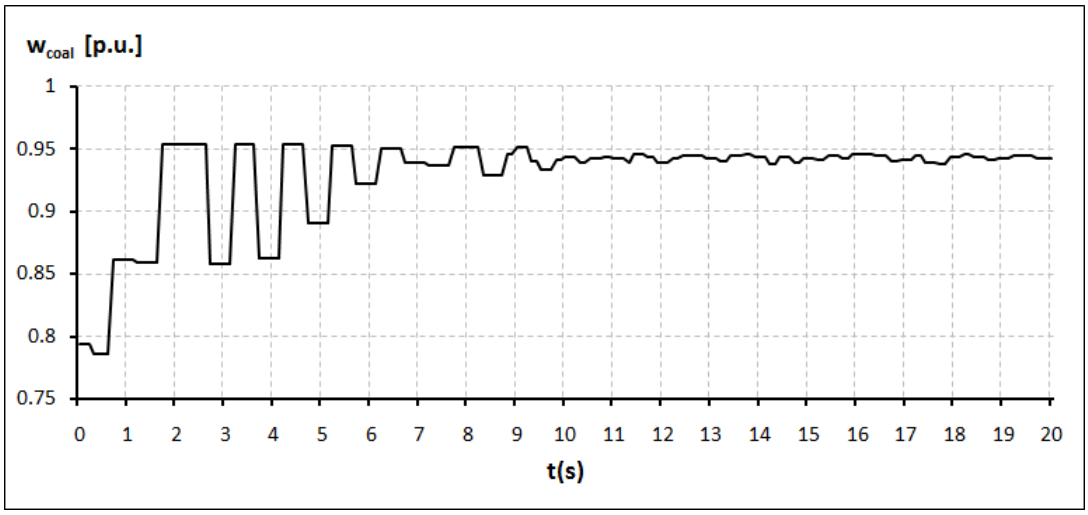

FIGURE 5.8 The unit step response model used to calculate the predicted outputs by the DMC controller

Analysing the unit step response model from Fig. 5.8, one can observe the similarity with the step response from a First Order Plus Time Delay (FOPTD) model. The mathematical expression defining the model is

$$G(s) = \frac{ke^{-\theta s}}{\tau s + 1} \tag{5.38}$$

where k is the static gain, θ is the time delay and τ is the time constant.

The parameters of the model were found by using the process reaction curve method, which is illustrated in Sung *et al.* [2009]. This method uses a step input test to

identify the approximated FOPTD model for a process. The step input u_∞ is applied to the process and its response follows the trajectory shown in Fig. 5.9, until it stabilises at the steady state value y_∞. Higher order processes, having a similar response can thus be assimilated by a FOPTD model.

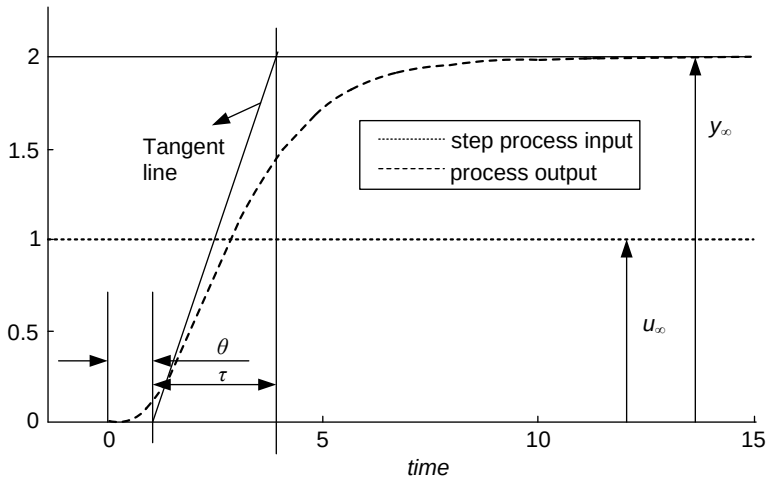

FIGURE 5.9 Typical response from a stable and overdamped process generated by a step input test [Sung *et al.*, 2009]

The tangent line is drawn at the point of inflexion and from a visual inspection the time delay θ and the time constant τ can be identified. The static gain k can then be calculated as the ratio of the process output y_∞ to the step input u_∞.

The parameters for the FOPTD model whose process response is illustrated in Fig. 5.8 are: $k = 0.9417$, $\theta = 0.6$, $\tau = 1.7$. Substituting these values into the expression of the model from (5.38) it results

$$G(s) = \frac{0.9417e^{-0.6s}}{1.7s + 1} \tag{5.39}$$

The sampling time recommended for discrete control should be less than 10% of the time constant [Moon and Lee, 2005]. With the calculated time constant and following the above recommendation, a time sample of 0.1 s was chosen for the discretisation of the model. The number of coefficients used to define the unit step response model for the DMC controller is determined by how many time samples are necessary until the process stabilises after a step change in the input [Tatjewski, 2007]. For this case, the model is defined by 147 coefficients.

5.5.2 Tuning parameters of the DMC controller

The performance of the DMC controller can be adjusted by manipulating four parameters: the predicted output weights, $\underline{\Psi}$ the control input weights, $\underline{\Lambda}$ the prediction horizon, N and the control horizon, N_u [Tatjewski, 2007].

If a more aggressive control action and a faster response from the system is expected from the DMC controller, then this can be achieved by decreasing the prediction horizon, N, increasing the number of control moves from the control horizon, N_u and decreasing the control weights, $\underline{\Lambda}$. There is a lower limit for the prediction horizon, an upper limit for the control horizon and lower limit on the control weights beyond which the closed loop system becomes unstable [Maciejowski, 2002].

In this research, scaling of the influence of the components from the error vector, $Y^{sp} - Y^{pred}$ was not considered, so the matrix of the predicted output weights, $\underline{\Psi}$, is equal with the identity matrix I of dimension $(N - N_1 + 1) \times (N - N_1 + 1)$. The matrix of the control input weights, $\underline{\Lambda}$, is considered to have the same influence over all the control moves and therefore in its form $\underline{\Lambda} = \lambda I$, with the identity matrix, I of

dimension $N_u \times N_u$, the parameter λ was found through the procedure of trial and error to have the best selected value of 80. Following the same procedure the optimal values for the prediction horizon and the control horizon were found to be 200 and 110 respectively. The values of the constraints considered by the QP problem were: $U_{min} = 0$, $U_{max} = 1$, $\Delta U_{max} = 0.004$, $Y_{min} = 0$, $Y_{max} = 1$.

5.6 Simulation tests of the DMC controller performance

The control system of the power plant simulator is based on PID controllers and adding to this the nonlinear dynamic behavior of the process, means that it can only be tuned to give an optimal performance at one operating point and just an acceptable performance at other operating points.

Two initial simulation tests were run to check the performance of both controllers:

- Test 1

With the power plant operating at steady state conditions, generating 550 MW, a step increase of 25 MW in the load demand signal is performed.

- Test 2

With the power plant operating at steady state conditions, generating 550 MW, a step decrease of 25 MW in the load demand signal is performed.

Throughout both simulation tests, the variables monitored were coal feeder speed command and coal flow rate. The simulation results gathered after the first test, were plotted in Fig. 5.10 - Fig. 5.13.

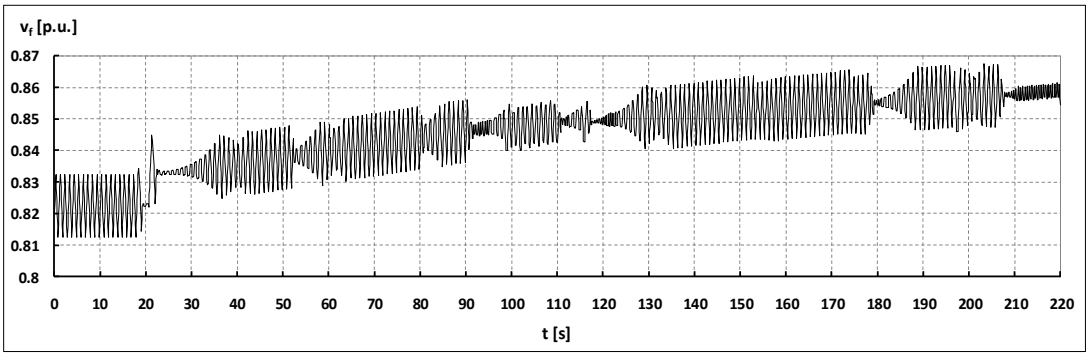

FIGURE 5.10 PID controller in operation. The evolution of the speed command signal sent to the coal feeder for a 25 MW step increase in the load demand.

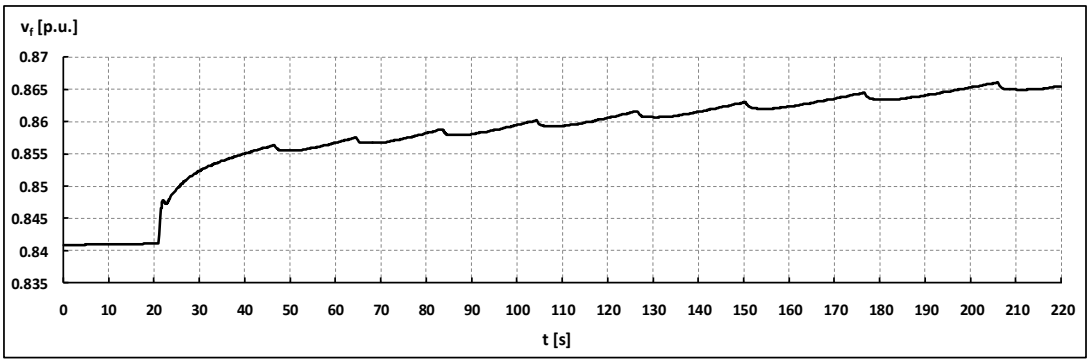

FIGURE 5.11 DMC controller in operation. The evolution of the speed command signal sent to the coal feeder for a 25 MW step increase in the load demand.

During the steady state operation, the signal sent by the PID controller is presenting a continuous variation in time, which is then manifested even more intensely after the step change in the load demand. Compared to this, the signal sent by the DMC controller presents the same amplitude before the test is initiated and afterwards its amplitude is increasing in a steady manner.

The service life of the electric motor of the coal feeder is increased for a more constant operation as is the case for the signal sent by the DMC controller and is shortened for a continuously varying control signal sent by the PID controller.

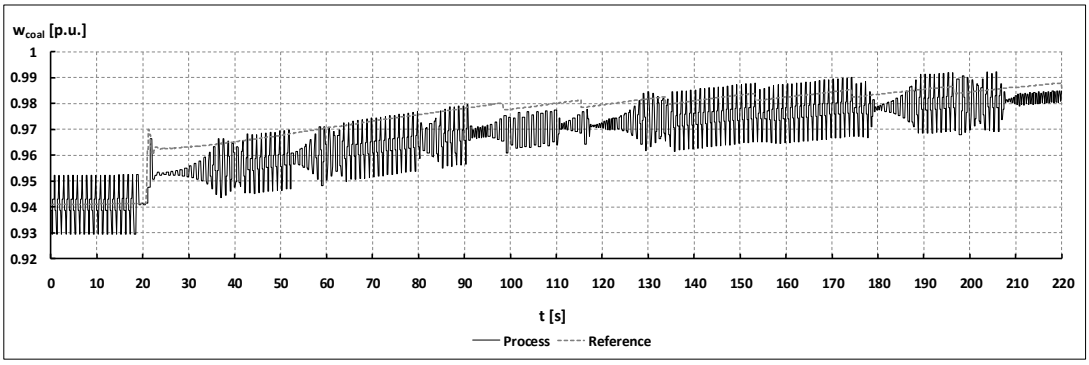

FIGURE 5.12 PID controller in operation. The evolution of the coal flow rate sent to the burners by the coal mill for a 25 MW step increase in the load demand.

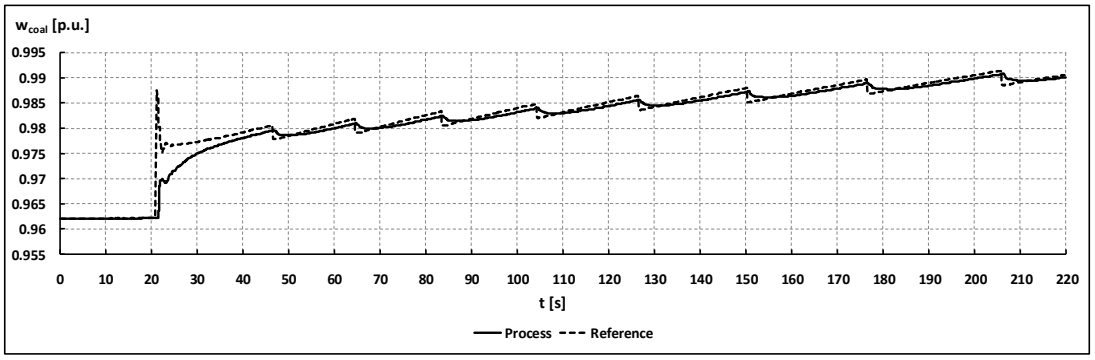

FIGURE 5.13 DMC controller in operation. The evolution of the coal flow rate sent to the burners by the coal mill for a 25 MW step increase in the load demand.

The set-points trajectory is very well tracked by the coal flow rate, when using the DMC controller and is poorly followed when the PID is in operation. The mean absolute error between the trajectories is 0.005 for the DMC controller and 0.01 for the PID controller.

There is a sudden increase in the set-points trajectory, immediately after the change in the load demand is initiated, which is followed by the output variable when the PID controller is used and which is ignored for the other controller. This behaviour

of the output variable is generated by the constraints applied by the DMC algorithm to the rate of change of the control signal.

All the results gathered from the second simulation test were processed into the graphs presented in Fig. 5.14 - Fig. 5.17.

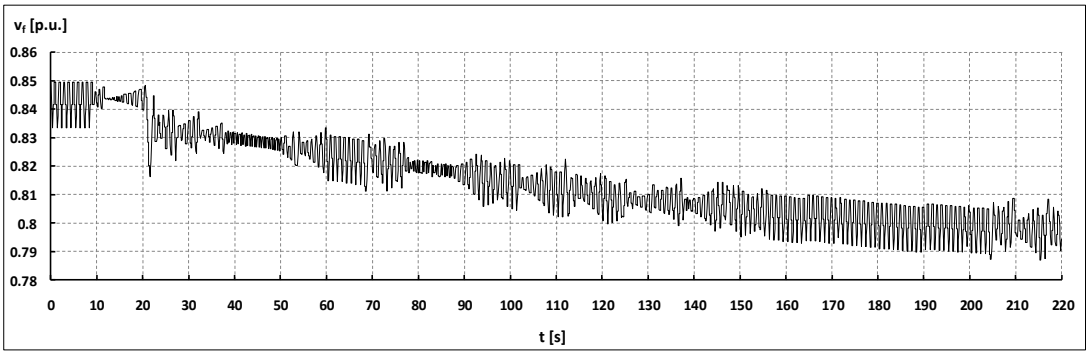

FIGURE 5.14 PID controller in operation. The evolution of the speed command signal sent to the coal feeder for a 25 MW step decrease in the load demand.

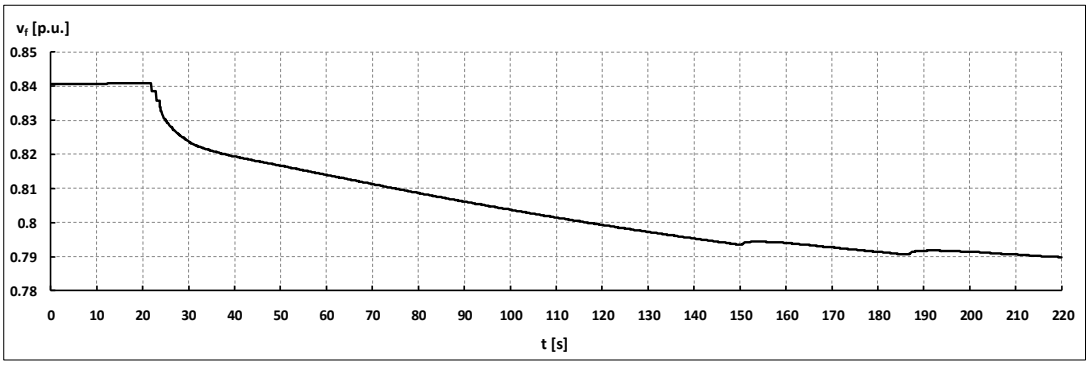

FIGURE 5.15 DMC controller in operation. The evolution of the speed command signal sent to the coal feeder for a 25 MW step decrease in the load demand.

Analysing both graphs from the above figures, it shows a very similar performance for both controllers during the second simulation test as compared to the first one.

The PID control signal is varying all the time, while the DMC control signal presents a very stable trajectory.

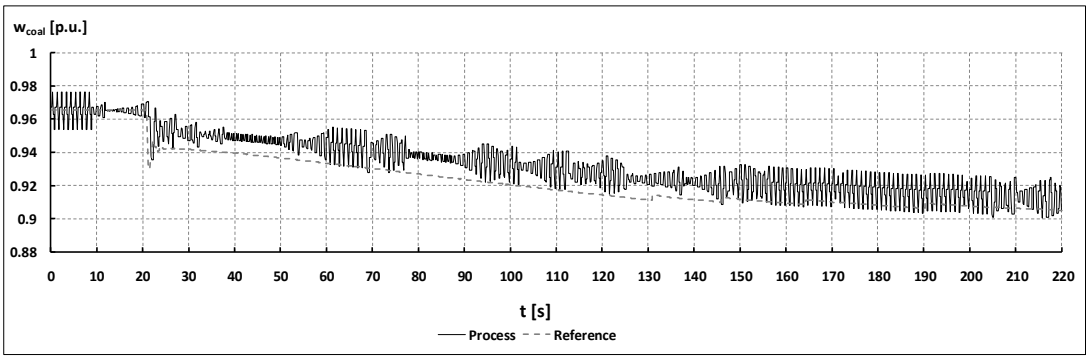

FIGURE 5.16 PID controller in operation. The evolution of the coal flow rate sent to the burners by the coal mill for a 25 MW step decrease in the load demand.

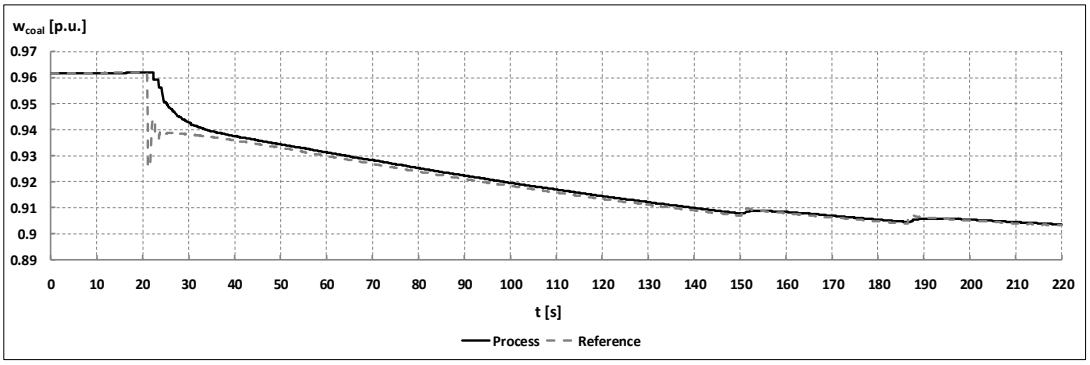

FIGURE 5.17 DMC controller in operation. The evolution of the coal flow rate sent to the burners by the coal mill for a 25 MW step decrease in the load demand.

The output variable, the coal flow rate follows very closely the set-points trajectory for the DMC controller in operation, having a mean absolute error of 0.001, compared to a value of 0.02, when using the PID controller. The constraints on the rate of change of the control signal prevents the undershoot of the coal flow rate,

after the step change in the load demand was initiated, for the case when DMC controller regulates the process.

For both simulation tests, the DMC controller outperformed the PID controller. The evolution in time of the control signal sent by the PID controller suggests that it might be poorly tuned for this operating point of the power plant.

Given the above consideration, another simulation test was performed, this time for the power plant operating at steady state conditions for 450 MW (75%) power output. From this operating level a step load change of 50 MW up to 500 MW (83%) nominal load is run. The evolution of the coal flowrate subject to PID control is presented in Fig. 5.18.

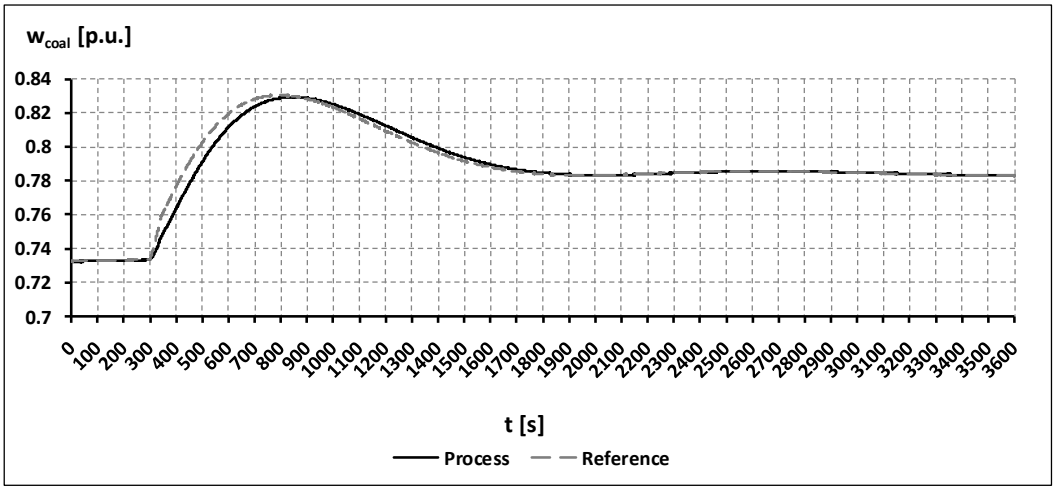

FIGURE 5.18 The evolution in time of the coal flow rate sent to the burners by the coal mill for a 50 MW step increase in the load demand under PID control

The parameters characterising the above controlled signal are:

- Overshoot [p.u.] = 5.94;
- Rise time [s] = 167.8;

- Settling time [s] = 1586.6.

The definition for the rise time is the time needed by the signal to get from 10% to 90% of the steady state value and the one for the settling time is the time needed by the signal to settle within ±5% of the steady state value. It can be observed that there is a good tracking of the reference trajectory with a maximum absolute error of 0.0132.

The trajectory of the coal flowrate using the DMC control strategy is illustrated in Fig. 5.19.

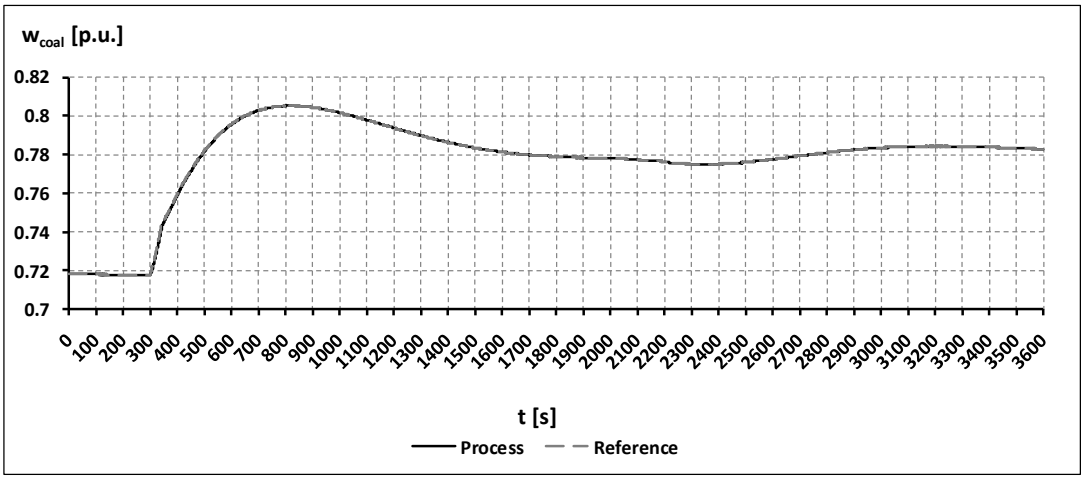

FIGURE 5.19 The evolution in time of the coal flow rate sent to the burners by the coal mill for a 50 MW step increase in the load demand under DMC control

The parameters characterizing the controlled signal are:

- Overshoot [p.u.] = 2.86;
- Rise time [s] = 207.5;
- Settling time [s] = 1540.5.

As is depicted in Fig. 5.19, there is almost no error between the reference and the process trajectory, with a maximum absolute error of 0.0018. This means the error is reduced with 86.4% compared to the PID case. A good tracking of the reference trajectory by the coal flowrate has a positive impact on the response time of the boiler to changes in the load demand.

For comparison purposes, both coal flowrate trajectories for PID and for DMC controller are plotted in the same graph, as presented in Fig. 5.20.

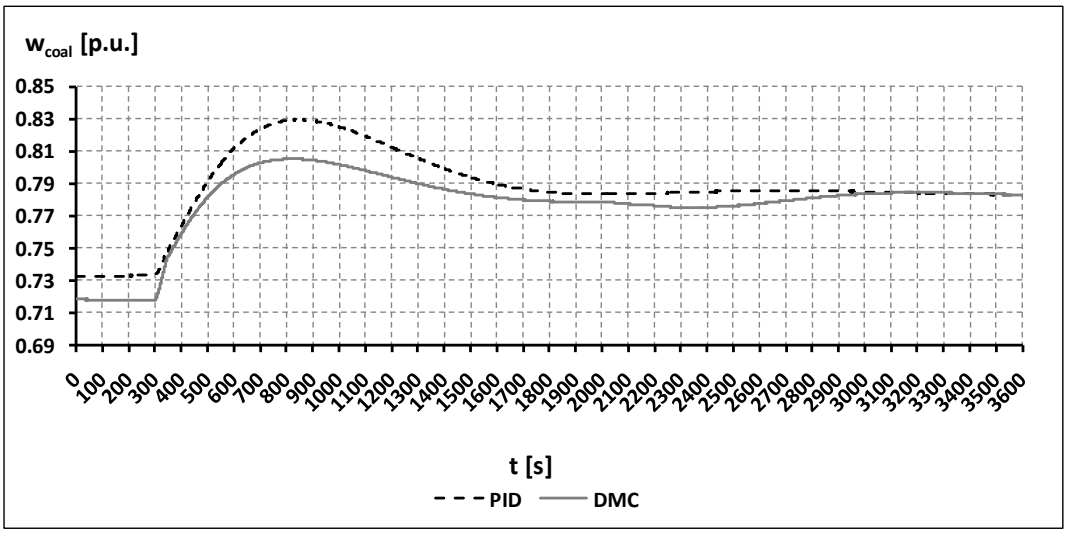

FIGURE 5.20 The trajectories followed by the coal flow rate signal under PID control and under DMC control

It shows that even for steady-state operation, DMC controller has a better management of the coal, the flowrate value being smaller than for PID controller.

After the step load change is sent to the power plant, the overshoot using DMC controller is less than 50% of the value when using PID controller. In the PID control

case the increase in coal flowrate is nearly 40 s faster, but the settling time is similar for both controllers.

The fact that the coal flowrate trajectory having the DMC controller on, is situated below the trajectory for the PID controller indicates that less coal is used to generate the same power output. For the ease of calculation the coal flowrate values are expressed in the simulator using the per unit system. The base quantity is obtained by considering that each coal mill is providing a coal flowrate of 13.168 kg/s. There are five working coal mills, so it results that the coal flowrate base value is 65.84 kg/s.

Integrating the area under each trajectory, it results that 186.71 t of coal were used with the PID on, compared with 184.44 t of coal when having the DMC controller implemented. The difference of the two values shows that a saving of 2.27 t was made during an hour operation by using the DMC controller. The control signal sent to the coal feeder motor during the test is plotted for both controllers in Fig. 5.21.

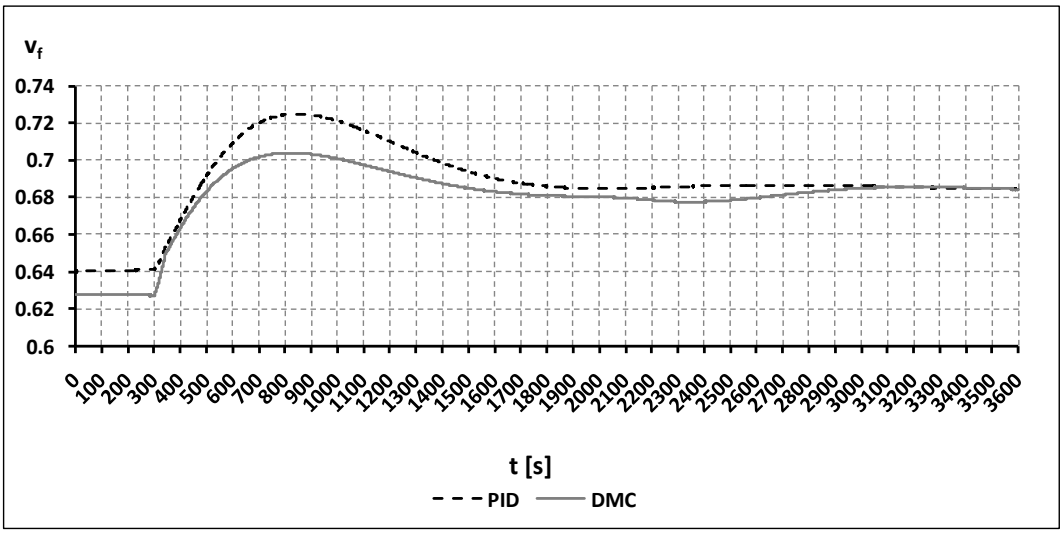

FIGURE 5.21 The trajectories followed by the control signal sent to the coal feeder by the PID controller and by the DMC controller.

The control signal is regulating the motor speed of the coal feeder and as is described by Fig. 10 it has smaller amplitudes when the DMC controller is in use. The maximum control amplitude is 3% smaller than the one sent by PID controller.

The response of the power plant, regarding the generated power is the same for both controllers and this is illustrated by Fig. 5.22.

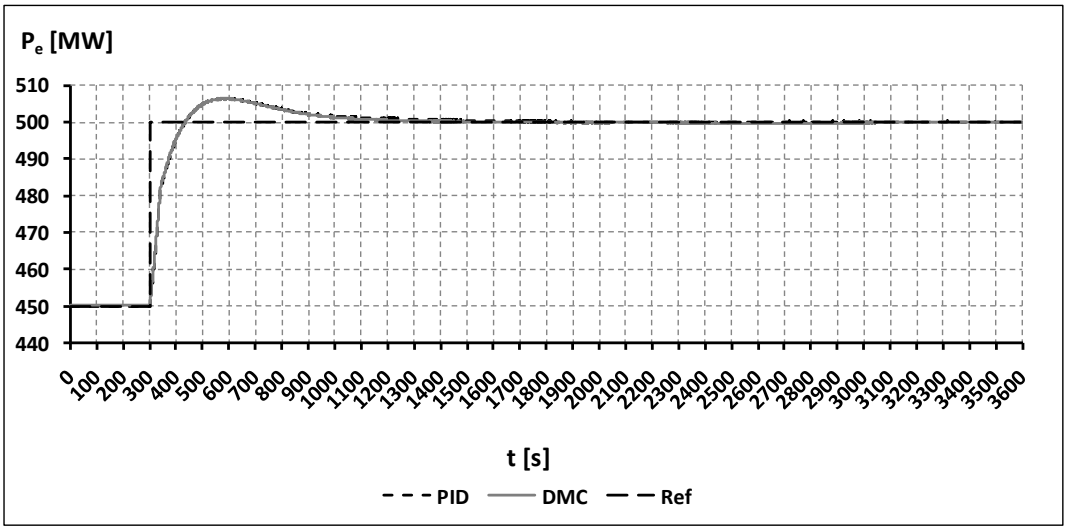

FIGURE 5.22 The trajectories of the power output generated by the power plant for PID controller and DMC controller in operation

During this test other significant process variables were monitored. The steam pressure evolution for both controllers is described in Fig. 5.23.

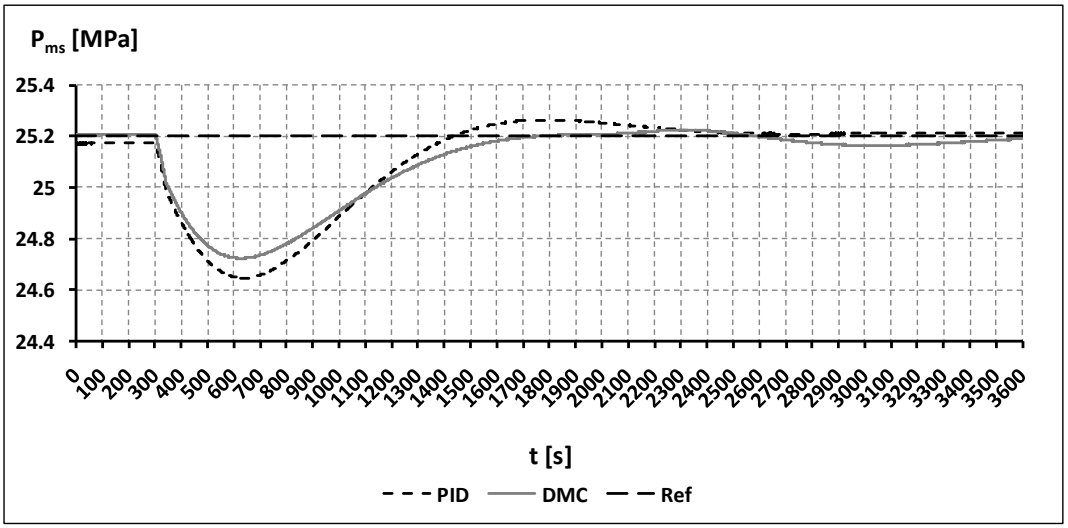

FIGURE 5.23 The evolution through time of the main steam pressure both for the PID controller and for the DMC controller in operation.

The set-point value for the pressure is 25.2 MPa. A comparative numerical analysis is given below:

PID controller in operation

- peak error -0.55 ~ 0.06 MPa
- standard deviation 0.19 MPa
- settling time 2500 s

DMC controller in operation

- peak error -0.48 ~ 0.03 MPa
- standard deviation 0.16 MPa
- settling time 1700 s

From steady-state operation there is no steady-state error when the DMC controller is operating. After the step load change occurs, the pressure drop is 14% more and the

settling time is with 800 s longer using the PID controller, than when the test is run with the DMC controller.

The superheated steam temperature values were recorded throughout the test for both controllers and the trajectories are plotted in Fig. 5.24.

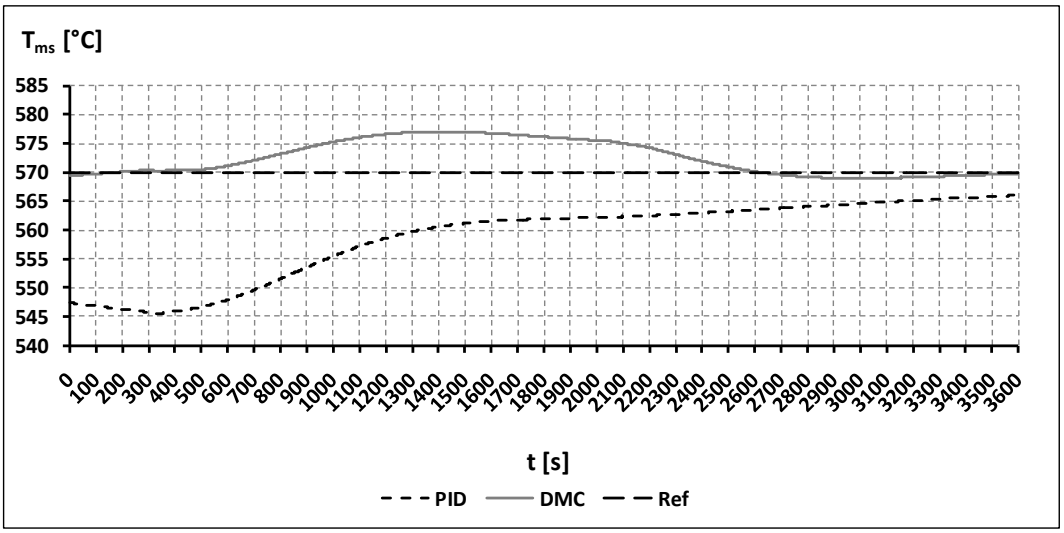

FIGURE 5.24 The evolution through time of the main steam temperature both for the PID controller and for the DMC controller in operation.

Using the DMC controller has a good effect on the superheated steam temperature even from the steady-state operation of the power plant. Its trajectory is very close to the reference trajectory, which is not the case when using the PID controller.

The performance of the controllers regarding the temperature is quantified by the following parameters:

<u>PID controller in operation</u>

- peak error -24.55 ~ -3.99 ºC
- standard deviation 6.8 ºC

- settling time >3600 s

DMC controller in operation

- peak error -1.03 ~ 7.05 ºC
- standard deviation 2.98 ºC
- settling time 2500 s

The set-point value for the superheated steam temperature is 570 ºC. The average steam temperature when the PID is in use, is 558.7 ºC, while its value is 572.48 ºC with the DMC controller in operation. So there is a 2% difference for the PID case and 0.43% for the DMC case. While the temperature is settled after nearly 42 minutes when the DMC is in operation, it takes more than 60 minutes to reach a stable value when the PID controller is used. Keeping the steam temperature at a constant value is very important for the power plant efficiency and also for the lifetime of the boiler and steam turbine, by minimizing the thermal stresses.

5.7 Summary

The chapter begins with an introduction to the advanced family of control algorithms entitled MPC. One algorithm that was successfully implemented in industrial applications is the DMC algorithm, whose structure is presented for the case of a SISO system. The control inputs are calculated by solving a QP problem, which is carried out in this research by using Hildreth's algorithm.

The power plant simulator is regulated by a CCS, whose operation is described and all the manipulated and control variables are defined. Of utter importance to the dynamic response of the power plant is the coal mill control. The existing control

strategy is based on a PID controller, which doesn't provide an optimal regulation. In order to improve the performance of the coal mill control system a DMC controller was proposed to replace the existing PID controller.

Several simulation tests were performed in order to assess the performance of the DMC controller against that of the existing PID one. Initial tests consisted in an increase/decrease with 25 MW of the 550 MW power output level, while the variables monitored were: the coal feeder speed command and the coal flow rate. Another test referred to a step load change of 50 MW from the power plant operating at 450 MW power output. During this test the monitored variables were: the coal flowrate, the coal feeder speed command, the power output, the steam pressure and the superheated steam temperature. The results gathered from all tests were used to perform a comparative numerical analysis and they were then plotted into graphs, all showing an improved performance when the DMC controller was in use.

Chapter 6

Superheated Steam Temperature Regulation Based on Generalized Predictive Control Algorithm

6.1 Introduction to superheater steam temperature control

Steam temperature control at the superheater's (SH) outlet is one of the most challenging control loop in a fossil fuelled power plant. The difficulty in controlling this system is mainly due to the high nonlinearity of the SH, long time delays and the disturbances coming from the flue gases [Hlava, 2010; Fu *et al.*, 2013].

If the temperature is kept constant, with only small variations, the set-point for the steam temperature can be higher, which will increase power plant efficiency. If the temperature is kept stable, the lifetime of the boiler and steam turbine are also increased, as the thermal stresses are minimized [Fu *et al.*, 2013].

The new regulations regarding CO_2 emissions, the increasing power generation from wind farms and the European energy market deregulation, have all changed the operating requirements for a power plant [Ziems and Weber, 2009]. Initially designed to operate at base load, at their almost full capacity, nowadays power plants need to be flexible, efficient and capable of following the changes in the load demand [Fu *et al.*, 2013]. Considering all the above mentioned, keeping the steam temperature in certain limits is of crucial importance.

Due to its good control performance, simplicity, technology maturity and good robustness [Sung *et al.*, 2009], the PID controller is still the most used in the steam temperature control loops. However, due to large changes in the load demand and the

transients which follow in the combustion process the performance of the PID controller is far from being optimal [Gough, 2000]. This motivates the use of other type of controllers, such as model-based controllers.

The MPC algorithm chosen for the regulation of the SH outlet steam temperature is Generalized Predictive Control (GPC). One characteristic of GPC algorithm is that it can deal with unstable and non-minimum phase plants [Camacho and Bordons, 2007]. The GPC algorithm was developed by Clarke *et al.* [1987] and it became popular both in industry and academia, with successful industrial applications [Clarke, 1988].

The use of the algorithm has been reported by Moelbak [1999], where the GPC controller showed a better performance against the existing PID controller, in regulating the superheated steam temperature in a real coal-fired power plant, equipped with a once-through boiler.

Another MPC algorithm, namely the DMC was used for the design of controllers intended to regulate the steam temperature and its successful implementation was reported in the following publications. A DMC controller for steam temperature control was developed by Fu *et al.* [2013] and tested in a power plant simulator and in a field operating coal-fired power plant having a drum boiler. According to the simulation tests, the DMC control strategy proved to outperform the PID based one.

Another successful implementation of a DMC controller for steam temperature regulation is reported by Kim *et al.* [2010], this time the controller was tested in a power plant simulator operating with a once-through boiler. Sanchez *et al.* [2004] developed a DMC and a fuzzy controller to regulate the steam temperature in a 300

MW power plant simulator. The controllers' performance is compared to the existing PID and the test results show a tighter temperature control when the advanced control strategies are used.

6.2 The GPC algorithm

The particularity of the GPC algorithm against the rest of the MPC algorithms is the use of a process model described by a discrete difference equation or equivalently a discrete transfer function. It can also deal with unstable systems as is the case with the SH. The part of the SH, which will be regulated by the new controller is a SISO process. The predictive controller is designed following the GPC algorithm for a SISO process, as it is described by Camacho and Bordons [2007] and by Clarke *et al.* [1987].

6.2.1 The prediction model

For a SISO process, the discretized model, linearized at a certain operating point, can be described by the following form:

$$A(z^{-1})y(t) = z^{-\theta}B(z^{-1})u(t-1) + C(z^{-1})\epsilon(t) \tag{6.1}$$

where $u(t)$ and $y(t)$ are the control and output sequences of the plant, θ is the dead time of the system and $\epsilon(t)$ is a zero mean white noise. A, B, C are polynomials in the backward shift operator z^{-1} of degrees n_a, n_b and n_c, respectively. The model described by the equation (6.1) is known as a Controller Auto-Regressive Moving-Average (CARMA) model.

6.2.2 The output predictions

To calculate the future plant output, $y(t+j)$ the following Diophantine equation is considered:

$$1 = \boldsymbol{E_j}(z^{-1})\bar{A}(z^{-1}) + z^{-j}\boldsymbol{F_j}(z^{-1}) \tag{6.2}$$

where the notation $\bar{A}(z^{-1}) = \Delta A(z^{-1})$ was used and the degrees of the polynomials $\boldsymbol{E_j}$ and $\boldsymbol{F_j}$ are $j-1$ and n_a.

Performing several manipulations with (6.1) and (6.2), the prediction $y(t+j)$ can be written as

$$y(t+j) = \boldsymbol{F_j}(z^{-1})y(t) + \boldsymbol{E_j}(z^{-1})B(z^{-1})\Delta u(t+j-\theta-1) + \\ + \boldsymbol{E_j}(z^{-1})\epsilon(t+j) \tag{6.3}$$

As the noise terms $\epsilon(t+j)$ are placed in the future, they can be disregarded and the output predictions have the expression,

$$\hat{y}(t+j|t) = \boldsymbol{G_j}(z^{-1})\Delta u(t+j-\theta-1) + \boldsymbol{F_j}(z^{-1})y(t) \tag{6.4}$$

where the notation $\boldsymbol{G_j}(z^{-1}) = \boldsymbol{E_j}(z^{-1})B(z^{-1})$ was used.

The vector y of N ahead predictions can be written as:

$$\mathbf{y} = \mathbf{G}\mathbf{u} + \mathbf{F}(z^{-1})y(t) + \mathbf{G}'(z^{-1})\Delta u(t-1) \tag{6.5}$$

where $\mathbf{y}$, $\mathbf{G}$, $\mathbf{u}$, $\mathbf{F}$, $\mathbf{G}'$ are defined as,

$$\mathbf{y} = \begin{bmatrix} \hat{y}(t+\theta+1|t) \\ \hat{y}(t+\theta+2|t) \\ \vdots \\ \hat{y}(t+\theta+N|t) \end{bmatrix} \quad \mathbf{u} = \begin{bmatrix} \Delta u(t) \\ \Delta u(t+1) \\ \vdots \\ \Delta u(t+N-1) \end{bmatrix}$$

$$\mathbf{G} = \begin{bmatrix} g_0 & 0 & \dots & 0 \\ g_1 & g_0 & \dots & 0 \\ \vdots & \vdots & \vdots & \vdots \\ g_{N-1} & g_{N-2} & \cdots & g_0 \end{bmatrix}$$

$$\mathbf{G}'(z^{-1}) = \begin{bmatrix} (G_{\theta+1}(z^{-1}) - g_0)z \\ (G_{\theta+2}(z^{-1}) - g_0 - g_1 z^{-1})z^2 \\ \vdots \\ \left(G_{\theta+N}(z^{-1}) - g_0 - g_1 z^{-1} - \cdots - g_{N-1} z^{-(N-1)}\right) z^N \end{bmatrix}$$

$$\mathbf{F}(z^{-1}) = \begin{bmatrix} F_{\theta+1}(z^{-1}) \\ F_{\theta+2}(z^{-1}) \\ \vdots \\ F_{\theta+N}(z^{-1}) \end{bmatrix} \tag{6.6}$$

It is noticed that the last two terms from (6.5) only depend on the past inputs and outputs and so they can be grouped together into **f**. Using this notation expression (6.5) can be written as

$$\mathbf{y} = \mathbf{Gu} + \mathbf{f} \tag{6.7}$$

6.2.3 The control law

At each sampling instant the GPC algorithm is minimizing a cost function of the form

$$J(N, N_u) = \sum_{j=1}^{N} \delta(j) \left[\hat{y}(t+j|t) - \mathrm{W}_{\mathrm{sp}}(t+j)\right]^2 + \cdots$$

$$+ \sum_{j=1}^{N_u} \lambda(j) \left[\Delta u(t+j-1)\right]^2 \tag{6.8}$$

where N is the prediction horizon, N_u is the control horizon, $\delta(j)$ and $\lambda(j)$ are weighting sequences and $\mathrm{W}_{\mathrm{sp}}(t+j)$ is the future reference trajectory.

The cost function from (6.8) can be rewritten using the matrices defined in (6.6) and (6.7), where for simplicity in derivation $\delta(j)$ is considered to have the value of unity and $\lambda(j)$ is set to the constant λ, which gives the following expression:

$$J = (\mathbf{Gu} + \mathbf{f} - \mathbf{W})^T (\mathbf{Gu} + \mathbf{f} - \mathbf{W}) + \lambda \mathbf{u}^T \mathbf{u} \tag{6.9}$$

where $\mathbf{W}$ is the vector of future reference trajectory, being defined as

$$\mathbf{W} = [\mathrm{W_{sp}}(t+\theta+1)\ \mathrm{W_{sp}}(t+\theta+2)\cdots\ \mathrm{W_{sp}}(t+\theta+N)]^T \qquad (6.10)$$

If no constraints are applied to the control signals, the solution to the optimization problem can be found by making the gradient of J equal to zero. The control inputs vector is

$$\mathbf{u} = (\mathbf{G}^T\mathbf{G} + \lambda\mathbf{I})^{-1}\mathbf{G}^T(\mathbf{W} - \mathbf{f}) \qquad (6.11)$$

From the vector $\mathbf{u}$ only the first element of the vector represents the control signal which is actually sent to the process.

6.3 Description of the SH process

6.3.1 Structure of the SH

The structure of the SH implemented in the power plant simulator, together with the process inputs and outputs is illustrated in Fig. 6.1.

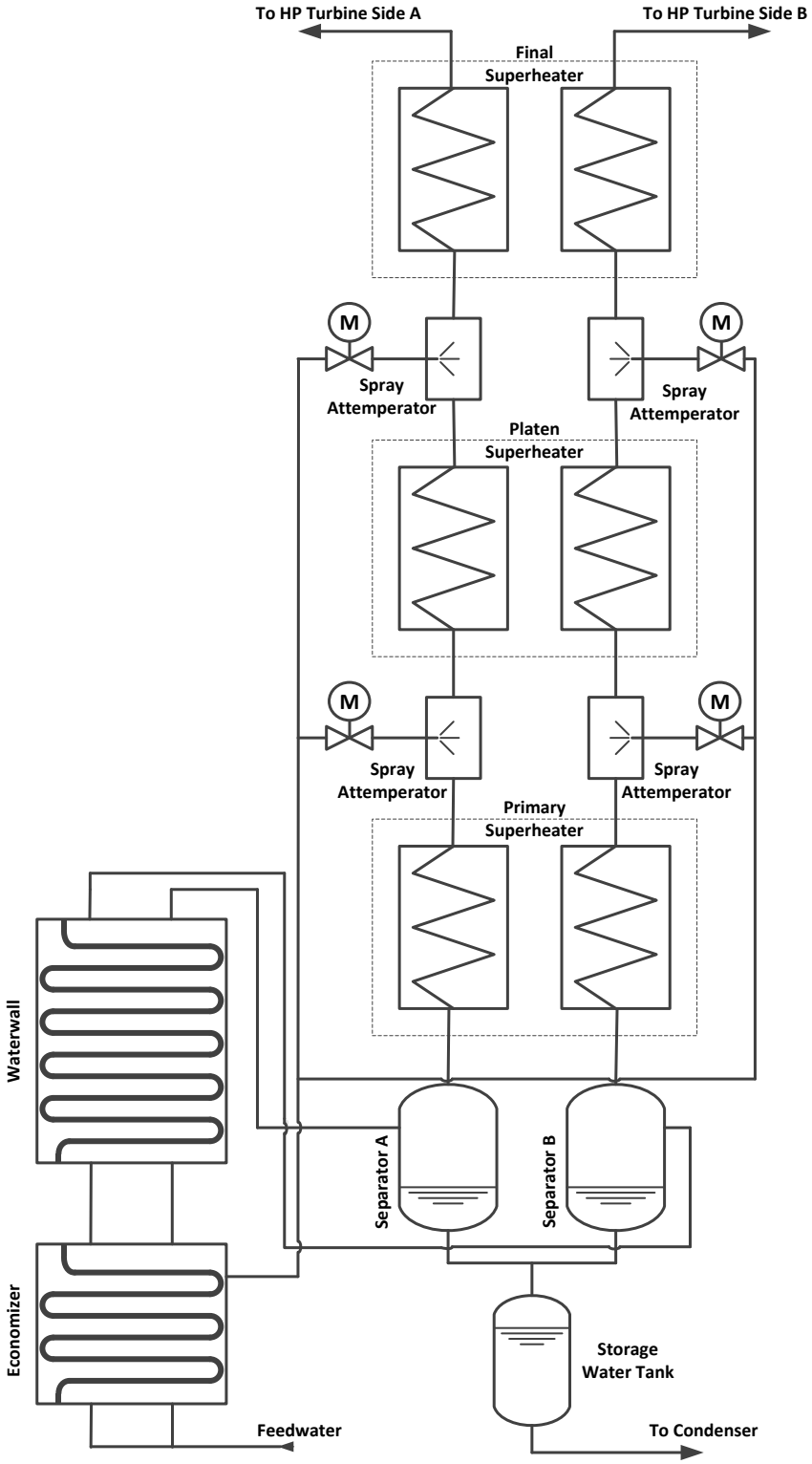

FIGURE 6.1 The structure of the SH and its connections to other systems

The SH is a heat exchanger which has the role of transferring the heat from the flue gases to the steam coming from the waterwall, to increase the steam temperature. The increased temperature means that more energy is available to be used by the turbine for conversion to mechanical and then electrical energy. Due to this added energy, the efficiency of the entire cycle is increased [Woodruff *et al*., 2004]. The efficiency of the turbine over a wide load range is affected, if the steam temperature is not maintained at constant over that range [Woodruff *et al*., 2004].

The predominant method used to control steam temperature is attemperation. The device is called a spray-type attemperator. Water is sprayed into steam, it will form steam through evapouration and the temperature of the final mixture will be regulated to lower than the initial one [Woodruff *et al*., 2004].

The SH from the simulator has three sections: Primary SH, Platen SH and Final SH. Each section is divided in two subsections, such that there are two steam paths going through the SH, denoted A and B in Fig. 6.1. There are two attemperators on each side, one after Primary SH and one after Platen SH. The first attemperator is controlling the steam temperature at the outlet of the Platen SH and the second attemperator is regulating the steam temperature at the outlet of the Final SH.

6.3.2 Steam temperature control structure

The temperature of the superheated steam exiting the Platen SH and Final SH is regulated by a Proportional-Integral (PI) Cascade control structure. This type of control structure is depicted in Fig. 6.2.

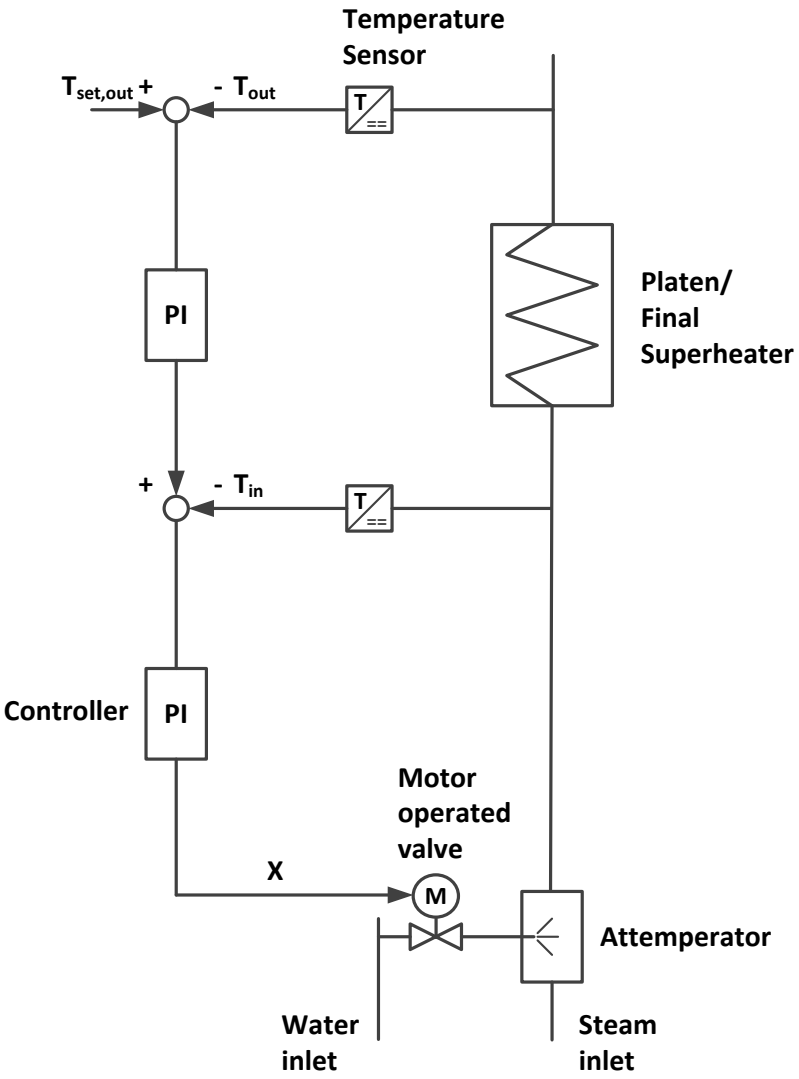

FIGURE 6.2 Cascade PI control structure regulating the steam temperature at the outlet of Final/Platen SH; $\mathbf{T_{in}}$ – inlet steam temperature [°C];$\mathbf{T_{out}}$ – outlet steam temperature [°C]; $T_{set,out}$ – outlet set-point steam temperature [°C]; **X** – valve position [%].

A PI cascade control structure uses an additional internal feedback loop to reject disturbances more effectively [Sung *et al.*, 2009]. When the valve position of the attemperator changes, the spray water pressure changes as well and as a result, the

spray water flow rate will be disturbed [Yu and Kim, 2011]. This disturbance can be rejected by using a cascade PI structure. Referring to Fig. 6.2, the control signal sent by the outer PI controller acts as the set-point for the inner control loop. In this loop, the temperature at the attemperator outlet is measured and the PI controller acts in such a way as to reduce the deviation between the set-point temperature from the outer controller and the temperature at the attemperator outlet. Because the inner loop is faster than the outer loop, the disturbance is rejected.

6.4 Development of the GPC controller

The most important temperature to be controlled is the steam temperature at the output of the last stage of the SH, namely at the Final SH outlet, just before entering the HP turbine [Hlava, 2010]. The aim of this research work is to achieve better control performance by replacing the PI Cascade control, which controls the steam temperature at the outlet of the Final SH, with a controller based on the GPC algorithm. The block diagram of the steam temperature control system employing the GPC controller is illustrated in Fig. 6.3, where $T_{set,out}$ is the set-point temperature, T_{in} is the temperature at the Final SH inlet, T_{out} is the temperature at the Final SH outlet and $\boldsymbol{\alpha}$ is the valve position of the attemperator.

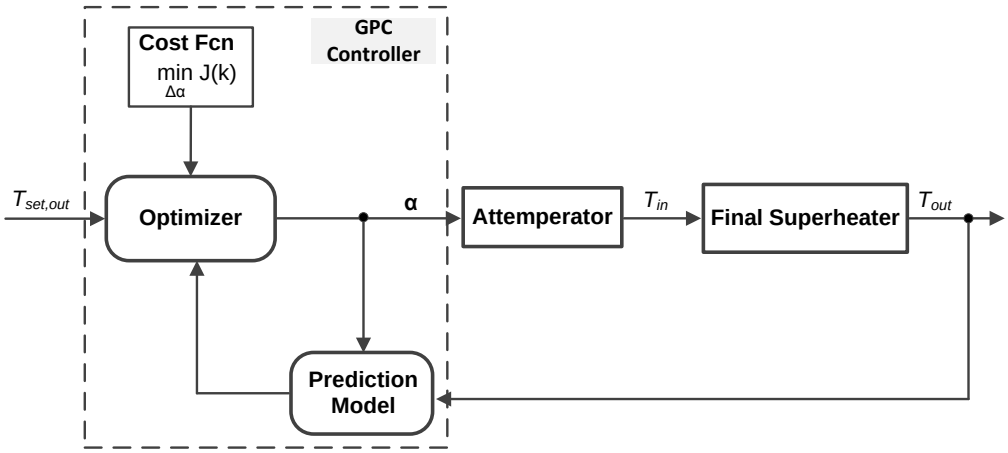

FIGURE 6.3 Final SH outlet steam temperature control loop based on GPC controller

6.4.1 Identification of the prediction model

The identification of the prediction model was carried out for the power plant operating at the steady-state conditions, generating 500 MW (83%) power output.

Having the control system of the attemperator's valve operating on manual (PI controller disconnected), a 10% step increase in the valve opening was added to existing control signal and sent to the motor operated valve. The step response of the process, namely the evolution in time of the Final SH outlet steam temperature was recorded at a sampling rate of $T_s = 0.1\ s$. After several trials were conducted, it was decided that a rank 4 model in the form of a discrete difference equation represents a good description of the process dynamics with a dead time θ of 4.8 s. Using expression (6.1), the prediction model has the following form:

$$y(t) + a_1 y(t-1) + a_2 y(t-2) + a_3 y(t-3) + a_4 y(t-4) =$$
$$= b_0 y(t-49) + b_1 y(t-50) + b_2 y(t-51) + b_3 y(t-52) +$$
$$+ b_4 y(t-53) \qquad (6.12)$$

where $a_1, \cdots, a_4$ and $b_0, \cdots, b_4$ are the parameters of the polynomials A and B.

Multiple Linear Regression method described in Chapra [2012] and was used to fit the model parameters to the points of the step response. This method represents an extension of the linear regression, where y is a linear function of two or more independent variables, expressed as:

$$y = \alpha_0 + \alpha_1 x_1 + \alpha_2 x_2 + \cdots \alpha_m x_m \tag{6.13}$$

In order to obtain the best fit, the sum of the squares of the residuals is minimized.

$$S_r = \sum_{i=1}^{n} e_i^2 = \sum_{i=1}^{n} \left(y_i - \alpha_0 - \alpha_1 x_{1,i} - \alpha_2 x_{2,i} - \cdots - \alpha_m x_{m,i}\right)^2 \tag{6.14}$$

This is achieved by differentiating relation (6.14) with respect to each of the unknown coefficients, which gives:

$$\begin{aligned}
\frac{\partial S_r}{\partial \alpha_0} &= -2 \sum_{i=1}^{n} \left(y_i - \alpha_0 - \alpha_1 x_{1,i} - \alpha_2 x_{2,i} - \cdots - \alpha_m x_{m,i}\right) \\
\frac{\partial S_r}{\partial \alpha_1} &= -2 \sum_{i=1}^{n} x_{1,i} \left(y_i - \alpha_0 - \alpha_1 x_{1,i} - \alpha_2 x_{2,i} - \cdots - \alpha_m x_{m,i}\right) \\
&\vdots \\
\frac{\partial S_r}{\partial \alpha_m} &= -2 \sum_{i=1}^{n} x_{m,i} \left(y_i - \alpha_0 - \alpha_1 x_{1,i} - \alpha_2 x_{2,i} - \cdots - \alpha_m x_{m,i}\right)
\end{aligned} \tag{6.15}$$

Setting the partial derivatives from (6.15) equal to zero gives the coefficients which minimise the sum of the squares of the residuals. This is expressed in the matrix format as

$$\begin{bmatrix} n & \sum_{i=1}^{n} x_{1,i} & \sum_{i=1}^{n} x_{2,i} & \cdots & \sum_{i=1}^{n} x_{m,i} \\ \sum_{i=1}^{n} x_{1,i} & \sum_{i=1}^{n} x_{1,i}^2 & \sum_{i=1}^{n} x_{1,i}x_{2,i} & \cdots & \sum_{i=1}^{n} x_{1,i}x_{m,i} \\ \vdots & \vdots & \vdots & \vdots & \vdots \\ \sum_{i=1}^{n} x_{m,i} & \sum_{i=1}^{n} x_{m,i}x_{1,i} & \sum_{i=1}^{n} x_{m,i}x_{2,i} & \cdots & \sum_{i=1}^{n} x_{m,i}^2 \end{bmatrix} \begin{bmatrix} \alpha_0 \\ \alpha_1 \\ \vdots \\ \alpha_m \end{bmatrix} = \begin{bmatrix} \sum_{i=1}^{n} y_i \\ \sum_{i=1}^{n} x_{1,i}y_i \\ \vdots \\ \sum_{i=1}^{n} x_{m,i}y_i \end{bmatrix}$$

(6.16)

Expression (6.16) represents a set of $(m+1)$ equations with $(m+1)$ unknown variables, to which a solution can be found. After the calculation of the parameters by using the method described above, the CARMA model was obtained.

$$(1 - 0.2412z^{-1} - 0.5614z^{-2} - 0.3602z^{-3} + 0.1686z^{-4})y(k) =$$

$$= z^{-48}(-0.0301 + 0.0073z^{-1} + 0.0169z^{-2} - 0.0516z^{-3} -$$

$$0.0131z^{-4})u(k-1) \quad (6.17)$$

From (6.17) the polynomials A and B can be identified as

$$A(z^{-1}) = 1 - 0.2412z^{-1} - 0.5614z^{-2} - 0.3602z^{-3} + 0.1686z^{-4}$$

$$B(z^{-1}) = -0.0301 + 0.0073z^{-1} + 0.0169z^{-2} - 0.0516z^{-3} -$$

$$-0.0131z^{-4} \quad (6.18)$$

The real step response of the system and the one of the fitted model are presented in Fig. 6.4.

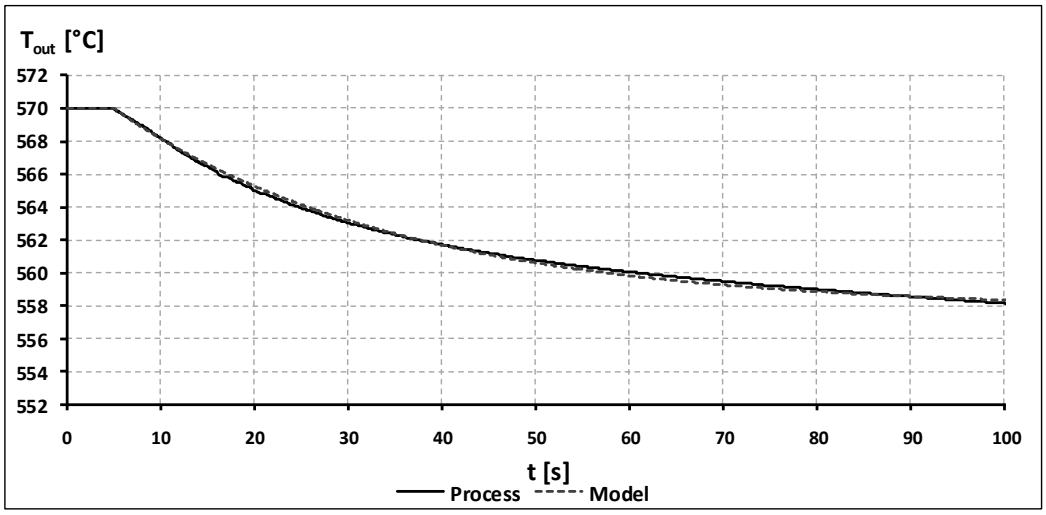

FIGURE 6.4 Step response of the real process and of the identified CARMA model

6.4.2 Tuning parameters of the GPC controller

The parameters of the GPC algorithm, which influence the control input values generated in the optimization process of the cost function are:

- N – prediction horizon,
- N_u – control horizon, $N_u \leq N$,
- $\delta(j)$ – weight of the predicted outputs,
- $\lambda(j)$ – weight of the control inputs.

It is suggested in Clarke *et al.* [1987] that the value of the prediction horizon, N should be larger than the rank of the polynomial B. If the value of N is chosen to be of an adequate value compared to process dynamics and the feedback control system operates correctly, then choosing a larger value for it will not improve the performance of the control system [Tatjewski, 2007].

The control horizon is considered an important design parameter [Clarke *et al.*, 1987]. If the value of N_u is increased, then the control and the corresponding process

response becomes more active. There is a limit for N_u beyond which there is no significant progress in the controller's performance. Since the number of decision variables in the optimization problem are related to the value of N_u, it is advised to give relatively small values for this parameter as this will ease the computational burden [Tatjewski, 2007].

The GPC algorithm devised by Clarke *et al.* [1987] disregards the effect of the weight δ on the predicted outputs values and sets its value equal to unity. The remaining tunable parameter λ affects the cost of the control input moves. With the increase of the value for this parameter, the control effort is forced to decrease, which leads to a slower response from the system. For a small value of λ the controller will tend to minimize the error between the predicted outputs and the set-point values, disregarding the control effort [Camacho, 2007], which in turn generates a fast response from the system.

The parameters of the GPC controller were tuned using trial-and-error procedure and the following values were found to deliver an optimal performance:

- prediction horizon $N = 5$
- control horizon $N_u = 5$
- control weight $\lambda = 300$
- output weight $\delta = 1$.

6.5 Simulation tests of the GPC controller performance

The initial conditions, common for all simulation tests run in the simulator, were considered to be for the power plant operating at steady-state 500 MW (83%)

generated power output. During all three simulation tests, the set-point value for the outlet Final SH steam temperature was 570°C. For the first simulation test, the disturbance is a step change in the load command signal from 500 MW (83%) to 600 MW (100%) generated power. The power plant load change rate is 10 MW/min. The results of the simulation test are presented in the Fig. 6.5 - Fig. 6.7.

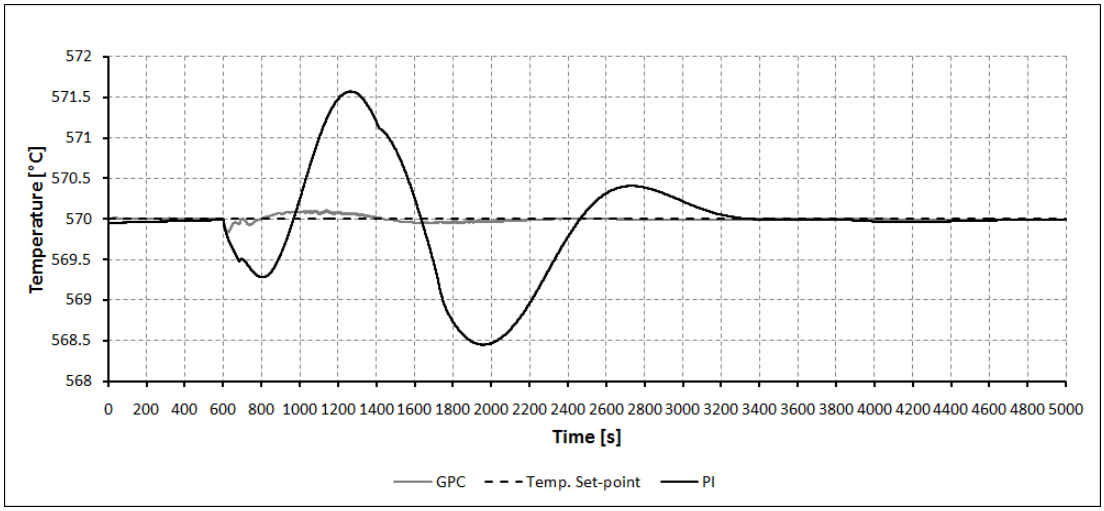

FIGURE 6.5 Superheated steam temperature response

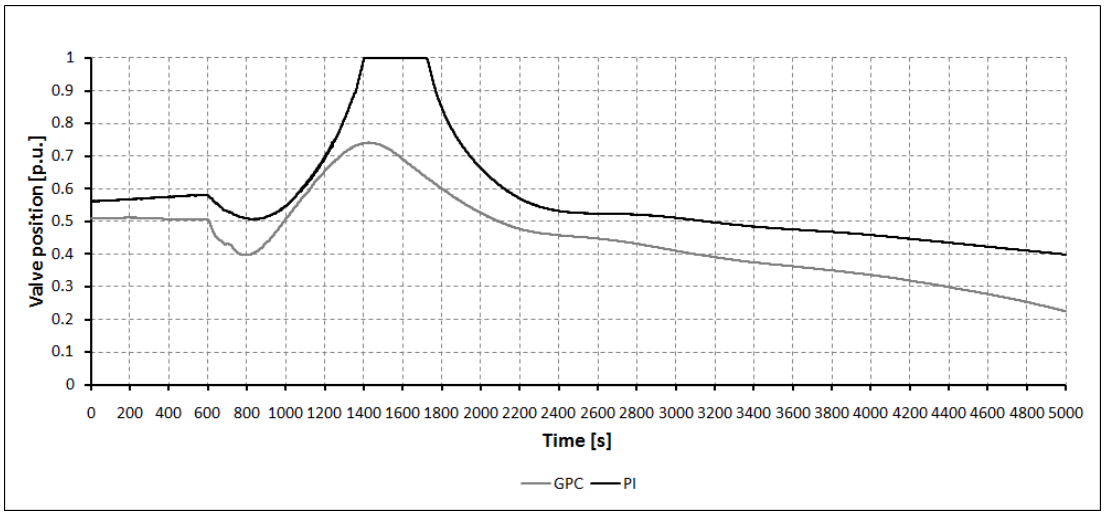

FIGURE 6.6 Control signal variation

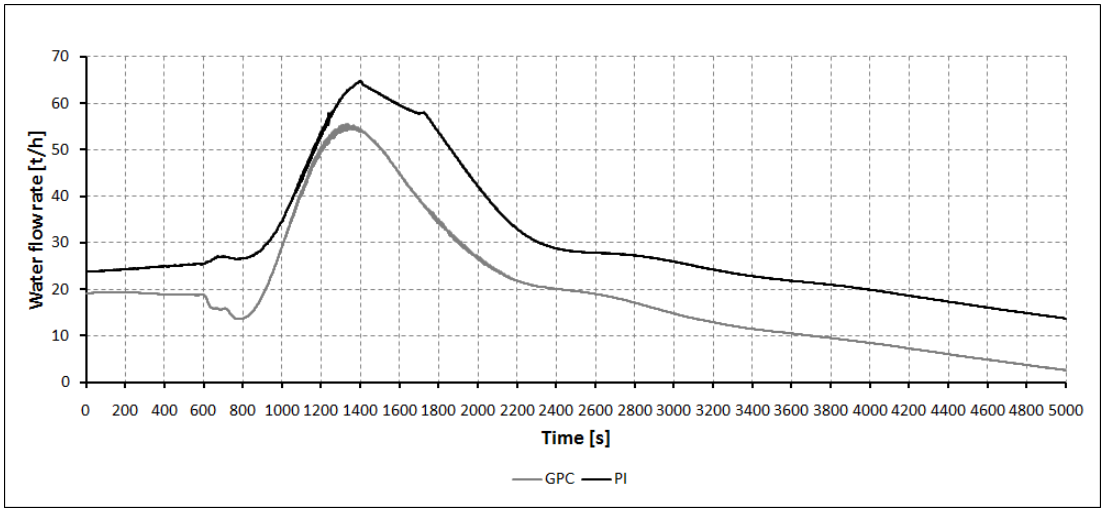

FIGURE 6.7 Spray water flow rate

The results of this simulation test show an improved stability of the steam temperature, for the case when the GPC controller was used. A comparative numerical analysis is given below:

PI control:

- peak error -1.55 ~1.57 °C
- standard deviation 0.62 °C
- settling time 4500 s

GPC control:

- peak error -0.16 ~ 0.11 °C
- standard deviation 0.03 °C
- settling time 2300 s

During the test, the average value for the valve opening area was 0.57 p.u., when the PI controller was used, compared to 0.45 p.u., with the GPC controller in operation. Regarding the water flow rate, the average value was 29.91 t/h, when using the PI controller and 19.51 t/h, when using the GPC controller. According to these results there is a smaller over/undershoot for the temperature, the system reaches steady-state twice quicker and the amount of spray water needed, was reduced with 35% with the GPC controller in operation. Analysing the control signal, it can be seen that

the PI control signal has significant variation in amplitude, while the GPC control signal has smaller variation.

In the second simulation test, the load demand signal has an initial ramp up trend from 500 MW (83%) to 600 MW (100% nominal load), with 10 MW/min load change rate, then it remains constant for 20 min and follows afterwards a ramp down trend from 600 MW (100%) to 500 MW (83% nominal load) with the same load change rate. The results obtained after this load demand signal was applied to the power plant, were used to plot the graphs illustrated in the Fig. 6.8 – Fig. 6.10.

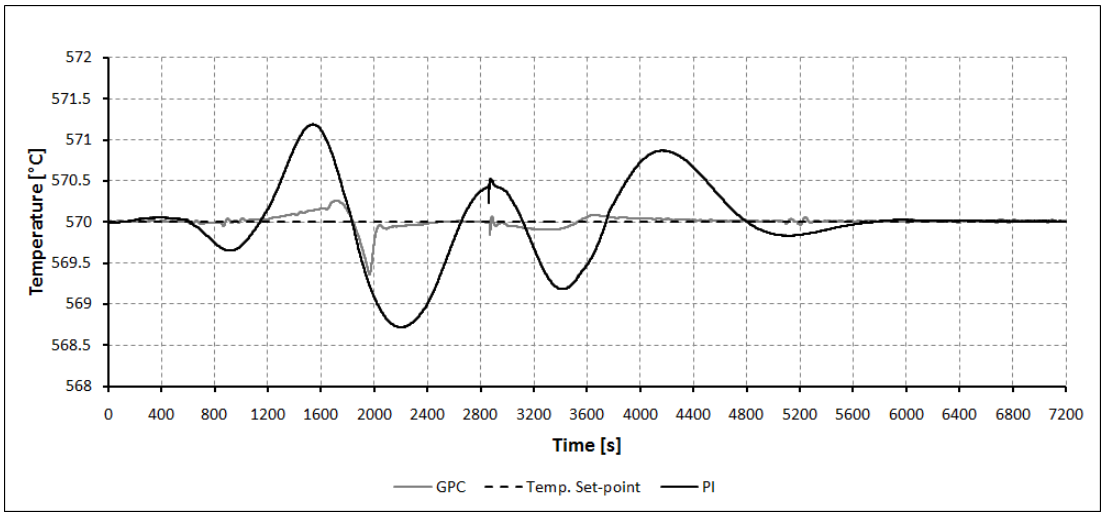

FIGURE 6.8 Superheated steam temperature response

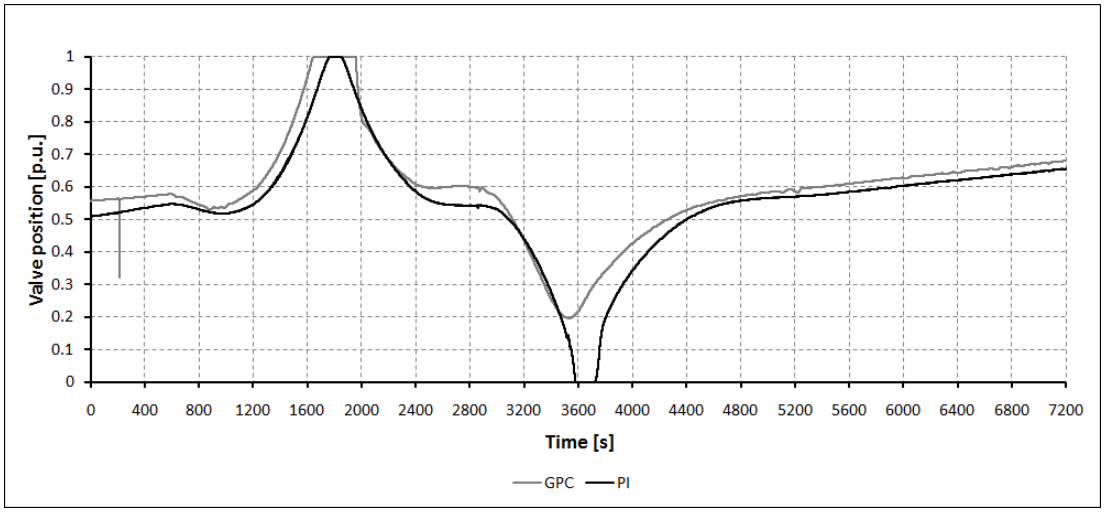

FIGURE 6.9 Control signal variation

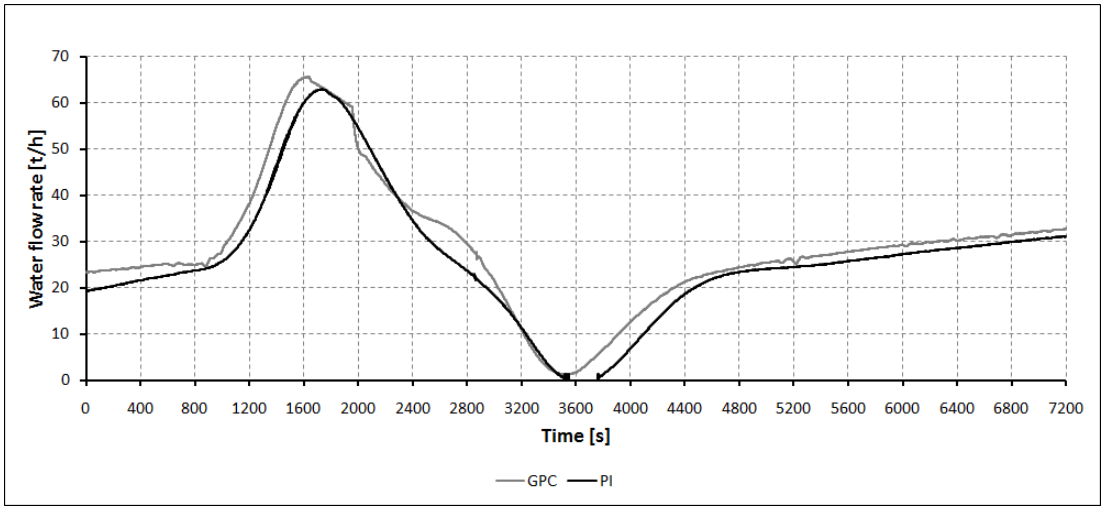

FIGURE 6.10 Spray water flow rate

The steam temperature shows again smaller variation, when the GPC controller is used. This is reflected as well by the numerical results given below.

PI control:

- peak error -1.28 ~1.19°C
- standard deviation 0.5 °C

GPC control:

- peak error -0.64 ~ 0.26 °C
- standard deviation 0.08 °C

- settling time 6100 s
- settling time 4800 s

During the test, the average value for the valve opening area was 0.55 p.u., when the PI controller was used, compared to 0.59 p.u., with the GPC controller in operation. Regarding the water flow rate, the average value was 26.19 t/h, when using the PI controller and 28.67 t/h, when using the GPC controller.

Analysing the values for the peak error and the standard deviation, it shows a smaller over/undershoot for the temperature, and a settling time with 21% shorter for the system, when the GPC controller is in operation. The average spray water needed is slightly higher for the GPC controller, but the valve opening area has smaller variations, than for the PI case. Again the control signal sent by the GPC controller is more stable, compared to the one sent by the PI controller which has a continuous variation.

The power plant modelled by the simulator is considered to have six coal mills, five of them in operation and one in stand-by. The disturbance considered for the third simulation test was a stop of a coal mill. This affects the combustion process, which results in a variation of the flue gases temperature and this, in turn generates disturbances of the steam temperature. The results of the simulation test are presented in Fig. 6.11 – Fig. 6.13.

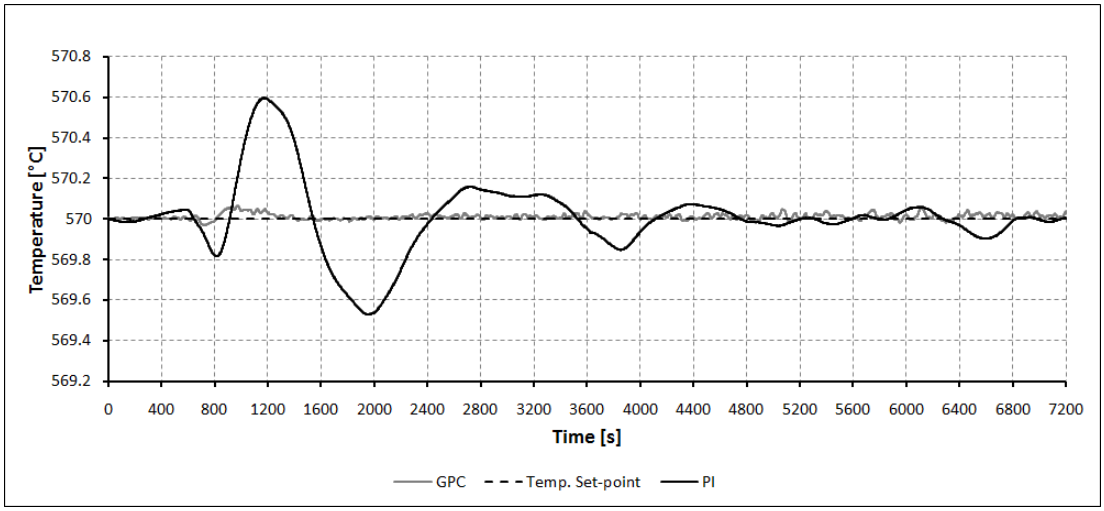

FIGURE 6.11 Superheated steam temperature response

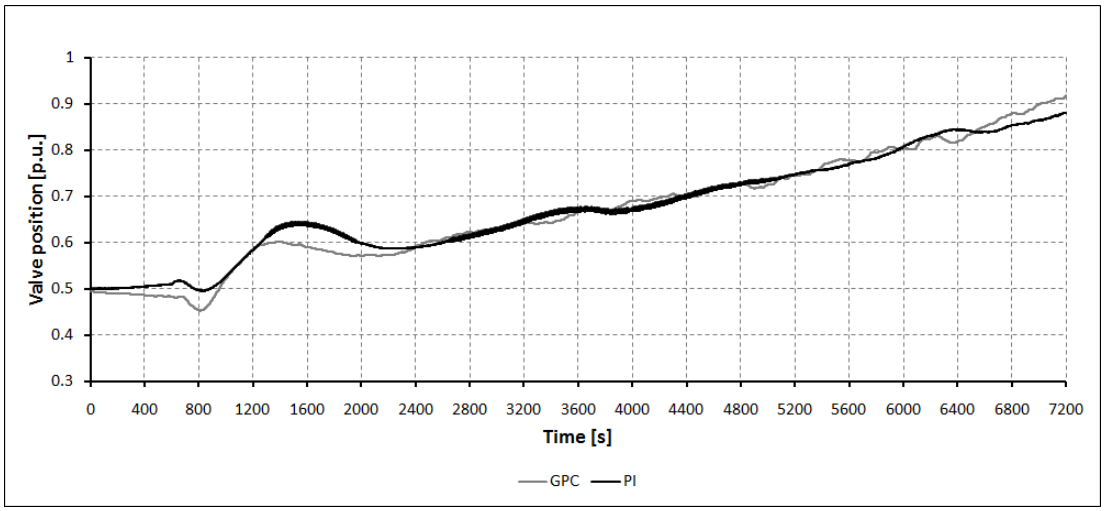

FIGURE 6.12 Control signal variation

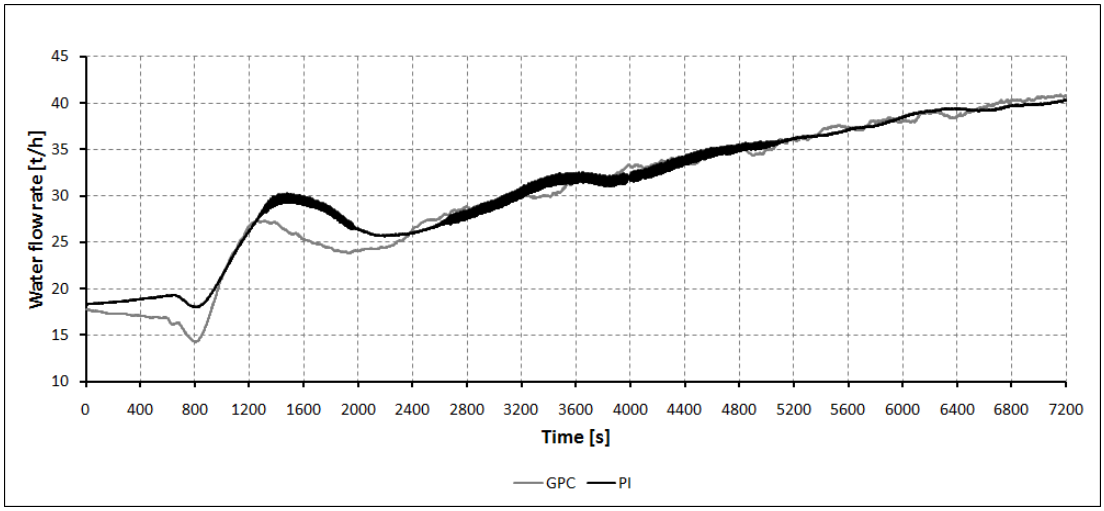

FIGURE 6.13 Spray water flow rate

Fig. 6.11 shows an improved stability of the steam temperature, when the GPC controller is tested. The graphic results are backed by the numerical data given below.

PI control:

- peak error -0.47 ~0.6°C
- standard deviation 0.18 °C
- settling time 4800 s

GPC control:

- peak error -0.03 ~ 0.07 °C
- standard deviation 0.01 °C
- settling time 1400 s

During the test, the average value for the valve opening area was 0.68 p.u., when the PI controller was used, compared to 0.67 p.u., with the GPC controller in operation. Regarding the water flow rate, the average value was 30.94 t/h, when using the PI controller and 30.32 t/h, when using the GPC controller.

The average value of the control signal and the water flow rate are very similar, but as it can be observed from Fig. 6.12, the signal sent by the PI controller has

considerable transients compared to the GPC one. The settling time is improved by 70% with the GPC controller in operation.

6.6 Summary

The chapter begins with an introduction to steam temperature control in power plants and its importance in the overall efficiency is underlined. Although PID control is still the most used control strategy to regulate the steam temperature, the new economic environment requires power plants to be more flexible in operation, which calls for more advanced control strategies. The controllers based on the algorithms belonging to MPC are able to deliver this new required control performance. The MPC algorithm chosen to develop the controller for regulating the steam temperature is GPC, because it can manage unstable systems as is the case with the SH.

Steam temperature is regulated in SH by using attemperators, one controlling the steam temperature at the outlet of Platen SH and another one at the outlet of Final SH. The existing control structure for each one of them is a PI Cascade control structure. Because the steam temperature at the last stage of the SH, namely at the outlet of Final SH is considered to be the most important, the research focused on replacing the PI Cascade control structure from this part with a GPC based controller.

After the CARMA model was identified, the GPC algorithm was coded in FORTRAN 95 and implemented in the power plant simulator. In order to assess the performance of the GPC controller against the PI Cascade control loop, three simulation tests were run for different scenarios. The variables monitored were the

steam temperature, the control signal sent to valve and the water flow rate from the attemperator. All scenarios were run both for the PI Cascade control loop and for the GPC controller.

In the first simulation test, having the power plant operating at 500 MW steady state power output, a step increase change of 100 MW was made to the load command signal. In the second scenario the load command signal is ramped up from 500 MW to 600 MW, with a 10 MW/min rate of change, maintained there for the next 20 minutes and then ramped down to the initial power output. In the third scenario, the combustion process is disturbed by a stop in operation of one of the coal mills.

The results gathered from the simulation tests show a better temperature regulation when the GPC controller was in operation as to when the PI cascade control loop was used.

Chapter 7

Conclusions and Suggestions for Future Research Work

7.1 Summary

The research work exposed in this thesis is concerned with the study of the dynamic responses of a supercritical coal-fired power plant, aiming to assess if it can comply with the frequency control requirements specified in the GB Grid Code.

A complex power plant simulator, developed in collaboration with Tsinghua University from Beijing, China was used for running simulation tests under different operating scenarios.

A study of the frequency control at power plant level was conducted and the requirements for a grid connected power plant were extracted from the GB Grid Code. A comparison of these requirements against eight other European and non-European grid codes was then conducted.

Based on the GB Grid Code frequency control requirements, several simulation tests were run and the results were processed and subjected to further analysis.

The control architecture implemented in the simulator was studied and two major control loops of subsystems, whose performance could be improved were identified.

Controllers based on MPC algorithms were designed and implemented in the power plant simulator to improve the performance of the previously identified control loops. Simulation tests for the existing control strategies and for the proposed ones

were run and the results and different performance indicators were compared and discussed afterwards.

The conclusions which can be drawn based on my PhD research work summarized above are presented in the next section.

7.2 Conclusions

The operation of a steam power plant is based on the thermodynamic cycles of Rankine and Reheat, from where its efficiency can be calculated. A supercritical power plant uses a variation of these cycles, where the parameters for steam, namely the pressure and temperature have been raised above the critical point of water in order to increase its efficiency. In this way the power plant can reach an efficiency of up to 46% compared to 35% for a subcritical one. The main structural difference between a supercritical and a subcritical power plant is the lack of the drum.

Power system frequency represents an indicator of the power system stability and its value is closely monitored at the power plant level and at the power system level. Frequency control requirements are specified in a technical document entitled Grid Code and an analysis of these requirements for several European and non-European countries was completed. The nominal frequency for all the analysed countries is 50 Hz, allowing a variation of ±5 Hz from this value during normal operation and of -3 Hz, +2 Hz in case of critical situations for the majority of the power systems. There are at least two frequency control strategies implemented by each country, which are generally named primary and secondary frequency control.

All the simulation tests performed in this research have been run on a complex power plant simulator designed after a field operating 600 MW supercritical coal-fired power plant. The requirements specified by the GB Grid Code for Primary Frequency Response and High Frequency Response were used to verify the dynamic responses of the power plant. The power plant was considered to operate first in fixed pressure control mode and then in variable pressure control mode and it resulted that the fastest response is achieved for the first control mode.

The simulation results indicate that both frequency control requirements can't be fulfilled by the power plant. The maximum load ramping of the power plant is not enough to comply with the requirements for Primary Frequency Response.

Power plant control system is based on PID controllers, which are easy to implement and operate but due to the nonlinearity of the regulated processes, their performance is far from being optimal. The regulation of two variables, namely the coal flow rate and the temperature of the superheated steam is of utter importance for the power plant operation, therefore MPC based controllers were designed to improve the performance of these control loops.

The new controller designed for the regulation of the coal flow rate is based on the DMC algorithm. Characteristic for this algorithm is the use of a discrete step response model to calculate the predictions of process outputs. Care needs to be taken of the choice for the amplitude of the step change signal, when the prediction model is identified. A set of linear inequality constrains on the amplitude of the control signal, on the rate of change of control inputs and on the amplitude of the

process outputs are considered by the controller when calculating the future control inputs. They represent the solution to a QP optimization problem which is solved at each time sample. Hildreth's Algorithm, which uses a Primal-Dual method belonging to the Active Set was chosen to solve this problem, motivated by its ability to provide a near optimal solution, even for the case of ill conditioned problems.

Simulation tests were run, consisting in a step increase/decrease of the load demand signal sent to the power plant, from power output levels of 550 MW and 450 MW, considering the case of the control loop being regulated by the PID controller and then by the DMC controller. The control loop performs better under DMC controller, with a steady evolution of the control input signal and with almost zero steady-state error between the set-point trajectory and the coal flow rate variable. There is also no need for re-identification of the prediction model or for re-tuning of the DMC controller's parameters when power plant operating level was changed, as the controller's performance didn't deteriorate. Other monitored variables, like main steam pressure and temperature were found to be better regulated when the DMC controller was in operation.

The control of the superheated steam temperature is of high importance, as it affects the efficiency of the power plant and the lifetime of the boiler and steam turbine. The high nonlinearity of this process makes it difficult for the PID controllers to regulate it. A controller based on GPC algorithm was designed to improve the performance of this control loop. The particularity of the GPC algorithm is the use of a discrete difference equation as the process model used to calculate the predicted outputs. A

rank four model was identified and describes with the required accuracy the process dynamics. The GPC controller replaced the two PI controllers from the cascade control loop.

Several simulation tests were conducted for different scenarios from the power plant operating level of 500 MW. The results show an improved stability of the steam temperature with a very good tracking of the set-point trajectory when the GPC controller is in operation. Also the control signal sent to the motor actuating the attemperator's valve is more stable in time, which means a longer service life for both the motor and the valve. Another improvement is represented by the decrease of the water flow rate sent by the attemperator. The GPC controller showed the same good performance when the power output level was changed to 600 MW, requiring no re-identification of the process model and no re-tuning of the parameters.

7.3 Suggestions for future research work

A power plant in general and a supercritical power plant in particular represents a very complex system, with many processes undergoing simultaneously and often interacting one with another. Therefore someone's research work can only cover certain aspects of this topic, while many other areas of research still remain uncovered.

As suggestions for future development of the software it should be investigated the introduction of a gain scheduling scheme for the PID controllers, which will allow an optimal performance of the power plant over a wider range of operating points.

It would also be beneficial for frequency control analysis if a simplified power system model would be connected to the simulator, so that more complex studies can be conducted and the impact on power system frequency as a result of power plant's actions to be better understood.

If the Grid Code requirements cannot be relaxed, than other technical solutions should be investigated, which will allow the supercritical coal-fired power plant to participate to frequency control in the grid.

The MPC based controllers that were designed and implemented in the power plant simulator, proved a better control performance of the respective processes against the existing PID controllers. Other control loops can benefit as well from the implementation of MPC based controllers.

A MIMO control strategy based on MPC algorithms should be investigated, as in this way the interactions between the simultaneously operating processes would be considered.

If the nonlinear model of the process plant is available, then this can be used as the prediction model in Nonlinear Model Predictive Control (NMPC). In this case the performance of the closed loop can be increased significantly. Although the complexity of the algorithm is much increased, with the development of the computation technology this can be implemented. Using NMPC might be another way of improving the performance of the power plant and research in this area should be conducted.

Due to frequent fluctuations of the energy markets, a power plant should be as flexible as possible in the choice of the fuel. As an example in this regard, studies can be carried on the feasibility of a supercritical power plant to operate on biomass.

The requirements on reducing the CO_2 emissions demand adoption of new technologies, which will increase efficiency and are also suitable for retrofit to existing power plants. In this aspect the impact of circulating fluidized beds and coal gasification technologies on supercritical power plant is another research theme.

Finally applying Carbon Capture and Storage technologies to a supercritical power plant should also be included in a future research work.

Appendix A
FORTRAN code for DMC Controller

```
      SUBROUTINE CONSTRAINED

      REAL, DIMENSION (147) :: Model = (/0.0,0.0,0.0,0.0,0.0,
     @   0.0,0.0,0.0538,0.1045,0.1523,0.1974,0.24,0.28,0.3178,
     @   0.3535,0.3871,0.4188,0.4486,0.4768,0.5034,0.5284,0.552,
     @   0.5743,0.5953,0.6151,0.6337,0.6513,0.6679,0.6835,0.6983,
     @   0.7122,0.7253,0.7377,0.7493,0.7603,0.7707,0.7804,0.7897,
     @   0.7983,0.8065,0.8143,0.8215,0.8284,0.8349,0.841,0.8467,
     @   0.8522,0.8573,0.8621,0.8666,0.8709,0.875,0.8788,0.8824,
     @   0.8858,0.889,0.892,0.8948,0.8975,0.9,0.9024,0.9046,0.9068,
     @   0.9088,0.9106,0.9124,0.9141,0.9157,0.9172,0.9186,0.9199,
     @   0.9211,0.9223,0.9234,0.9245,0.9254,0.9264,0.9272,0.9281,
     @   0.9288,0.9296,0.9303,0.9309,0.9315,0.9321,0.9327,0.9332,
     @   0.9337,0.9341,0.9346,0.935,0.9354,0.9357,0.9361,0.9364,
     @   0.9367,0.937,0.9372,0.9375,0.9377,0.938,0.9382,0.9384,
     @   0.9386,0.9387,0.9389,0.9391,0.9392,0.9394,0.9395,0.9396,
     @   0.9397,0.9399,0.94,0.9401,0.9402,0.9402,0.9403,0.9404,
     @   0.9405,0.9405,0.9406,0.9407,0.9407,0.9408,0.9408,0.9409,
     @   0.9409,0.941,0.941,0.9411,0.9411,0.9411,0.9412,0.9412,
     @   0.9412,0.9413,0.9413,0.9413,0.9413,0.9413,0.9414,0.9414,
     @   0.9414,0.9414,0.9414,0.9415/)

      INTEGER, PARAMETER :: D = SIZE ( Model )       ! size of the model
      INTEGER, PARAMETER :: N1 = 8                   ! process delay
      INTEGER, PARAMETER :: N = 147                  ! prediction horizon
      INTEGER, PARAMETER :: NU = 100                 ! control horizon
      REAL, PARAMETER :: Lambda = 10.00              ! control weight
      REAL, DIMENSION(N-N1+1, D-1) :: MP             ! matrix to calc. free component
      REAL, DIMENSION(N-N1+1, NU) :: M               ! dynamic matrix for forced component
      REAL, DIMENSION(NU, NU) :: ID                  ! identity matrix
      REAL, DIMENSION(NU, NU) :: H                   ! matrix H from cost function, hessian
      REAL, DIMENSION(NU, NU) :: J                   ! lower triangular matrix for input control
      REAL, DIMENSION(2*(2*NU+N-N1+1), NU) :: A      ! left hand constraints matrix
      REAL, DIMENSION(NU, 1) :: Umin                 ! minimum input amplitude matrix
      REAL, DIMENSION(NU, 1) :: Umax                 ! maximum input amplitude matrix
      REAL, DIMENSION(N-N1+1, 1) :: Ymin             ! minimum output amplitude matrix
      REAL, DIMENSION(N-N1+1, 1) :: Ymax             ! maximum output amplitude matrix
      REAL, DIMENSION(NU, 1) :: DUmax                ! maximum rate input matrix
      REAL, DIMENSION(N-N1+1, 1) :: Y                ! current measurements matrix
      REAL, DIMENSION(NU,1) :: U                     ! last control input
      REAL, SAVE, DIMENSION(D-1) :: DUp_vec = (/0.0,0.0,0.0,
     @   0.0,0.0,0.0,0.0,0.0,0.0,0.0,0.0,0.0,0.0,0.0,0.0,0.0,0.0,0.0,
     @   0.0,0.0,0.0,0.0,0.0,0.0,0.0,0.0,0.0,0.0,0.0,0.0,0.0,0.0,0.0,
     @   0.0,0.0,0.0,0.0,0.0,0.0,0.0,0.0,0.0,0.0,0.0,0.0,0.0,0.0,0.0,
     @   0.0,0.0,0.0,0.0,0.0,0.0,0.0,0.0,0.0,0.0,0.0,0.0,0.0,0.0,0.0,
     @   0.0,0.0,0.0,0.0,0.0,0.0,0.0,0.0,0.0,0.0,0.0,0.0,0.0,0.0,0.0,
     @   0.0,0.0,0.0,0.0,0.0,0.0,0.0,0.0,0.0,0.0,0.0,0.0,0.0,0.0,0.0,
     @   0.0,0.0,0.0,0.0,0.0,0.0,0.0,0.0,0.0,0.0,0.0,0.0,0.0,0.0,0.0,
     @   0.0,0.0,0.0,0.0,0.0,0.0,0.0,0.0,0.0,0.0,0.0,0.0,0.0,0.0,0.0,
     @   0.0,0.0,0.0,0.0,0.0,0.0,0.0,0.0,0.0,0.0,0.0,0.0,0.0,0.0,0.0,
     @   0.0,0.0,0.0,0.0,0.0,0.0,0.0,0.0,0.0,0.0,0.0,0.0,0.0,0.0,0.0,
     @   0.0,0.0,0.0,0.0/)                           ! (D-1) past control inputs vector
      REAL, DIMENSION(D-1,1) :: DUp                  ! (D-1) past control inputs
      REAL, DIMENSION(N-N1+1,1) :: Y_zero            ! free component trajectory
      REAL, DIMENSION(2*(2*NU+N-N1+1), 1) :: B       ! right hand constraints matrix
      REAL, DIMENSION(N-N1+1,1) :: Ysp               ! set point matrix
      REAL, DIMENSION(NU,1) :: F                     ! matrix F from cost function, gradient
      INTEGER MX, Lim
      REAL, DIMENSION(NU, NU) :: INV_H               ! the inverse of matrix H
      REAL, DIMENSION(NU,1) :: DU                    ! future control inputs
      REAL, DIMENSION(D) :: DUp_vecR                 ! updated vector for (D-1) past control
      INTEGER, SAVE :: T=0

      T=T+1

      CALL Matrix_MMP(Model, N1, N, D, NU, MP, M)

      CALL Matrix_ID(NU, ID)

      H = 2*(MATMUL(TRANSPOSE(M), M) + Lambda*ID)

      CALL Matrix_J(NU, J)

      CALL Matrix_A(N1, N, NU, ID, J, M, A)

      Umin = 0
      Umax = 1
```

```
Ymin = 0
Ymax = 1

DUmax = 0.004

Y = CBFF_TOTALFUELQn

U = CBFF_DBM

DUp = RESHAPE ( DUp_vec, (/D-1,1/) )

Y_zero = Y + MATMUL(MP, DUp)

CALL Matrix_B(NU, N, N1, Umin, Umax, Ymin, DUmax, U, Y_zero, B)

Ysp = CBFF_TOTALFUELCMDn

F = (-2) * MATMUL(TRANSPOSE(M),(Ysp - Y_zero))

MX = NU
Lim = MX

CALL MATINV (H, Lim, MX)

INV_H = H

CALL HILDRETH (NU, INV_H, H, F, A, B, DU)

IF (T==1) THEN
CBFF_DBM_DMC=CBFF_DBM+DU(1,1)
ELSE
CBFF_DBM_DMC=CBFF_DBM_DMC+DU(1,1)
END IF

DUp_vecR = (/DU(1,1),DUp_vec/)
DO i = 1, D-1
     DUp_vec(i) = DUp_vecR(i)
END DO

END SUBROUTINE CONSTRAINED

SUBROUTINE Matrix_MMP(EModel1, EN1, EN, ED, ENU, EMP, EM)

INTEGER EN1
INTEGER EN
INTEGER ED
REAL, DIMENSION(ED) :: EModel1
REAL, DIMENSION(EN-EN1+1, ED-1):: EMP
REAL, DIMENSION(EN-1) :: EModel2
REAL, DIMENSION(EN+ED-1) :: EModel3
INTEGER k
INTEGER ENU
REAL, DIMENSION(EN-EN1+1, ENU) :: EM
REAL, DIMENSION(EN-ED) :: EModel4
REAL, DIMENSION(EN) :: EModel5

DO i = 1, EN-1
         EModel2(i) = EModel1(ED)
END DO

         EModel3 = (/EModel1, EModel2/)

DO j = 1, ED-1
        k=0
    DO i = EN1+j, EN+j
            k = k+1
            EMP(k,j) = EModel3(i) - EModel3(j)
    END DO
END DO

DO i = 1, EN-ED
         EModel4(i) = EModel1(ED)
END DO

EModel5 = (/EModel1, EModel4/)

DO i = 1, EN-EN1+1
        DO j = 1, ENU
                IF(i < j) THEN
                        EM(i,j) = 0
                ELSE
                        EM(i,j) = EModel5(i-j+EN1)
                END IF
        END DO
END DO
```

```
        END SUBROUTINE Matrix_MMP

        SUBROUTINE Matrix_ID(ENU, EID)

        INTEGER ENU
        REAL, DIMENSION(ENU, ENU) :: EID

        DO i = 1, ENU
                DO j = 1, ENU
                        IF(i == j) THEN
                                EID(i,j) = 1
                        ELSE
                                EID(i,j) = 0
                        END IF
                END DO
        END DO

        END SUBROUTINE Matrix_ID

        SUBROUTINE Matrix_J(ENU, EJ)

        INTEGER ENU
        REAL, DIMENSION(ENU, ENU) :: EJ

        DO i = 1, ENU
                DO j = 1, ENU
                        IF(i >= j) THEN
                                EJ(i,j) = 1
                        ELSE
                                EJ(i,j) = 0
                        END IF
                END DO
        END DO

        END SUBROUTINE Matrix_J

        SUBROUTINE Matrix_A(EN1, EN, ENU, EID, EJ, EM, EA)

        INTEGER EN1
        INTEGER EN
        INTEGER ENU
        REAL, DIMENSION(ENU, ENU) :: EJ
        REAL, DIMENSION(EN-EN1+1, ENU) :: EM
        REAL, DIMENSION(ENU, ENU) :: EID
        REAL, DIMENSION(2*(2*ENU+EN-EN1+1), ENU) :: EA
        REAL, DIMENSION(ENU*ENU) :: vecJ
        REAL, DIMENSION((EN-EN1+1)*ENU) :: vecM
        REAL, DIMENSION(ENU*ENU) :: vecID
        REAL, DIMENSION(:), ALLOCATABLE :: vecA

        vecJ = RESHAPE(TRANSPOSE(EJ), SHAPE=(/ENU*ENU/))
        vecM = RESHAPE(TRANSPOSE(EM), SHAPE=(/(EN-EN1+1)*ENU/))
        vecID = RESHAPE(TRANSPOSE(EID), SHAPE=(/ENU*ENU/))
C
        IF(ALLOCATED(vecA)) DEALLOCATE(vecA)
        ALLOCATE( vecA(2*(2*ENU+EN-EN1+1)*ENU) )
C
        vecA = (/(-1)*vecID, vecID, (-1)*vecJ, vecJ, (-1)*vecM, vecM/)
        EA = RESHAPE(vecA,SHAPE=(/2*(2*ENU+EN-EN1+1),ENU/),ORDER=(/2,1/))
C
        IF(ALLOCATED(vecA)) DEALLOCATE(vecA)
C
        END SUBROUTINE Matrix_A

        SUBROUTINE Matrix_B(ENU, EN, EN1, EUmin, EUmax, EYmin, EDUmax, EU, EY_zero, EB)

        INTEGER ENU, EN, EN1
        REAL, DIMENSION(ENU, 1) :: EUmin
        REAL, DIMENSION(ENU, 1) :: EUmax
        REAL, DIMENSION(EN-EN1+1, 1) :: EYmin
        REAL, DIMENSION(EN-EN1+1, 1) :: EYmax
        REAL, DIMENSION(ENU, 1) :: EDUmax
        REAL, DIMENSION(ENU,1) :: EU
        REAL, DIMENSION(EN-EN1+1,1) :: EY_zero
        REAL, DIMENSION(2*(2*ENU+EN-EN1+1), 1) :: EB
        REAL, DIMENSION(ENU) :: Uminvec
        REAL, DIMENSION(ENU) :: Umaxvec
        REAL, DIMENSION(EN-EN1+1) :: Yminvec
        REAL, DIMENSION(EN-EN1+1) :: Ymaxvec
        REAL, DIMENSION(ENU) :: DUmaxvec
        REAL, DIMENSION(:), ALLOCATABLE :: EBvec

        DUmaxvec = RESHAPE(EDUmax,SHAPE=(/ENU/))
        Uminvec = RESHAPE((-1)*EUmin + EU,SHAPE=(/ENU/))
```

```
         Umaxvec = RESHAPE(EUmax - EU,SHAPE=(/ENU/))
         Yminvec = RESHAPE((-1)*EYmin + EY_zero,SHAPE=(/EN-EN1+1/))
         Ymaxvec = RESHAPE(EYmax - EY_zero,SHAPE=(/EN-EN1+1/))
C
         IF(ALLOCATED(EBvec)) DEALLOCATE(EBvec)
         ALLOCATE( EBvec(2*(2*ENU+EN-EN1+1)) )
C
         EBvec = (/DUmaxvec, DUmaxvec, Uminvec, Umaxvec, Yminvec, Ymaxvec/)
         EB = RESHAPE(EBvec,SHAPE=(/2*(2*ENU+EN-EN1+1), 1/))
C
         IF(ALLOCATED(EBvec)) DEALLOCATE(EBvec)
C
         END SUBROUTINE Matrix_B

         SUBROUTINE MATINV (A, LDA, N)

!
!   * INDICATES PARAMETERS REQUIRING INPUT VALUES
!
         PARAMETER (MX=100)
         DIMENSION A(LDA,*),IEX(MX,2)
         IFLAG = 0
!
!--- CHECK CONSISTENCY OF PASSED PARAMETERS
!
         IF (N.GT.LDA) THEN
             IFLAG = -1
             RETURN
         END IF
!
!--- COMPUTE A = LU BY THE CROUT REDUCTION WHERE L IS LOWER TRIANGULAR
!--- AND U IS UNIT UPPER TRIANGULAR
!
         NEX = 0
         DO K = 1, N
           DO I = K, N
             S = A(I,K)
              DO L = 1, K-1
                S = S-A(I,L)*A(L,K)
              END DO
             A(I,K) = S
           END DO
!
!--- INTERCHANGE ROWS IF NECESSARY
!
         Q = 0.0
         L = 0
          DO I = K, N
             R = ABS(A(I,K))
             IF (R.GT.Q) THEN
                Q = R
                L = I
             END IF
          END DO
         IF (L.EQ.0) THEN
            IFLAG = K

            RETURN
         END IF
         IF (L.NE.K) THEN
            NEX = NEX+1
            IF (NEX.GT.MX) THEN
               IFLAG = -2
               RETURN
            END IF
            IEX(NEX,1) = K
            IEX(NEX,2) = L
            DO J = 1, N
               Q = A(K,J)
               A(K,J) = A(L,J)
               A(L,J) = Q
            END DO
         END IF
!
!--- END ROW INTERCHANGE SECTION
!
          DO J = K+1, N
             S = A(K,J)
             DO L = 1, K-1
                S = S-A(K,L)*A(L,J)
             END DO
             A(K,J) = S/A(K,K)
          END DO
         END DO
!
```

```
!--- INVERT THE LOWER TRIANGLE L IN PLACE
!
         DO K = N, 1, -1
            A(K,K) = 1.0/A(K,K)
          DO I = K-1, 1, -1
             S = 0.0
             DO J = I+1, K
                S = S+A(J,I)*A(K,J)
             END DO
             A(K,I) = -S/A(I,I)
          END DO
         END DO
!
!--- INVERT THE UPPER TRIANGLE U IN PLACE
!
         DO K = N, 1, -1
            DO I = K-1, 1, -1
                 S = A(I,K)
               DO J = I+1, K-1
                  S = S+A(I,J)*A(J,K)
               END DO
                 A(I,K) = -S
            END DO
         END DO
!
!--- COMPUTE INV(A) = INV(U)*INV(L)
!
         DO I = 1, N
            DO J = 1, N
              IF (J.GT.I) THEN
                 S = 0.0
                 L = J
              ELSE
                 S = A(I,J)
                 L = I+1
              END IF
              DO K = L, N
                 S = S+A(I,K)*A(K,J)
              END DO
              A(I,J) = S
            END DO
         END DO
!
!--- INTERCHANGE COLUMNS OF INV(A) TO REVERSE EFFECT OF ROW
!--- INTERCHANGES OF A
!
         DO I = NEX, 1, -1
            K = IEX(I,1)
            L = IEX(I,2)
           DO J = 1, N
              Q = A(J,K)
              A(J,K) = A(J,L)
              A(J,L) = Q
           END DO
         END DO
C
         END SUBROUTINE MATINV

         SUBROUTINE HILDRETH (NX, Hinv, H, F, A, B, eta)

            INTEGER NX
            REAL, DIMENSION (NX,NX) :: H
            REAL, DIMENSION (NX,1) :: F
            REAL, DIMENSION (4*NX,NX) :: A
            REAL, DIMENSION (4*NX,1) :: B
            REAL, DIMENSION (NX,1) :: eta
C           REAL, DIMENSION (4*NX,1) :: X_ini
            REAL, DIMENSION(:,:), ALLOCATABLE :: X_ini
            REAL, DIMENSION(:,:), ALLOCATABLE :: Lambda
            REAL, DIMENSION(:,:), ALLOCATABLE :: Lambda_p
            REAL, DIMENSION (NX,NX) :: Hinv
C           REAL, DIMENSION (NX,NX) :: NHinv
            REAL, DIMENSION(:,:), ALLOCATABLE :: NHinv
C           REAL, DIMENSION (4*NX,4*NX) :: P
            REAL, DIMENSION(:,:), ALLOCATABLE :: P
C           REAL, DIMENSION (4*NX,1) :: D
            REAL, DIMENSION(:,:), ALLOCATABLE :: D
            REAL, DIMENSION (1,1) :: EL
            REAL, DIMENSION (4*NX) :: Z
            REAL, DIMENSION (NX) :: C
            INTEGER k, i, km
            REAL AL, W, LA, G
!
!   * CALCULATES THE NEGATIVE OF MATRIX H
!
```

```
        IF(ALLOCATED(NHinv)) DEALLOCATE(NHinv)
        ALLOCATE( NHinv(NX,NX) )
!
           NHinv = (-1)*Hinv
!
!   * CALCULATES THE GLOBAL OPTIMAL SOLUTION
!
           eta = MATMUL(NHinv, F)
           k = 0
!
!   * CHECKS THE INEQUALITY CONSTRAINTS FOR THE GLOBAL SOLUTION
!
           DO i = 1, 4*NX
               C = A(i,:) * eta(:,1)
               G = SUM(C)
                IF (G > B(i,1)) THEN
                   k = k + 1
                ELSE
                   k = k + 0
                END IF
           END DO

           IF (k == 0) THEN
               RETURN
           END IF
!
!   * CALCULATES THE MATRICES FOR THE DUAL PROBLEM
!
        IF(ALLOCATED(P)) DEALLOCATE(P)
        ALLOCATE( P(4*NX,4*NX) )
C

           P = MATMUL(MATMUL(A, Hinv), TRANSPOSE(A))
C
        IF(ALLOCATED(D)) DEALLOCATE(D)
        ALLOCATE( D(4*NX,1) )
C
           D = B + MATMUL(MATMUL(A, Hinv), F)
!
!   * INITIATES THE LAGRANGE MULTIPLIERS
!
        IF(ALLOCATED(X_ini)) DEALLOCATE(X_ini)
        ALLOCATE( X_ini(4*NX,1) )
C
          X_ini = 0.0
C
        IF(ALLOCATED(Lambda)) DEALLOCATE(Lambda)
        ALLOCATE( Lambda(4*NX,1) )
C
          Lambda = X_ini
          AL = 10.0
!
!   * CALCULATES THE LAGRANGE MULTIPLIERS THROUGH ITTERATIONS
!
        IF(ALLOCATED(Lambda_p)) DEALLOCATE(Lambda_p)
        ALLOCATE( Lambda_p(4*NX,1) )
C
        DO km = 1, 38
            Lambda_p = Lambda
            DO i = 1, 4*NX
               Z = P(i,:) * Lambda(:,1)
               W = SUM(Z) - P(i,i) * Lambda(i,1)
               W = W + D(i,1)
               LA = -W / P(i,i)
               Lambda(i,1) = MAX(0.0,LA)
            END DO
            EL = MATMUL(TRANSPOSE(Lambda - Lambda_p), (Lambda - Lambda_p))
            AL = EL(1,1)
            IF (AL < 10E-8) THEN
                EXIT
            END IF
        END DO
!
!   * CALCULATES THE PRIMAL VARIABLES
!
        eta = MATMUL(NHinv, F) - MATMUL(MATMUL(Hinv, TRANSPOSE(A)), Lambda)
        IF(ALLOCATED(P)) DEALLOCATE(P)
        IF(ALLOCATED(D)) DEALLOCATE(D)
        IF(ALLOCATED(NHinv)) DEALLOCATE(NHinv)
        IF(ALLOCATED(Lambda_p)) DEALLOCATE(Lambda_p)
        IF(ALLOCATED(Lambda)) DEALLOCATE(Lambda)
        IF(ALLOCATED(X_ini)) DEALLOCATE(X_ini)
C
        END SUBROUTINE HILDRETH
```

Appendix B
FORTRAN code for GPC Controller

```
          SUBROUTINE GPCATTEMP

          INTEGER, PARAMETER :: Na = 4
          INTEGER, PARAMETER :: Nb = 52
          INTEGER, PARAMETER :: N = 5
          REAL, DIMENSION(N*(Na+1)) :: F_vector
          REAL, DIMENSION(N, Na+1) :: F
          REAL, DIMENSION(N*Nb) :: G_prime_vector
          REAL, DIMENSION(N, Nb) :: G_prime
          REAL, DIMENSION(N*N) :: K_vector
          REAL, DIMENSION(N, N) :: K
          REAL, DIMENSION(N, 1) :: W
          REAL, SAVE, DIMENSION(Na+1) :: Yp_vector = 0.0
          REAL, DIMENSION(Na+1, 1) :: Yp
          REAL, DIMENSION(Na+2) :: Yp_vec
          REAL, SAVE, DIMENSION(Nb) :: DUp_vector = 0.0
          REAL, DIMENSION(Nb, 1) :: DUp
          REAL, DIMENSION(Nb+1) :: DUp_vec
          REAL, DIMENSION(N, 1) :: DU
          REAL, DIMENSION(N, 1) :: Y_zero
!
!=======Horizon N=5====================================================
!
C         GO TO 500
          F_vector = (/ 26.1532, 26.6303, 27.1058, 27.5798, 28.0522,
     @                   -5.8311, -5.9477, -6.0639, -6.1798, -6.2953,
     @                  -14.3220,-14.5909,-14.8591,-15.1264,-15.3927,
     @                   -9.3289, -9.5011, -9.6727, -9.8436,-10.0142,
     @                    4.3287,  4.4094,  4.4899,  4.5700,  4.6500 /)

          F = RESHAPE ( F_vector, (/N, Na+1/) )

          G_prime_vector = (/ -0.0301,-0.0300,-0.0925,-0.1155,-0.1561,
     @                         -0.0300,-0.0925,-0.1155,-0.1561,-0.2014,
     @                         -0.0925,-0.1155,-0.1561,-0.2014,-0.2328,
     @                         -0.1155,-0.1561,-0.2014,-0.2328,-0.2766,
     @                         -0.1561,-0.2014,-0.2328,-0.2766,-0.3142,
     @                         -0.2014,-0.2328,-0.2766,-0.3142,-0.3516,
     @                         -0.2328,-0.2766,-0.3142,-0.3516,-0.3922,
     @                         -0.2766,-0.3142,-0.3516,-0.3922,-0.4291,
     @                         -0.3142,-0.3516,-0.3922,-0.4291,-0.4679,
     @                         -0.3516,-0.3922,-0.4291,-0.4679,-0.5063,
     @                         -0.3922,-0.4291,-0.4679,-0.5063,-0.5439,
     @                         -0.4291,-0.4679,-0.5063,-0.5439,-0.5822,
     @                         -0.4679,-0.5063,-0.5439,-0.5822,-0.6198,
     @                         -0.5063,-0.5439,-0.5822,-0.6198,-0.6575,
     @                         -0.5439,-0.5822,-0.6198,-0.6575,-0.6952,
     @                         -0.5822,-0.6198,-0.6575,-0.6952,-0.7325,
     @                         -0.6198,-0.6575,-0.6952,-0.7325,-0.7699,
     @                         -0.6575,-0.6952,-0.7325,-0.7699,-0.8071,
     @                         -0.6952,-0.7325,-0.7699,-0.8071,-0.8441,
     @                         -0.7325,-0.7699,-0.8071,-0.8441,-0.8811,
     @                         -0.7699,-0.8071,-0.8441,-0.8811,-0.9179,
     @                         -0.8071,-0.8441,-0.8811,-0.9179,-0.9546,
     @                         -0.8441,-0.8811,-0.9179,-0.9546,-0.9912,
     @                         -0.8811,-0.9179,-0.9546,-0.9912,-1.0277,
     @                         -0.9179,-0.9546,-0.9912,-1.0277,-1.0640,
     @                         -0.9546,-0.9912,-1.0277,-1.0640,-1.1003,
     @                         -0.9912,-1.0277,-1.0640,-1.1003,-1.1364,
     @                         -1.0277,-1.0640,-1.1003,-1.1364,-1.1724,
     @                         -1.0640,-1.1003,-1.1364,-1.1724,-1.2082,
     @                         -1.1003,-1.1364,-1.1724,-1.2082,-1.2440,
     @                         -1.1364,-1.1724,-1.2082,-1.2440,-1.2796,
     @                         -1.1724,-1.2082,-1.2440,-1.2796,-1.3152,
     @                         -1.2082,-1.2440,-1.2796,-1.3152,-1.3506,
     @                         -1.2440,-1.2796,-1.3152,-1.3506,-1.3859,
     @                         -1.2796,-1.3152,-1.3506,-1.3859,-1.4211,
     @                         -1.3152,-1.3506,-1.3859,-1.4211,-1.4561,
     @                         -1.3506,-1.3859,-1.4211,-1.4561,-1.4911,
     @                         -1.3859,-1.4211,-1.4561,-1.4911,-1.5259,
     @                         -1.4211,-1.4561,-1.4911,-1.5259,-1.5606,
     @                         -1.4561,-1.4911,-1.5259,-1.5606,-1.5952,
     @                         -1.4911,-1.5259,-1.5606,-1.5952,-1.6297,
     @                         -1.5259,-1.5606,-1.5952,-1.6297,-1.6641,
     @                         -1.5606,-1.5952,-1.6297,-1.6641,-1.6984,
     @                         -1.5952,-1.6297,-1.6641,-1.6984,-1.7325,
     @                         -1.6297,-1.6641,-1.6984,-1.7325,-1.7666,
     @                         -1.6641,-1.6984,-1.7325,-1.7666,-1.8005,
```

```
     @                         -1.6984,-1.7325,-1.7666,-1.8005,-1.8344,
     @                         -1.7325,-1.7666,-1.8005,-1.8344,-1.8681,
     @                         -1.7666,-1.8005,-1.8344,-1.8681,-1.0573,
     @                         -1.8005,-1.8344,-1.8681,-1.0573,-1.2814,
     @                         -1.8344,-1.8681,-1.0573,-1.2814,-1.7782,
     @                         -1.8681,-1.0573,-1.2814,-1.7782,-0.3613 /)

          G_prime = RESHAPE ( G_prime_vector, (/N, Nb/) )
!
!========Lambda = 10=================================================
!
          GO TO 100
          K_vector = (/ -0.0030, 4.58E-06, 2.14E-06, 1.87E-06, 1.04E-06,
     @                  -0.0030,  -0.0030, 3.52E-06, 2.98E-06, 1.88E-06,
     @                  -0.0030,  -0.0030,  -0.0030, 3.51E-06, 2.14E-06,
     @                  -0.0092,  -0.0030,  -0.0030,  -0.0030, 4.58E-06,
     @                  -0.0115,  -0.0092,  -0.0030,  -0.0030,  -0.0030 /)
100       CONTINUE
!====================================================================
!
!========Lambda = 1000===============================================
!
          GO TO 200
          K_vector = (/ -3.0099E-05, 4.5954E-10, 2.1527E-10, 1.8810E-10,
     @                   1.0464E-10,
     @                  -3.0099E-05,-3.0099E-05, 3.5325E-10, 2.9880E-10,
     @                   1.8844E-10,
     @                  -2.9999E-05,-3.0099E-05,-3.0100E-05, 3.5253E-10,
     @                   2.1527E-10,
     @                  -9.2497E-05,-2.9998E-05,-3.0099E-05,-3.0099E-05,
     @                   4.5945E-10,
     @                  -1.1550E-04,-9.2497E-05,-2.9999E-05,-2.9999E-05,
     @                  -3.0099E-05 /)
200       CONTINUE
!====================================================================
!
!========Lambda = 500================================================
!
          GO TO 300
          K_vector = (/ -6.0197E-05, 1.8381E-09, 8.6106E-10, 7.5235E-10,
     @                   4.1854E-10,
     @                  -6.0195E-05,-6.0197E-05, 1.4129E-09, 1.1951E-09,
     @                   7.5374E-10,
     @                  -5.9994E-05,-6.0196E-05,-6.0198E-05, 1.4101E-09,
     @                   8.6106E-10,
     @                  -1.8499E-04,-5.9992E-05,-6.0196E-05,-6.0197E-05,
     @                   1.8377E-09,
     @                  -2.3098E-04,-1.8499E-04,-5.9994E-05,-5.9995E-05,
     @                  -6.0197E-05 /)
300       CONTINUE
!====================================================================
!
!========Lambda = 100================================================
!
          GO TO 400
          K_vector = (/ -3.0093E-04, 4.5938E-08, 2.1520E-08, 1.8803E-08,
     @                   1.0460E-08,
     @                  -3.0088E-04,-3.0092E-04, 3.5312E-08, 2.9869E-08,
     @                   1.8838E-08,
     @                  -2.9986E-04,-3.0091E-04,-3.0096E-04, 3.5241E-08,
     @                   2.1520E-08,
     @                  -9.2469E-04,-2.9980E-04,-3.0091E-04,-3.0092E-04,
     @                   4.5928E-08,
     @                  -1.1545E-03,-9.2469E-04,-2.9986E-04,-2.9988E-04,
     @                  -3.0093E-04 /)
400       CONTINUE
!====================================================================
!
!========Lambda = 300================================================
!
C         GO TO 40
          K_vector = (/ -1.0033E-04, 5.1055E-09, 2.3917E-09, 2.0898E-09,
     @                   1.1626E-09,
     @                  -1.0032E-04,-1.0032E-04, 3.9246E-09, 3.3197E-09,
     @                   2.0936E-09,
     @                  -9.9984E-05,-1.0032E-04,-1.0033E-04, 3.9167E-09,
     @                   2.3917E-09,
     @                  -3.0830E-04,-9.9978E-05,-1.0032E-04,-1.0032E-04,
     @                   5.1045E-09,
     @                  -3.8495E-04,-3.0830E-04,-9.9984E-05,-9.9987E-05,
     @                  -1.0033E-04 /)
C40       CONTINUE
!====================================================================
C500      CONTINUE
!========End Horizon N=5=============================================
```

```
!========Horizon N=10================================================
         GO TO 600
         F_vector = (/ 222.4921, 231.9219, 240.9855, 249.6511, 257.8897,
     @                  265.6751, 272.9839, 279.7956, 286.0927, 291.8607,
     @                 -427.9897,-446.8949,-465.1119,-482.5755,-499.2258,
     @                 -515.0084,-529.8746,-543.7810,-556.6902,-568.5708,
     @                  206.4977, 215.9731, 225.1266, 233.9246, 242.3363,
     @                  250.3335, 257.8908, 264.9855, 271.5976, 277.7102 /)
         F = RESHAPE ( F_vector, (/N, Na+1/) )

         G_prime_vector = (/ 0.0039, 0.0087, 0.0152, 0.0235, 0.0334,
     @                       0.0447, 0.0575, 0.0717, 0.0870, 0.1034,
     @                       0.0087, 0.0152, 0.0235, 0.0334, 0.0447,
     @                       0.0575, 0.0717, 0.0870, 0.1034, 0.1209,
     @                       0.0152, 0.0235, 0.0334, 0.0447, 0.0575,
     @                       0.0717, 0.0870, 0.1034, 0.1209, 0.1392,
     @                       0.0235, 0.0334, 0.0447, 0.0575, 0.0717,
     @                       0.0870, 0.1034, 0.1209, 0.1392, 0.1583,
     @                       0.0334, 0.0447, 0.0575, 0.0717, 0.0870,
     @                       0.1034, 0.1209, 0.1392, 0.1583, 0.1780,
     @                       0.0447, 0.0575, 0.0717, 0.0870, 0.1034,
     @                       0.1209, 0.1392, 0.1583, 0.1780, 0.1983,
     @                       0.0575, 0.0717, 0.0870, 0.1034, 0.1209,
     @                       0.1392, 0.1583, 0.1780, 0.1983, 0.2190,
     @                       0.0717, 0.0870, 0.1034, 0.1209, 0.1392,
     @                       0.1583, 0.1780, 0.1983, 0.2190, 0.2401,
     @                       0.0870, 0.1034, 0.1209, 0.1392, 0.1583,
     @                       0.1780, 0.1983, 0.2190, 0.2401, 0.2614,
     @                       0.1034, 0.1209, 0.1392, 0.1583, 0.1780,
     @                       0.1983, 0.2190, 0.2401, 0.2614, 0.2828,
     @                       0.1209, 0.1392, 0.1583, 0.1780, 0.1983,
     @                       0.2190, 0.2401, 0.2614, 0.2828, 0.3041,
     @                       0.1392, 0.1583, 0.1780, 0.1983, 0.2190,
     @                       0.2401, 0.2614, 0.2828, 0.3041, 0.3254,
     @                       0.1583, 0.1780, 0.1983, 0.2190, 0.2401,
     @                       0.2614, 0.2828, 0.3041, 0.3254, 0.3466,
     @                       0.1780, 0.1983, 0.2190, 0.2401, 0.2614,
     @                       0.2828, 0.3041, 0.3254, 0.3466, 0.3674,
     @                       0.1983, 0.2190, 0.2401, 0.2614, 0.2828,
     @                       0.3041, 0.3254, 0.3466, 0.3674, 0.3878,
     @                       0.2190, 0.2401, 0.2614, 0.2828, 0.3041,
     @                       0.3254, 0.3466, 0.3674, 0.3878, 0.4078,
     @                       0.2401, 0.2614, 0.2828, 0.3041, 0.3254,
     @                       0.3466, 0.3674, 0.3878, 0.4078, 0.4273,
     @                       0.2614, 0.2828, 0.3041, 0.3254, 0.3466,
     @                       0.3674, 0.3878, 0.4078, 0.4273, 0.4461,
     @                       0.2828, 0.3041, 0.3254, 0.3466, 0.3674,
     @                       0.3878, 0.4078, 0.4273, 0.4461, 0.4643,
     @                       0.3041, 0.3254, 0.3466, 0.3674, 0.3878,
     @                       0.4078, 0.4273, 0.4461, 0.4643, 0.4817,
     @                       0.3254, 0.3466, 0.3674, 0.3878, 0.4078,
     @                       0.4273, 0.4461, 0.4643, 0.4817, 0.4982,
     @                       0.3466, 0.3674, 0.3878, 0.4078, 0.4273,
     @                       0.4461, 0.4643, 0.4817, 0.4982, 0.5140,
     @                       0.3674, 0.3878, 0.4078, 0.4273, 0.4461,
     @                       0.4643, 0.4817, 0.4982, 0.5140, 0.5288,
     @                       0.3878, 0.4078, 0.4273, 0.4461, 0.4643,
     @                       0.4817, 0.4982, 0.5140, 0.5288, 0.5426,
     @                       0.4078, 0.4273, 0.4461, 0.4643, 0.4817,
     @                       0.4982, 0.5140, 0.5288, 0.5426, 0.5555,
     @                       0.2078, 0.2173, 0.2265, 0.2354, 0.2438,
     @                       0.2519, 0.2595, 0.2666, 0.2733, 0.2794 /)
         G_prime = RESHAPE ( G_prime_vector, (/N, Nb/) )
!
!========Lambda = 10==================================================
!
         GO TO 700
         K_vector = (/ 0.0001, 0.0000, 0.0000, 0.0000, 0.0000,
     @                 0.0000, 0.0000, 0.0000, 0.0000, 0.0000,
     @                 0.0004, 0.0001, 0.0000, 0.0000, 0.0000,
     @                 0.0000, 0.0000, 0.0000, 0.0000, 0.0000,
     @                 0.0009, 0.0004, 0.0001, 0.0000, 0.0000,
     @                 0.0000, 0.0000, 0.0000, 0.0000, 0.0000,
     @                 0.0015, 0.0009, 0.0004, 0.0001, 0.0000,
     @                 0.0000, 0.0000, 0.0000, 0.0000, 0.0000,
     @                 0.0023, 0.0015, 0.0009, 0.0004, 0.0001,
     @                 0.0000, 0.0000, 0.0000, 0.0000, 0.0000,
     @                 0.0033, 0.0023, 0.0015, 0.0009, 0.0004,
     @                 0.0001, 0.0000, 0.0000, 0.0000, 0.0000,
     @                 0.0045, 0.0033, 0.0023, 0.0015, 0.0009,
     @                 0.0004, 0.0001, 0.0000, 0.0000, 0.0000,
     @                 0.0057, 0.0044, 0.0033, 0.0023, 0.0015,
     @                 0.0009, 0.0004, 0.0001, 0.0000, 0.0000,
     @                 0.0071, 0.0057, 0.0044, 0.0033, 0.0023,
```

```
     @                 0.0015, 0.0009, 0.0004, 0.0001, 0.0000,
     @                 0.0087, 0.0071, 0.0057, 0.0045, 0.0033,
     @                 0.0023, 0.0015, 0.0009, 0.0004, 0.0001 /)
700      CONTINUE
!=====================================================================
!
!========Lambda = 5=================================================
!
         GO TO 800
         K_vector = (/ 0.0002, 0.0000, 0.0000, 0.0000, 0.0000,
     @                 0.0000, 0.0000, 0.0000, 0.0000, 0.0000,
     @                 0.0008, 0.0002, 0.0000, 0.0000, 0.0000,
     @                 0.0000, 0.0000, 0.0000, 0.0000, 0.0000,
     @                 0.0017, 0.0008, 0.0002, 0.0000, 0.0000,
     @                 0.0000, 0.0000, 0.0000, 0.0000, 0.0000,
     @                 0.0030, 0.0017, 0.0008, 0.0002, 0.0000,
     @                 0.0000, 0.0000, 0.0000, 0.0000, 0.0000,
     @                 0.0047, 0.0030, 0.0017, 0.0008, 0.0002,
     @                 0.0000, 0.0000, 0.0000, 0.0000, 0.0000,
     @                 0.0066, 0.0047, 0.0030, 0.0017, 0.0008,
     @                 0.0002, 0.0000, 0.0000, 0.0000, 0.0000,
     @                 0.0089, 0.0066, 0.0047, 0.0030, 0.0017,
     @                 0.0008, 0.0002, 0.0000, 0.0000, 0.0000,
     @                 0.0114, 0.0089, 0.0066, 0.0047, 0.0030,
     @                 0.0017, 0.0008, 0.0002, 0.0000, 0.0000,
     @                 0.0142, 0.0114, 0.0089, 0.0066, 0.0047,
     @                 0.0030, 0.0017, 0.0008, 0.0002, 0.0000,
     @                 0.0172, 0.0142, 0.0114, 0.0089, 0.0066,
     @                 0.0047, 0.0030, 0.0017, 0.0008, 0.0002 /)
800      CONTINUE
!=====================================================================
!
!========Lambda = 1=================================================
!
         GO TO 900
         K_vector = (/ 0.0100, 0.0000, 0.0000, 0.0000, 0.0000,
     @                 0.0039, 0.0100, 0.0000, 0.0000, 0.0000,
     @                 0.0087, 0.0039, 0.0100, 0.0000, 0.0000,
     @                 0.0152, 0.0087, 0.0039, 0.0100, 0.0000,
     @                 0.0235, 0.0152, 0.0087, 0.0039, 0.0100 /)
900      CONTINUE
!=====================================================================
!
!========Lambda = 0.1===============================================
!
         GO TO 1000
         K_vector = (/ 0.0990, -0.0006, -0.0003, -0.0002, -0.0002,
     @                 0.0381, 0.0994, -0.0003, -0.0002, -0.0002,
     @                 0.0856, 0.0382, 0.0994, -0.0003, -0.0003,
     @                 0.1497, 0.0856, 0.0382, 0.0994, -0.0006,
     @                 0.2313, 0.1497, 0.0856, 0.0381, 0.0990 /)
1000     CONTINUE
!=====================================================================
600      CONTINUE
!========End Horizon N=10===========================================

         K = RESHAPE ( K_vector, (/N, N/) )

         W = CTSS_LIM53_Y

         Yp_vec = (/ CTSS_PVX2AL, Yp_vector /)

         DO I = 1, Na+1
            Yp_vector(I) = Yp_vec(I)
         END DO

         Yp = RESHAPE ( Yp_vector, (/Na+1, 1/) )

         DUp = RESHAPE ( DUp_vector, (/Nb, 1/) )

         Y_zero = MATMUL(F, Yp) + MATMUL(G_prime, DUp)

         DU = MATMUL(K, (W - Y_zero))

         DUp_vec = (/ DU(1,1), DUp_vector /)

         IF (SWITCH_ATTEMP == 1) THEN
             CTSS_GPC_ATTEMP = CTSS_PID52_Y + DU(1,1)
         END IF

         DO I = 1, Nb
            DUp_vector (I) = DUp_vec (I)
         END DO

         END SUBROUTINE GPCATTEMP
```

Appendix C.1
Control Diagrams of the coal mills control – Fuel calculation

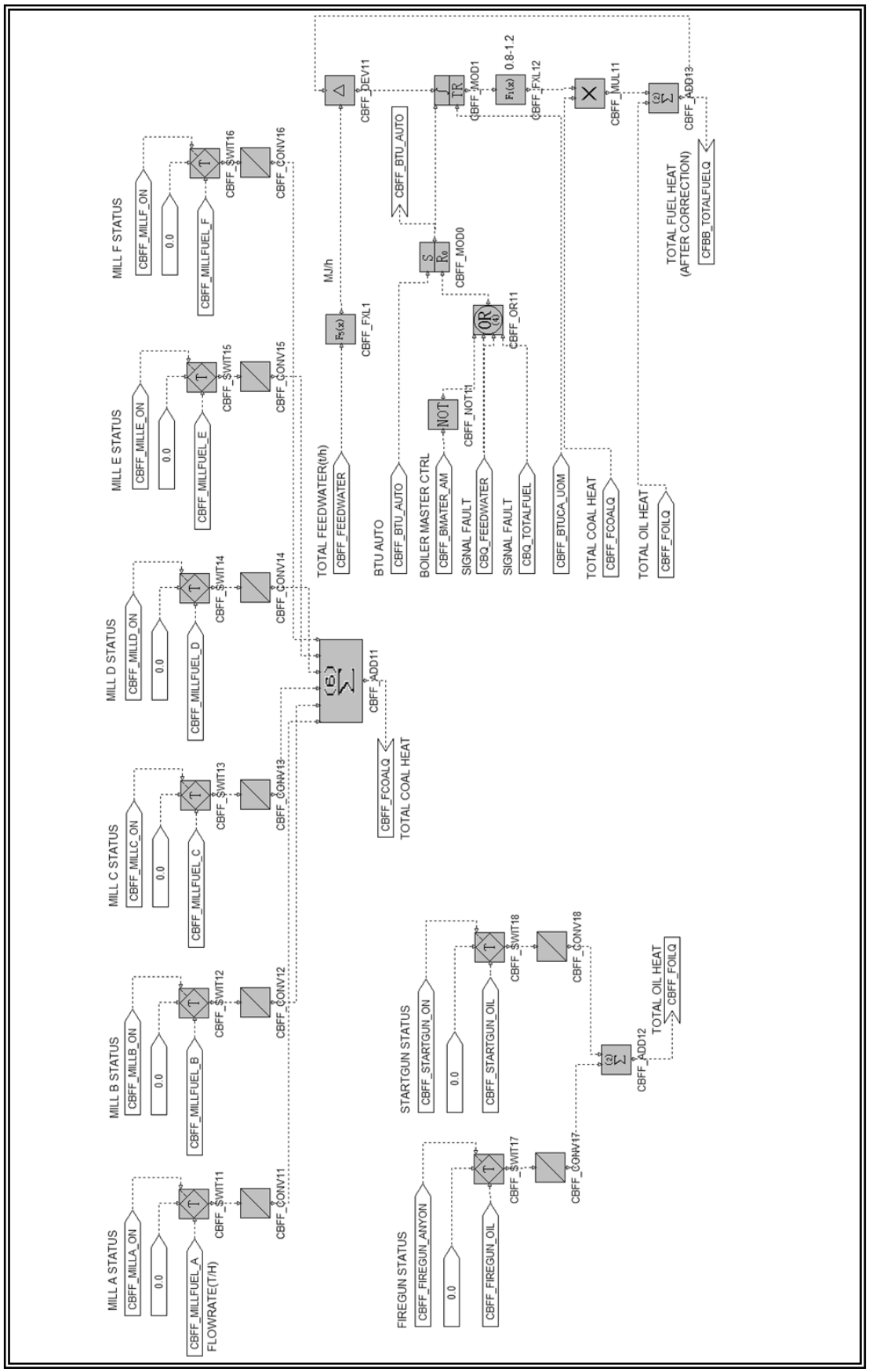

Appendix C.2
Control Diagrams of the coal mills control – Fuel control

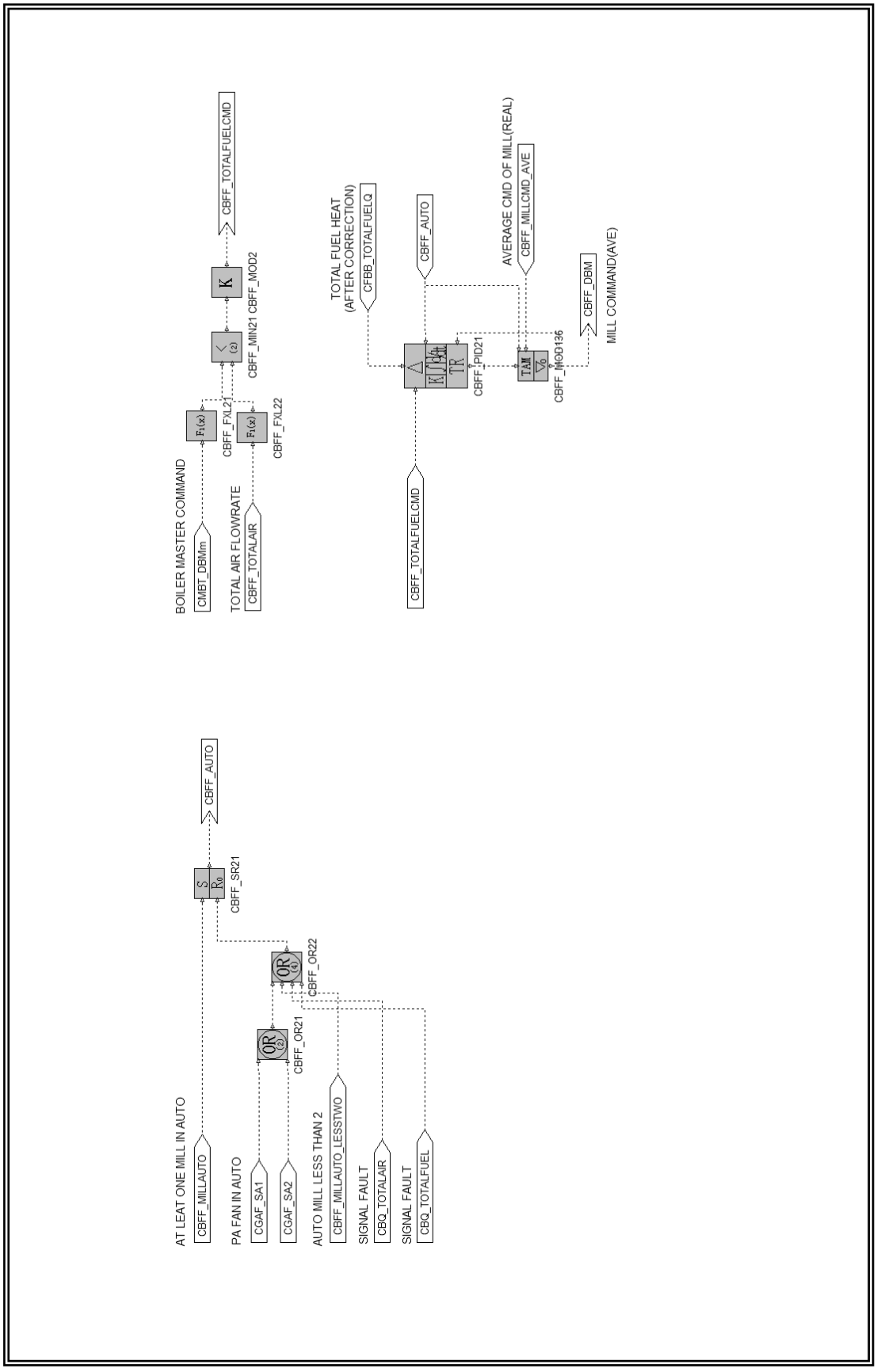

Appendix C.3
Control Diagrams of the coal mills control – Fuel command

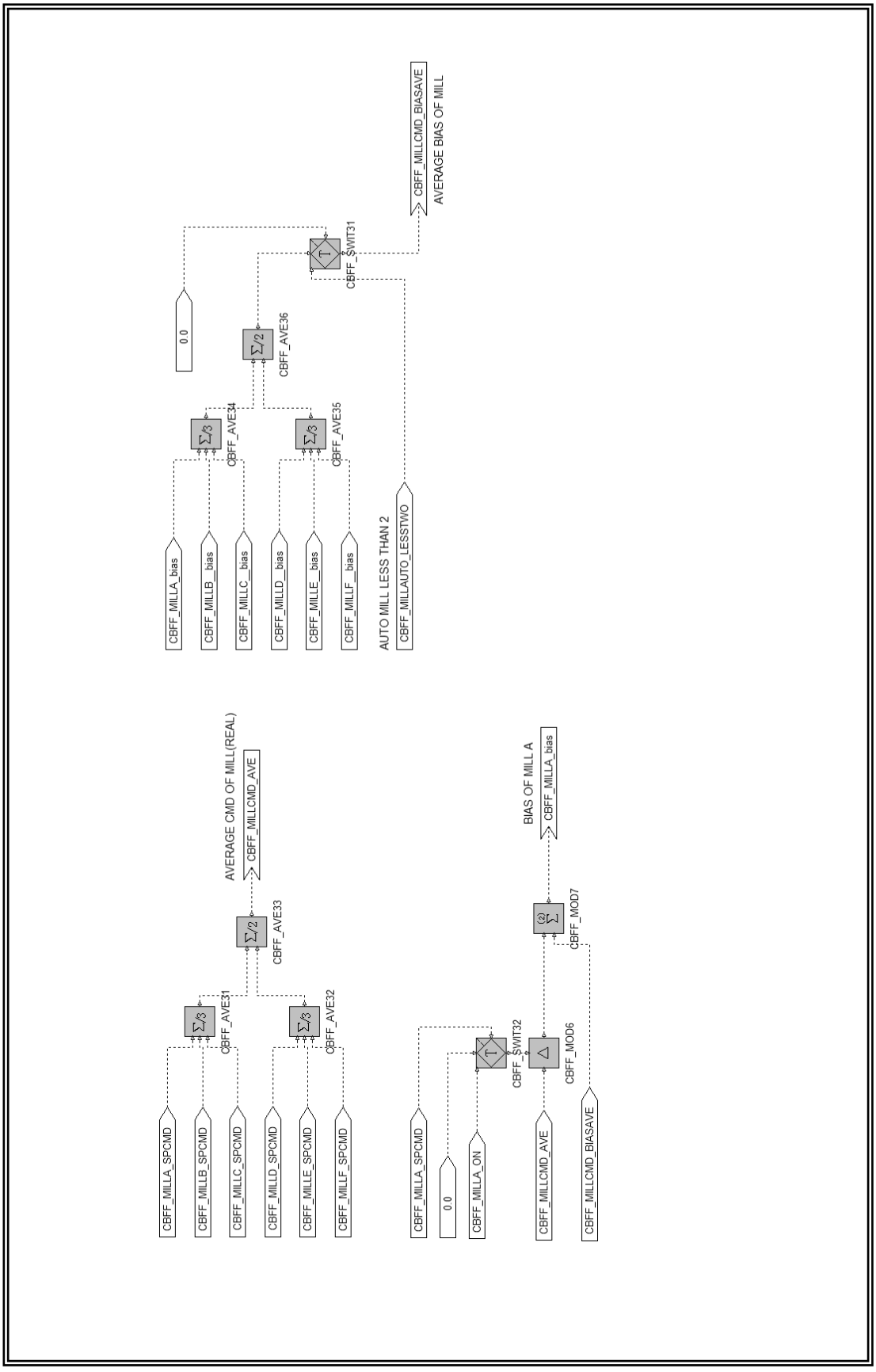

Appendix C.4
Control Diagrams of the coal mills control – Fuel feeder speed

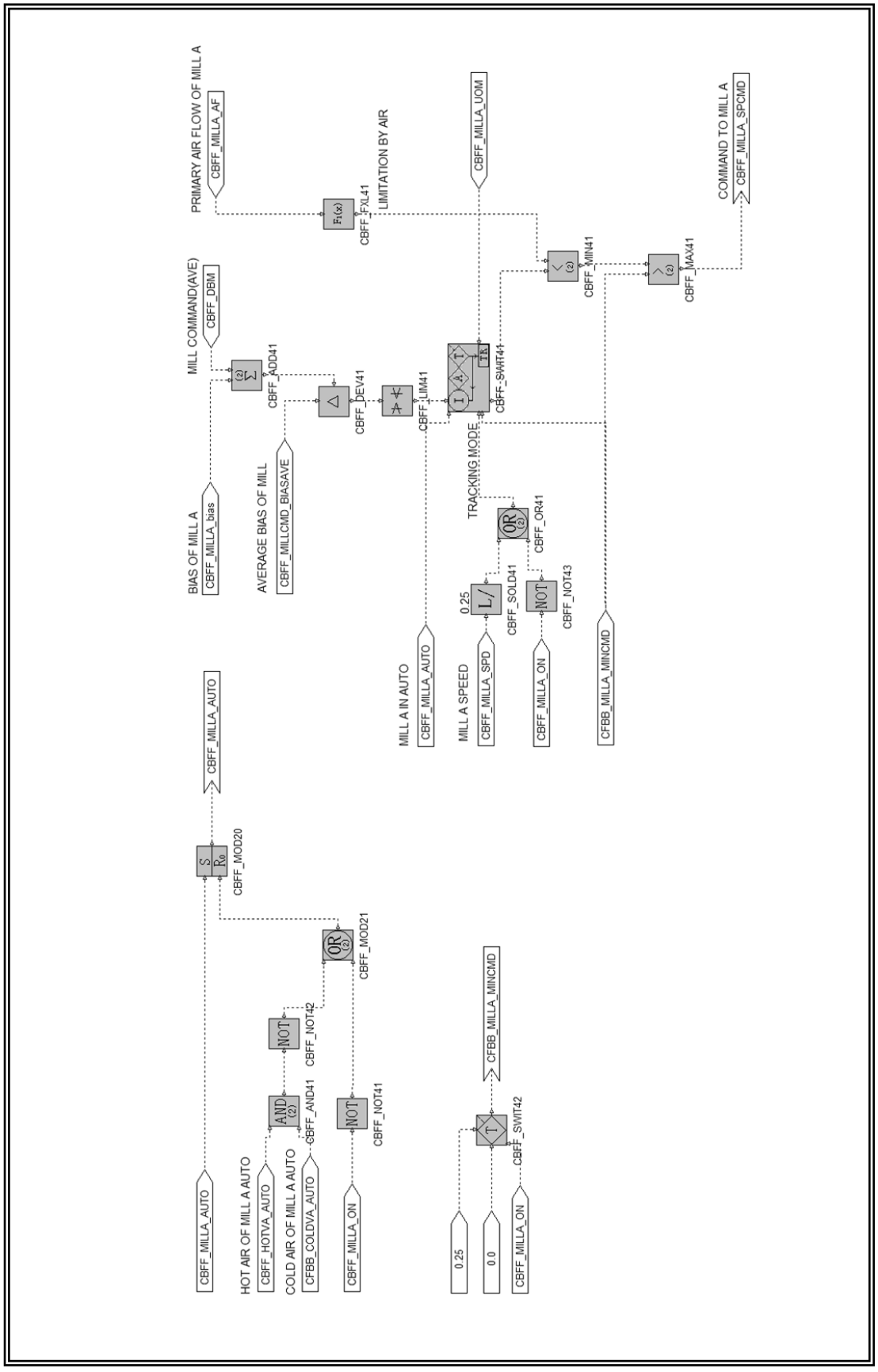

Appendix D
Control Diagram of the second stage SH temperature control

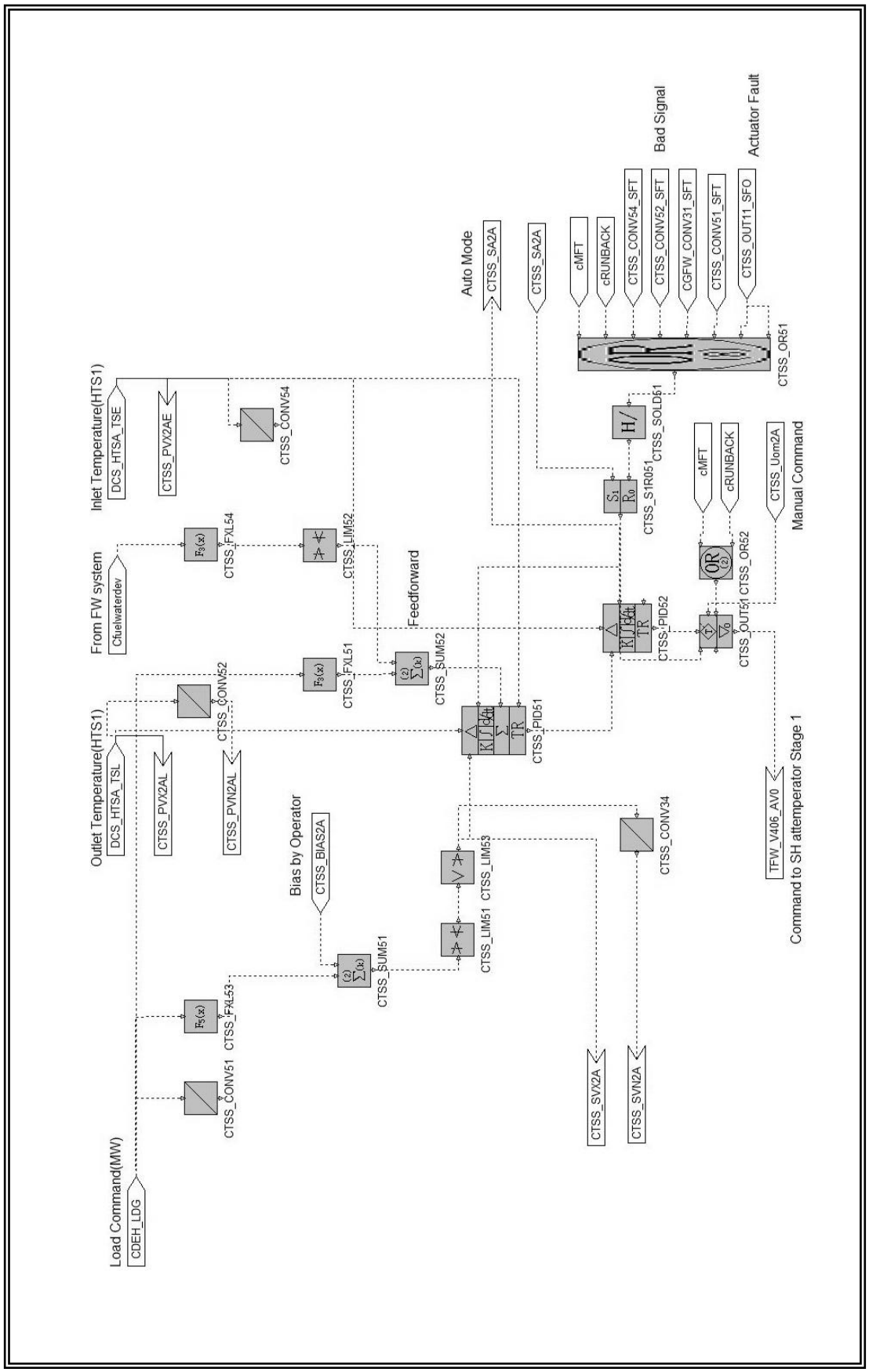

References

AEMC, 2001, *Reliability Panel, Frequency operating standards*.

AEMO, 2010, *Guide to Ancillary Services in the National Electricity Market*.

Aurora, C., Magni, L., Scattolini, R., Colombo, P., Pretolani, F., Villa, G., 2004, Predictive control of thermal power plants, *Int. J. Robust Nonlinear Control,* vol. 14, pp. 415-433.

Bucciero, J., Terbrueggen, M., 1998, *Dynamics of interconnected power systems*, Electric Power Research Institute.

Camacho, E. F., 2007, *Model Predictive Control*, Springer.

Camacho, E. F., Bordons, C., 2007, *Model Predictive Control*, 2nd ed., Springer, pp. 47-48.

Chapra, S. C., 2012, *Applied Numerical Methods with MATLAB for Engineers and Scientists*, 3rd ed., McGraw-Hill.

Clarke, D. W., Mohtadi, C., Tuffs, P. S., 1987, Generalised predictive control –Parts I and II, Automatica, vol. 23, issue (2), pp. 137-160.

Clarke, D. W., 1988, Application of Generalized Predictive Control to Industrial Processes, *IEEE Control Systems Magazine*, vol. 8, issue (2), pp. 49-55.

Clarke, D. W., Mohtadi, C., 1989, Properties of generalized predictive control, *Automatica - Identification and systems parameter estimation*, vol. 25, issue (6), pp. 859-875.

CN Transelectrica SA, 2004, *Codul tehnic al retelei electrice de transport*.

Cutler, C. R., Ramaker, B. L., 1980, Dynamic Matrix Control – a computer control Algorithm, *In Proceedings of Joint Automatic Control Conference, San Francisco*.

Department of Energy & Climate Change, 2008, *2008 Climate Change Act*.

Department of Energy & Climate Change, 2013, *UK energy in brief 2013.*

Dougherty, D., Cooper, D. J., 2003, Tuning guidelines of a dynamic matrix controller for integrating (non-self-regulating) processes, *Ind. Eng. Chem. Res.*, vol. 42, pp. 1739-1752.

EirGrid, 2009, *EirGrid Code*.

Energie-Control Austria, 2008, *Technische und organisatorische Regeln für Betreiber und Benutzer von Netzen*.

ETSU coal R&D Programme, 1997, *Technology status report: NO_x control for pulverised coal-fired power plant*.

EWEA, December 2005, *Large scale integration of wind energy in the European power supply: analysis, issues and recommendations*.

Flynn, D., 2003, *Thermal Power Plant Simulation and Control*, The Institution of Electrical Engineers.

Fu, X., Jiang, D., Zhou, Y., 2013, Model identification and predictive control of steam temperature in coal-fired power plant, *International Conference on Power, Energy and Control (ICPEC)*, 6-8 Feb., pp.509-513.

Ganguly, J., 2008, *Thermodynamics in Earth and Planetary Sciences*, Springer.

Garcia, C. E., Morshedi, A. M., 1986, Quadratic programming solution of dynamic matrix control (QDMC), *Chemical Eng. Communications*, vol. 46, pp. 73–87.

Gawthrop, P. J., Nomikos, P. E., 1990, Automatic tuning of commercial PID controllers for single loop and multiloop applications, *IEEE Control Systems Magazine*, vol. 10, no. 1, pp. 34-42.

Gomez Ortega, J., Camacho, E. F., 1996, Mobile Robot Navigation in a Partially Structured Environment using Neural Predictive Control, *Control Engineering Practice*, vol. 4, pp. 1669-1679.

Gough, B., 2000, Advanced control of steam superheat temperature on a utility boiler, *Universal Dynamics Technologies Inc., Richmond, Canada*.

Gu, J. J., Zhang, L. Y., Li, J. Q., Study on mathematical model of coordinated control system for supercritical units, *In 2009 International Conference on Machine Learning and Cybernetics, July 12, 2009-July 15, 2009*, Baoding, China: IEEE, pp. 2158-2163.

Herman, G. T., Lent, A., 1978, A family of iterative quadratic optimization algorithms for pairs of inequalities with applications in diagnostic radiology, *Mathematical Programming Study*, issue(9), pp. 15-29.

Hildreth, C., 1957, A quadratic programming procedure, *Naval Research Logistics Quarterly*, issue (4), pp. 79-85.

Hlava, J., 2010, Model predictive control of the superheater temperature based on a piecewise affine model, *Control 2010, UKACC International Conference*, 7-10 Sept., pp.1-6.

Hou, G., Xi, Y., Liu, J., Zhang, J., Simulation research of the multi-variable generalized predictive control in 500 MW unit plant coordinated control system. 2011 *International Conference on Advanced Mechatronic Systems (ICAMechS), 11-13 Aug. 2011*, pp. 196-201.

Institute of Thermal Dynamic Simulation and Control - Tsinghua University, 2012, *SimuEngine Technical Documentation*.

International Energy Agency, 2013, *Monthly Electricity Statistics, August 2013.*

Kiameh, P., 2002, *Power generation handbook*, McGraw-Hill Professional.

Kim, W., Moon, U., Lee, K. Y., Jung, W. H., Kim, S. H., 2010, Once-through boiler steam temperature control using Dynamic Matrix Control technique, *Power and Energy Society General Meeting, 2010 IEEE,* 25-29 July, pp.1-6.

Kitto, J. B., Stultz., S. C., 2005, *Steam. Its generation and use*, The Babcock & Wilcox Company.

Kocaarslan, I., Cam, E., Tiryaki, H., 2006, A fuzzy logic controller application for thermal power plants. *Energy Conversion and Management*, vol. 47, issue (4), pp. 442-458.

Laubli, F., Fenton, F. H., 1971, The Flexibility of the Supercritical Boiler as a Partner in Power System Design and Operation Part II: Application and Field Test Results. *IEEE Transactions on Power Apparatus and Systems*, PAS-90, issue (4), pp. 1725-1733.

Lee, J., Cooley, B., 1996, Recent advances in model predictive control and other related areas, *Chemical Process Control,* pp. 201-216.

Li, Z. J., Li, Z. X., Tan, W., Liu, J. Z., 2006, Constrained Dynamic Matrix Control for a Boiler-Turbine Unit, *International Conference on Machine Learning and Cybernetics*, pp. 665-670.

Linkers, D. A., Mahfonf, M., 1994, *Advances in Model-Based Predictive Control*, Oxford University Press.

Luenberger, D. G., 1969, *Optimization by vector space methods*, John Wiley and Sons, New York.

Maciejowski, J. M., 2002, *Predictive Control with Constraints*, 2nd ed., Prentice Hall.

Marquis, P., Broustail, J. P., 1988, SMOC, a bridge between state space and model predictive controllers: Application to the automation of a hydrotreating unit, *Proceedings of the IFAC Workshop on Model Based Process Control*, pp. 37-43.

Moelbak, T., 1999, Advanced control of superheater steam temperatures – an evaluation based on practical applications, *Control Engineering Practice*, vol. 7, issue 1, pp. 1–10.

Mohamed, O., Wang, J., Al-Duri, B., Lu, J., Gao, Q., Xue, Y., Liu, X., 2012, Predictive Control of Coal Mills for Improving Supercritical Power Generation Process Dynamic Responses, *IEEE 51st Annual Conference on Decision and Control (CDC)*.

Moon, U., Lee, K. Y., 2005, Step-Response Model Development for Dynamic Matrix Control of a Drum-Type Boiler–Turbine System, *IEEE Transactions on Power Systems*, vol. 20, no. 4, pp. 1922-1928.

Nakamura, H., Akaike, H., 1981, Statistical identification for optimal control of supercritical thermal power plants, *Automatica*, vol. 17, issue (1), pp. 143-155.

National Grid Electricity Transmission plc, 2010, *The Grid Code*.

National Development and Reform Commission, 2007, *The grid operation code DL/T 1040*.

Nicholls, R. J., Maxim, C., 5th December 2013, *Supercritical coal fired plant requirements and the Grid Code*, E.ON UK, [Online], Available: http://www.nationalgrid.com.

Prett, D. M., Gillette, R. D., 1980, Optimization and constrained multivariable control of catalytic cracking unit, *In Proceedings of Joint Automatic Control Conference, San Francisco*.

PSE Operator S.A., 2006, *Instruction of transmission system operation and maintenance*.

Réseau de Transport d'électricité, 2009, *Documentation technique de référence*.

Richalet, J., Rault, A., Testud, J. L., Papon, J., 1976, Algorithmic control of industrial Processes, *In Proceedings of 4th IFAC Symposium on Identification and System Parameter Estimation*, pp. 1119-1167.

Richalet, J., Rault, A., Testud, J. L., Papon, J., 1978, Model predictive heuristic control: Applications to industrial processes, *Automatica*, vol. 14, pp. 413-428.

Richalet, J., 1993, Industrial Applications of Model Based Predictive Control, *Automatica*, vol. 29, issue (5), pp. 1251-1274.

Rogers, G., Mayhew, Y., 1992, *Engineering Thermodynamics, Work and Heat Transfer*, Longman Scientific & Technical.

Rossiter, J. A., 2004, *Model Based Predictive Control, a Practical Approach*,1st ed., CRC Press.

Rovnak, J. A., Corlis, R., 1991, Dynamic matrix based control of fossil power plants. IEEE Transactions on Energy Conversion, vol. 6, issue (2), pp. 320-326.

Sanchez-Lopez, A., Arroyo-Figueroa, G., Villavicencio-Ramirez, A., 2004, Advanced control algorithms for steam temperature regulation of thermal power plants, *International Journal of Electrical Power & Energy Systems*, vol. 26, issue 10, pp. 779-785.

Smith, J. W., 1998, Supercritical (once through) boiler technology, *Babcock & Wilcox, Barberton, Ohio, US, BR- 1658*.

Sung, S. W., Lee, J., Lee, I. B., 2009, *Process Identification and PID Control*, 1st ed., John Wiley & Sons.

Susta, M. R., 2008, Development in Supercritical Steam Tech, *Powergen Asia 2008, Kuala Lumpur*.

System Operator for Northern Ireland, 2011, *Soni Grid Code*.

Tatjewski, P., 2007, *Advanced Control of Industrial Processes*, Springer.

Taylor, B., 7-9 Sept. 2008, The keynotes presentation from E.ON, *U21 Energy Conference*, Birmingham, UK.

Terna, 2011, *Codice di trasmissione dispacciamento, sviluppo e sicurezza della rete*.

UCTE, 2004, *UCTE Operation Handbook*.

U.S. Energy Information Administration, 2013, *International Energy Outlook 2013*.

Waddington, J., Maples, G. C., 1987, The control of large coal- and oil-fired generating units. *Power Engineering Journal*, vol. 1, issue (1), pp. 25-36.

Wang, J., 2009, *Study of Supercritical Coal Fired Power Plant Dynamic Responses and Control for Grid Code Compliance*, Case for support, Power Systems and Control Research Lab, University of Birmingham.

Wang, L., 2009, *Model Predictive Control System Design and Implementation Using MATLAB*, 1st ed., Springer.

Wismer, D. A., Chattergy, R., 1978, *Introduction to nonlinear optimization, a problem solving approach*, North-Holland, New York.

Woodruff, E. B., Lammers, H. B., Lammers, T. F., 2004, *Steam plant operation*, 8th ed., McGraw-Hill, pp. 60-63.

Yu, K. M., Kim, J., 2011, Model reference PID control and tuning for steam temperature in thermal power plant, *11th International Conference on Control, Automation and Systems (ICCAS)*, 26-29 Oct., pp. 415-419.

Ziems, C., Weber, H., 2009, Effects of wind turbine generated power fluctuations to thermal power generation, *Proceedings of IFAC Symposium on Power Plants and Power Systems Control, Tampere, Finland*.